Copy No. _____

Guide for Mechanistic-Empirical Design
OF NEW AND REHABILITATED PAVEMENT STRUCTURES

FINAL DOCUMENT

APPENDIX LL:
PUNCHOUTS IN CONTINUOUSLY REINFORCED CONCRETE PAVEMENTS

NCHRP

Prepared for
National Cooperative Highway Research Program
Transportation Research Board
National Research Council

Submitted by
ARA, Inc., ERES Division
505 West University Avenue
Champaign, Illinois 61820

July 2003

Acknowledgment of Sponsorship

This work was sponsored by the American Association of State Highway and Transportation Officials (AASHTO) in cooperation with the Federal Highway Administration and was conducted in the National Cooperative Highway Research Program which is administered by the Transportation Research Board of the National Research Council.

Acknowledgements

The research team for NCHRP Project 1-37A: Development of the 2002 Guide for the Design of New and Rehabilitated Pavement Structures consisted of Applied Research Associates, Inc., ERES Consultants Division (ARA-ERES) as the prime contractor with Arizona State University (ASU) as the primary subcontractor. Fugro-BRE, Inc., the University of Maryland, and Advanced Asphalt Technologies, LLC served as subcontractors to either ARA-ERES or ASU along with several independent consultants.

Research into the subject area covered in this Appendix was conducted at ARA-ERES. The authors of this appendix were Dr. Olga Selezneva, Dr. Michael Darter and Dr. Chetana Rao. Dr. Dan Zollinger provided the technical approach for mechanistic-empirical modeling of crack spacing and crack load transfer deterioration which leads to punchout development. Dr. Lev Khazanovich developed the neural networks to compute stresses at the critical locations in CRCP. The database used in model calibration and verification was assembled by Mr. Leslie Titus-Glover.

Foreword

This appendix is a supporting reference to the CRCP design guidance presented in PART 3, Chapters 4 and 7 of the Design Guide. Some sections of the referenced chapter are repeated here for emphasis and continuity. Of particular interest are sections on CRCP inputs, CRCP design procedure, performance calibration, sensitivity analysis, and reliability.

APPENDIX LL – PUNCHOUTS IN CONTINUOUSLY REINFORCED CONCRETE PAVEMENTS

INTRODUCTION

Background

Continuously reinforced concrete pavement (CRCP) is constructed with continuous longitudinal steel reinforcement and no intermediate transverse contraction joints. Over a 2 to 4 year period after construction, CRCP develops a transverse cracking pattern with cracks typically spaced 0.6 to 1.8 m (2 to 6 ft) apart. For newly constructed CRCP, transverse cracks are held together tightly by the longitudinal reinforcement. The absence of the transverse contraction joints and a well-defined pattern of transverse cracks are the major attributes that identify CRCP.

Historically, CRCP has shown good performance. However, one structural distress type—typically called an edge punchout, or structural punchout—may develop over time and traffic for this type of pavement (*1-8*). Punchouts develop between two closely spaced transverse cracks as a result of crack load transfer efficiency (LTE) loss and a longitudinal fatigue crack that defines the punchout segment along the pavement edge as shown in figure 1.

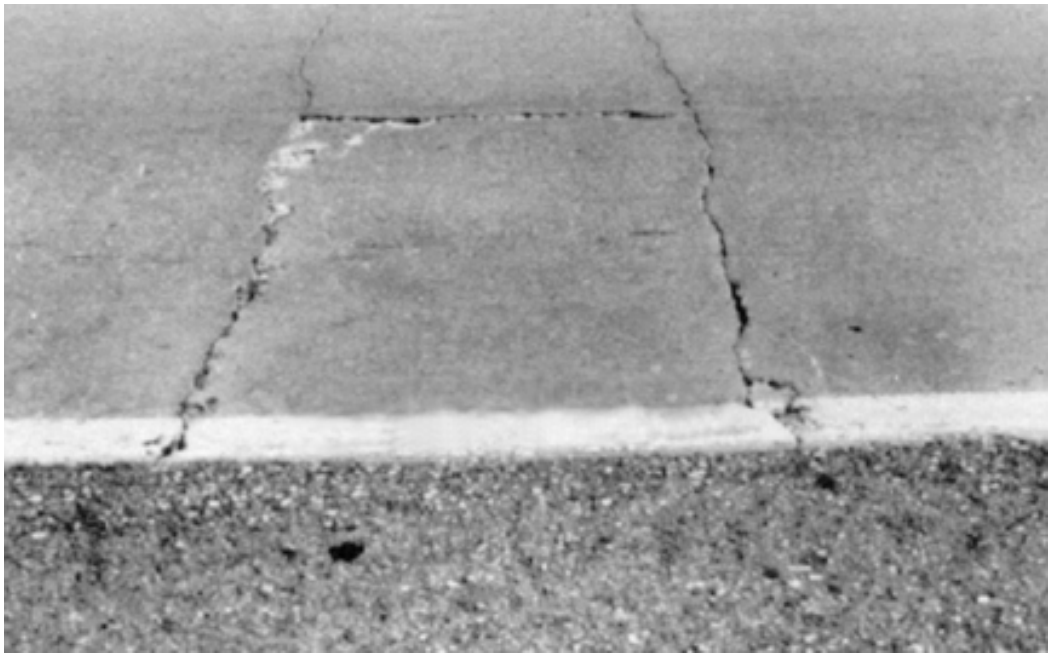

Figure 1. Illustration of a typical CRCP edge punchout.

The isolated piece of concrete settles down into voids created by erosion from traffic loads resulting in the loss of ride quality and eventually requires full depth repair. Controlling the development of punchouts is the focus of the mechanistic-empirical CRCP structural design procedure.

The causes and factors associated with CRCP punchouts have been the topic of many investigations. One of the first studies by LaCourserie and Darter (*1, 2*) in 1977 describes the mechanism of edge punchout based on the field investigations of punchout distress in CRCP in Illinois. This study showed the development of high tensile stress at the top of the slab about 1-2 m from the longitudinal edge of the slab as a result of poor load transfer at the surrounding transverse cracks. Crack spacing has also been shown to significantly affect the magnitude of the critical tensile lateral stresses on the top of the slab. These conclusions were reaffirmed by Selezneva (*3, 4*) in a recent analysis of CRCP distress data for the LTPP sections located in 22 States. About 90 percent of all punchouts observed on LTPP sections were on CRCP segments bound by a pair of transverse cracks spaced at 0.6 m or less.

Zollinger et al. (*5*) reported that punchouts in field studies were invariably accompanied by severe base erosion and loss of support. As was pointed out by Zollinger and Barenberg (*6*), poor support conditions can cause rapid deterioration of crack LTE capacity due to excessive shear stresses induced by high deflection. Environmentally induced upward slab curling and warping, coupled with loss of crack load transfer, also contribute to high tensile stresses at the top of the slab.

Deterioration of load transfer effectively isolates the loaded portion of the slab between the deteriorated transverse cracks from the adjacent pavement. As a result, only a narrow concrete panel bounded by two transverse cracks carries the wheel load. This situation leads to the development of high top tensile stresses. As repetitive heavy truck loading continues, a short longitudinal fatigue crack forms between the two transverse cracks. Any further wheel loads cause the portion of the concrete slab bounded by the transverse cracks to develop a short longitudinal fatigue crack, and the pavement edge to break off and settle into the eroded area resulting in an edge punchout.

The mechanism of punchout development is shown schematically in figure 2. The important stages of pavement deterioration leading to longitudinal cracking are indicated as 1 through 5.

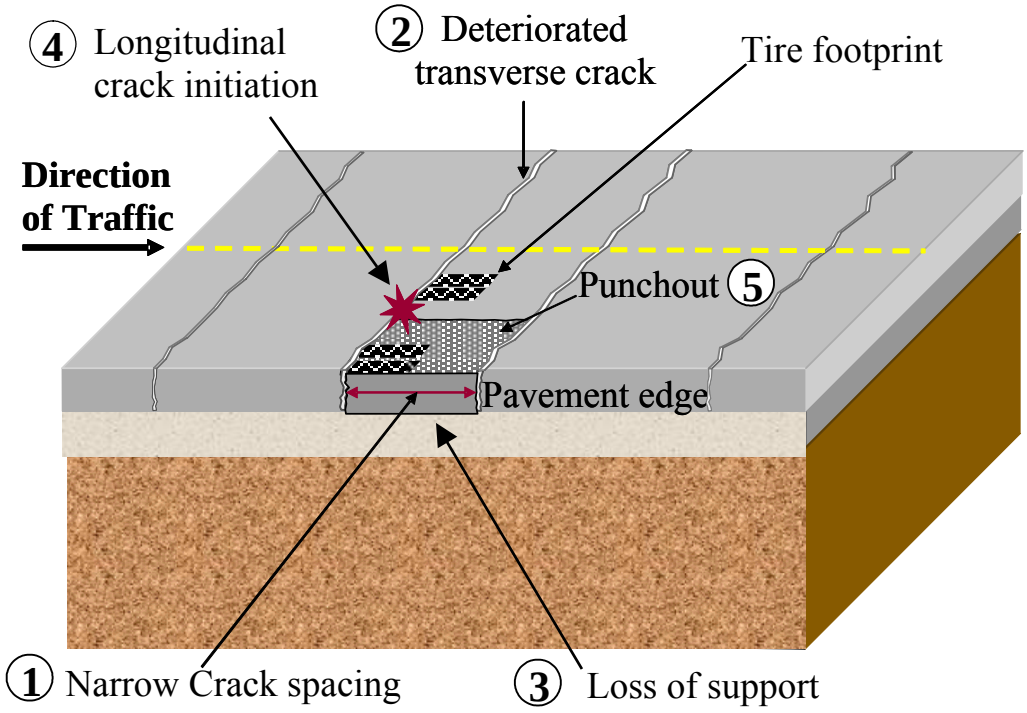

Figure 2. Mechanism of punchout development (*4*).

In summary, for a punchout to develop, several field conditions typically occur:

1. Presence of narrow transverse crack spacing (0.6 m or less) (2 foot or less) in the crack spacing distribution.
2. Loss of load transfer efficiency (LTE) across the transverse cracks due to aggregate interlock deterioration from excessive crack opening and heavy repeated loads.
3. Loss of support along the pavement edge due to base erosion.
4. Negative temperature gradients through the slab thickness and top of slab drying shrinkage further magnify bending stresses.
5. Passages of heavy axles causing repetitive cycles of excessive tensile bending stresses leading to longitudinal fatigue cracking that defines the punchout.

The above considerations were utilized in the development of the mechanistic-empirical punchout prediction model presented in this appendix.

Appendix Organization

This appendix consists of the following sections:

- Overview of Existing CRCP Design Models
- Overview of NCHRP 1-37A CRCP Punchout Model
- Step-by-Step Punchout Prediction Procedure

- Calibration of NCHRP 1-37A CRCP Punchout Model
- Sensitivity Analysis
- Implementation Considerations

OVERVIEW OF EXISTING CRCP DESIGN MODELS

Existing Models

The design of continuously reinforced concrete pavements (CRCP) has traditionally focused on the design of the steel reinforcement relative to the development of the transverse crack pattern. Punchout development was not directly considered in the 1993 AASHTO design guide. Over the years, a variety of tools have been developed for the analysis of CRC pavement systems relative to the prediction of transverse crack spacing, crack width, and steel stress. A brief review of different CRCP analysis and design procedures is presented below.

AASHTO CRCP Design Procedure

The AASHTO design procedure is based on the AASHO Road Test pavement serviceability equation. This procedure is based on the analysis of data collected from the doweled jointed concrete pavement sections. No CRCP sections were included in the road test. Current, 1993, AASHTO design procedure for the CRCP pavements consists of two parts (*9*):

- Longitudinal reinforcement design
- Thickness design

Longitudinal Reinforcement Design

Longitudinal steel is principal reinforcement in the CRCP. Its primary purpose is to control transverse crack spacing that form in the pavement due to concrete volumetric changes. Longitudinal reinforcement is designed to satisfy three limiting criteria: crack spacing, crack width, and allowable steel stress.

Crack spacing recommendations are derived from consideration of spalling and punchouts. To minimize the occurrence of spalling, the maximum spacing between consecutive cracks should be no more than 8 feet. To minimize the potential for the development of punchouts, the minimum desirable crack spacing recommended by AASHTO is 3.5 feet.

Crack width control criterion is based on a consideration of spalling and water penetration. AASHTO recommends that the allowable crack width should not exceed 0.04 inch. To prevent steel fracture and permanent deformation, AASHTO recommends limiting steel stress values to the 75 percentile of the ultimate tensile strength.

Thickness Design

The AASHTO thickness design procedure for CRCP is the same as the thickness design procedure for the jointed pavements. The structural slab thickness design is based upon an

extension of the field performance models developed from the AASHO Road Test. The fundamental approach is based on an empirical relationship between pavement serviceability loss, which is a measure of how well the pavement serves the user, and the magnitude, configuration, and repetition of traffic axle loads.

The original empirical model derived from the road test data was modified and extended using the Spangler corner stress equation. This modification provided means of incorporation of the material properties in the thickness design procedure (*10*). A drainage coefficient (C_d) based on the quality of drainage and on the time that the pavement structure is exposed to moisture levels approaching saturation was also added in 1986 (*11*). A loss of support factor was added to the design model in 1986 to account for the potential loss of support arising from base erosion. The resulting 1993 AASHTO structural design model is given as follows (*11*):

$$Log_{10}W_{18} = Z_R \cdot S_0 + 7.35 \cdot Log_{10}(D+1) - 0.06 + \frac{Log_{10}\left(\frac{\Delta PSI}{4.5-1.5}\right)}{1+\frac{1.624\cdot 10^7}{(D+1)^{8.46}}} + (4.22-0.32p_t) \cdot Log_{10}\left[\frac{S_c' \cdot C_d[D^{0.75}-1.132]}{215.63 \cdot J\left[D^{0.75}-\frac{18.42}{(E_c/k)^{0.25}}\right]}\right] \quad (1)$$

Where:

$W_{18} = W_{18} / F_R = W_{18} / 10^{(-Z_R S_0)}$ = Predicted number of 18-kip single axle load applications (ESAL)
F_R = Reliability design factor
Z_R= Standard normal deviate corresponding to selected level of reliability
S_0 = Overall standard deviation for rigid pavement
D = Slab thickness, inches
P_i = Initial serviceability index
p_t = Terminal serviceability index
S'_c = Flexural strength at 28 days of the PCC for specific project, psi
J = Load transfer coefficient used to adjust for load transfer characteristics across the cracks
C_d = Drainage coefficient
E_c = Modulus of elasticity of the concrete, psi
k = Modulus of subgrade reaction, psi/inch

With respect to the evaluation of traffic, the mixed traffic stream is converted into the number of 18-kip equivalent single axle loads. The load equivalency factors were derived from the AASHO Road Test and are discussed in the following section. The tridem axles were not included in the original Road Test and the factors given are the result of additional research. The Guide provides the capability to consider several design factors, such as load transfer at cracks, subdrainage and shoulder design, but provides inadequate guidance for the required empirical design input values.

The entire procedure is empirical. A Federal Highway Administration (FHWA) study of the CRCP performance published in 1998 (*5*) indicated that the applicability of the AASHTO procedures for thickness design for CRC pavements has never been verified. This equation actually has nothing to do with CRCP performance as it was derived strictly for jointed concrete pavements.

NCHRP 1-15 Design of CRCP for Highways

This design procedure is based on the prediction of transverse crack spacing, crack width, and steel stress to ensure CRCP performance. The design equations are derived from expressions of static equilibrium between the forces due to volumetric change in the concrete and the stiffness restraint developed within the bond between the steel reinforcement and the concrete and along the base interface.

The procedure developed as a result of the NCHRP 1-15 project has been implemented over the years in the series of software releases (latest is CRCP 9) (*12, 13*). Key design features of this procedure are the consideration of the following:

1. Concrete strength (f_c) and modulus of elasticity (E_c) as a function of age.
2. Steel percentages (p) and sizes (d_b) (in a single layer configuration; note: $q = 4p/d_b$)
3. Seasonal concrete temperature (relative to the difference from the concrete setting temperature)
4. Concrete (CTE_c) and steel (CTE_s) coefficient of thermal expansion values
5. Subbase friction value

The procedure also accounts for the effect on crack width and stress level in the concrete and steel due to bond-slip between the reinforcing steel and the concrete relative to the distance from the transverse crack. Punchout prediction is not explicitly stated in this procedure.

The CRCP9 program and others similar to it (*14 – 16*) are useful to develop crack spacing relationships applicable to design in terms of the key features noted above.

CRCP Design Parameters

Reis et al (*17*) provide a set of the closed form equations that could be used to predict key parameters used in the AASHTO and NCHRP 1-15 CRCP design procedures. Both design procedures concentrate on the analysis of the parameters affecting steel reinforcement design rather that analysis of CRCP structure to minimize structural distress in a form of a punchout.

Crack Width Prediction

Reis et al (*17*) suggested closed-form algorithms to represent the effect of bond slip on the average crack width ($\overline{cw}$) through the pavement section:

$$cw = L\left\{ z + \Delta t\alpha_c - \frac{c_2 f_t}{E_c} \right\} = \frac{c_1 d_b f_t}{U_m p}\left\{ z + \alpha\Delta t - \frac{c_2 f_t}{E_c} \right\} \quad (2)$$

Where

$\overline{L}$ = Average crack spacing (L)

$\overline{z}$ = Average unrestrained concrete drying shrinkage (LL^{-1})

$\overline{\Delta t}$ = Average difference between concrete temperature and the setting temperature (°F)

α_c = Concrete Coefficient of Thermal Expansion (CTE) $(°F)^{-1}$

c_1 = Bond slip coefficient

c_2 = Bond-slip coefficient

f_t = Maximum tensile stress in the concrete (FL^{-2})

E_c = Concrete modulus of elasticity (FL^{-2})

Crack width is averaged to represent the variation through the full section of the pavement. Crack width is the primary factor affecting the degree of load transfer and stiffness that can be provided across a transverse crack. As indicated in equation (2), the width of the transfer cracks is expected to vary as the average temperature of the concrete varies which implies that load transfer will vary according to daily and seasonal temperature conditions.

Steel Stress Prediction

Reis et al (*17*) provides the following expression to determine the stress in the steel (f_s) for the average crack spacing ($\overline{L}$):

$$f_s = 2nf_t - E_s\left\{\Delta t\left(\alpha_c - \alpha_s\right) + \left(z - \varepsilon_{crp}\right)\right\} + \frac{U_m \overline{L}}{d_b c_1} \quad (3)$$

Where

n = Modular ratio = $\frac{E_s}{E_c}$

E_s = Steel modulus of elasticity (FL^{-2})

Z = Unrestrained concrete drying shrinkage at the steel position located depth ζ below the pavement surface (LL^{-1})

ε_∞ = Ultimate shrinkage

rh_{PCC} = Percent relative humidity divided by 100 at depth ζ below the pavement surface

Δt = Difference in pavement temperature at the steel level from the concrete setting temperature (°F)

$$\Delta t = T_{set} - T(\zeta) \quad (4)$$

$$T_{set} = 0.95(T_{conc} + \Delta T) \quad (5)$$

T_{conc} = Temperature of fresh concrete at the time of construction (°F)

ΔT = Change in concrete temperature due to the heat of hydration (°F)

$$\Delta T = \frac{H_u C \alpha}{c_p \rho} \tag{6}$$

H_u = Heat of hydration per unit weight (W)

$$H_u = -0.0787 + 0.007(T_{conc}) - 3x10^{-5}(T^2_{conc}) \tag{7}$$

C = Amount of cement per unit volume (F)
α = Degree of hydration
c_p = Specific heat of cement ($Wmass^{-1}(°F/C)^{-1}$) = 1.1 $\frac{KJ}{kg°C}$

ρ = Density of concrete (FL^{-3})
T(ζ) = Temperature of the concrete at depth ζ below the pavement surface (°F/C)

$$T(\zeta) = T_{surf} - R_o e^{-\zeta\sqrt{\frac{\Pi}{h^2\gamma}}} \tag{8}$$

T_{surf} = Temperature of the concrete surface (°F/C)
R_o = Range in surface temperature over time period γ (°F/C)
h^2 = Concrete thermal diffusivity (L^2t^{-1})
α_c = Steel CTE $(°F/C)^{-1}$
ε_{crp} = Concrete creep strain (LL^{-1})
U_m = Peak bond stress (FL^{-2})

$$U_m = \frac{0.24 k_1 E_c \varepsilon_{tot}}{1 + 3\frac{g_a}{g_b}} \tag{9}$$

d_b = Reinforcing steel bar diameter (L)
c_1 = Bond-slip coefficient
k_1 = Bond coefficient
g_a = d_b
g_b = Reinforcing steel spacing (L)

Equation (2.11) is determined based on concrete shrinkage and temperature changes occurring at the level of the steel located a given distance below the surface of the pavement. In this manner, the effect of steel cover can be considered on the design steel stresses. The closer the steel is positioned to the pavement surface, the greater will be the stress in the steel. The coefficient c_1 takes into account the effect of bond-slip. The value of k_1 depends upon the deformation pattern of the steel reinforcement and has been reported (*17*) to be as low as 1.6.

Concrete Stress Prediction

Reis et al (*17*) also suggested an equation form for the longitudinal stress in the concrete pavement (at the depth of the steel) that is also a function of the bond-slip characteristics of the reinforcing steel. A modification to this form, based on work of Westergaard (*21*) and Bradbury

(*22*) will also allow consideration of stresses due to curling and warping as it may contribute to the stress level resulting in transverse crack development of a single layer of steel:

$$f_\sigma = \bar{L}\frac{f}{4} + \frac{\bar{L}U_m p}{c_1 d_b} + C\sigma_0\left(1 - \frac{2\zeta_1}{H}\right) \tag{10}$$

Where

$\bar{L}$ = Mean crack spacing
f = friction
U_m = Peak bond stress (FL^{-2})
p = Area of steel reinforcement (A_s) per area of concrete (A_c) in percent
= A_s/A_c
d_b = Reinforcing steel bar diameter (L)
c_1 = Bond-slip coefficient
C = Curling/warping stress coefficient (*22*)

$$\sigma_0 = \frac{E_c \Delta\varepsilon_{tot}}{2(1-\nu_c)} \tag{11}$$

ν_c = Concrete Poisson ratio
$\Delta\varepsilon_{tot}$ = Unrestrained curling and warping strain

$$\Delta\varepsilon_{tot} = \alpha_{PCC}\Delta t_{eqv\ m} + \varepsilon_\infty \Delta(1 - rh_{PCC}{}^3)_{eqv} \tag{12}$$

H = Slab thickness
ζ_1 = Depth to steel
Δt_{eqv} = equivalent temperature difference between the pavement surface and bottom (Mohamed and Hansen (*23*))
$\Delta(1\text{-}h_{PCC}{}^3)_{eqv}$ = equivalent relative humidity difference between the pavement surface and bottom (Mohamed and Hansen (*23*))

Mean Crack Spacing

The following expression can be used to predict the mean crack spacing (*17*):

$$\bar{L} = \frac{\left\{f_t - C\sigma_0\left(1 - \frac{2\zeta}{H}\right)\right\}}{\frac{f}{2} + \frac{U_m p}{c_1 d_b}} \tag{13}$$

Where

$\bar{L}$ = Mean crack spacing
f_t = tensile strength of the concrete
f = friction
U_m = Peak bond stress (FL^{-2})
p = Area of steel reinforcement (A_s) per area of concrete (A_c) in percent
= A_s/A_c

d_b = Reinforcing steel bar diameter (L)
c_1 = Bond-slip coefficient
C = Curling/warping stress coefficient (*22*)
σ_0 = from equation 18
p = Area of steel reinforcement (A_s) per area of concrete (A_c) in percent
= A_s/A_c
ν_c = Concrete Poisson ratio
$\Delta\varepsilon_{tot}$ = Unrestrained curling and warping strain
ν_c = Concrete Poisson ratio
$\Delta\varepsilon_{tot}$ = Unrestrained curling and warping strain from equation 19
H = Slab thickness
ζ = Depth to steel
Δt_{eqv} = equivalent temperature difference between the pavement surface and bottom (Mohamed and Hansen (*23*))
$\Delta(1\text{-}h_{PCC}^3)_{eqv}$ = equivalent relative humidity difference between the pavement surface and bottom (Mohamed and Hansen (*23*)).

CRCP Punchout Prediction

CRCP performance studies have resulted in the development of empirical models that predict CRCP punchouts. These models are based on field data collected in Illinois and describe punchouts as a function of pavement design features, construction techniques and traffic loadings expressed as ESALs. The following model predicts the development of localized CRCP failures (based on extensive field data from over 400 projects) as a function of pavement design features, construction techniques and traffic loadings (*24*):

$$\log_e(FAIL) = 6.8004 - 0.0334 * HPCC^2 - 6.5858 * PSTEEL$$

$$+ 1.2875 * \log_e(CESAL) - 1.1408 * BAM - 0.9367 * CAM \qquad (14)$$

$$- 0.8908 * GRAN - 0.1258 * CHAIRS$$

Where

FAIL	=	localized failures (punchouts) in the outer lane, failures/mile.
HPCC	=	CRCP slab thickness, in.
PSTEEL	=	longitudinal reinforcement, %.
CESAL	=	cumulative ESALs, millions.
BAM	=	1 if subbase material is bituminous-aggregate mixture, 0 otherwise.
CAM	=	1 if subbase material is cement-aggregate mixture, 0 otherwise.
GRAN	=	1 if subbase material is granular, 0 otherwise.
CHAIRS	=	1 if chairs used for reinforcement placement, 0 if tubes used.

Based on this model, an increase in ESALs corresponds to increase in localized failures, implying that increased load magnitude and/or frequency contribute to higher incidence of

punchouts. Similarly, structural improvements (e.g., increased slab thickness, greater amounts of reinforcing, stabilized foundation materials) are associated with fewer localized failures. An example of a sensitivity plot from this model is given in Figure 3.

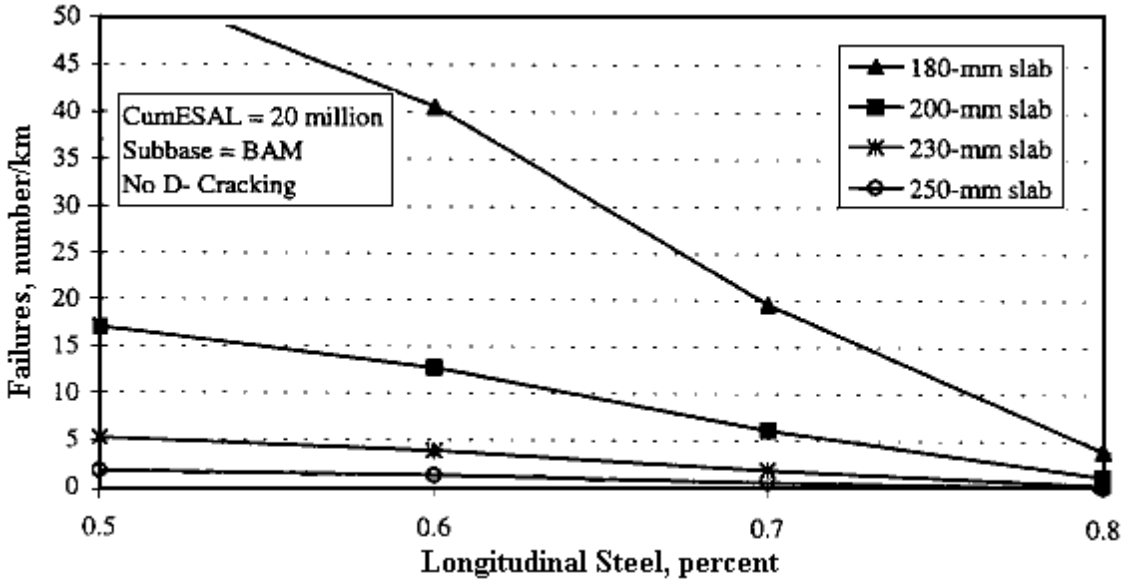

Figure 3. Effect of steel reinforcement content and slab thickness on CRCP punchout (failures/km). (*24*).

Limited research investigations on the subject of the mechanistic punchout prediction were found in the literature. This subject was previously investigated by Barenberg and Zollinger (*6*) in application to Illinois mechanistic design procedure for PCC pavements and then by Zollinger et al (*5*) in a recent 6-year CRCP performance study sponsored by the FHWA. However, no calibrated mechanistic model for punchout prediction was developed.

The results of the FHWA 6-year CRCP performance study did strengthen the importance of punchout consideration in the CRCP design. The investigators outlined the CRCP thickness design principles that take into account punchout development. These principles were considered in the development of the methodology for mechanistic-empirical CRCP damage assessment presented in this study.

Evaluation Summary

The results of the literature review indicate that there is no CRCP design procedure that takes into account minimization of the punchout development as a design criterion. Specific limitations of the existing design procedures for the CRCP pavements are the following:

- 1993 AASHTO design procedure is based on satisfaction of a certain serviceability level rather than on a prediction of particular structural distress.
- Punchouts are not considered as a direct design criterion in the 1993 AASHTO CRCP design procedure. The procedure indirectly implies that limiting minimum desirable

crack spacing to 3.5 feet would minimize the potential for punchout development. Although crack spacing is an important factor, no other design factors that may have an affect on the development of the excessive tensile stresses (leading to the punchout in the CRCP) are accounted for.

- The procedure assumes that CRCP critical structural responses are not different form those predicted for the jointed pavements. However, CRCP critical tensile stresses are totally different from the stresses in the jointed PCC pavements due to differences in the structural behavior between jointed slabs and a continuous PCC slab traversed by unequally-spaced transverse cracks with different degrees of load transfer.
- The existing design procedures were developed using ESAL approach for traffic characterization. No consideration of the effect of many different traffic characteristics on the pavement responses was included (e.g., tandem axle effect, lateral location).
- The results of the FHWA 6-year CRCP performance study strengthened the importance of punchout consideration in the CRCP design. Zollinger et al outlined the CRCP thickness design principles that take into account punchout development. These principles were considered in the development of the CRCP design methodology in this Guide.

OVERVIEW OF THE NCHRP 1-37A PUNCHOUT PREDICTION MODEL

Approach

The method for predicting CRCP performance is based on the process associated with the incremental development of punchout distress. Development of punchout distress is directly related to the formation of a longitudinal crack between two adjacent transverse cracks. This crack initiates at the top of the slab and propagates downward through the CRCP. The development of the longitudinal crack is in turn related to the accumulated fatigue damage caused by a slab bending in the transverse direction. Therefore, the prediction of punchout distress can be considered in the design process in terms of the accumulated fatigue damage associated with the formation of specific longitudinal cracks between two closely spaced transverse cracks (*2-7*).

CRCP punchouts are the result of a combination of:

- Repeated heavy axle loads.
- Loss of LTE across two closely spaced transverse cracks (crack width is primary factor).
- Inadequate PCC slab thickness.
- Free moisture beneath the CRCP.
- Erosion of the supporting base or subgrade material along edge of CRCP.
- Negative slab curling and moisture warping (drying shrinkage).

Crack width is a primary factor in the loss of load transfer across transverse cracks. This can occur due to cold temperatures and continuing shrinkage of the PCC slab over time. Wider cracks have less aggregate interlock and thus with repeated loading tend to deteriorate.

Loss of support along CRCP longitudinal joints has been identified as a key factor in the development of punchout distress (*3, 6*). It plays a prominent role, since it directly affects top-of-slab tensile stress and crack shear stress on the faces of transverse cracks where aggregate interlock occurs to transfer load between adjacent slab segments. An increase in shear stress increases the rate of aggregate wear-out that ultimately leads to lower LTE and increased lateral bending stress. However, as long as support conditions can be maintained and wear-out of aggregate interlock minimized, bending stresses in CRCP will be relatively small—which results, for all practical purposes, in long fatigue lives. For this reason, it is critical to maintain high load transfer across the cracks (narrow crack width) and full support conditions beneath the CRCP slab.

Erosion potential is greatest where upward curling and warping along the edge and corner areas pump trapped water back and forth along the slab/base interface under applied wheel loads. When combined with the relatively viscous nature of water, this pumping action creates a shearing stress that erodes the base material. Representation of erosion performance in the design of CRCP focuses on the use of material models and equation forms suggested in past research (*25, 26*). Erosion of the base along the CRCP slab edge has been approximately related to material erodibility potential, precipitation, and presence of a granular layer beneath a stabilized base.

Structural modeling of CRCP systems, from a design standpoint, focuses on four areas: (1) crack pattern development due to climatic stresses, (2) deterioration of LTE across the cracks (crack width), (3) the development of the loss of support along the longitudinal joint or slab edge, and (4) top of slab PCC fatigue cracking due to repeated applied wheel load configurations.

Critical truck axle loading includes a single, tandem, or tridem axle located as close as possible to the corner formed by transverse crack and slab edge possible, as shown in Figure 2. The magnitude of the stresses induced at the top surface of the CRCP is greater at nighttime when CRCP panels are curled upward. Loss of LTE across transverse cracks due to temperature movements and crack deterioration, accelerated by base erosion, also significantly increase critical tensile stresses.

Neural networks developed using a finite element structural model (*27*) were used to compute critical top tensile stresses for combination of various design parameters, crack spacings, crack LTE, wheel loads, and climatic conditions. LTE across the transverse cracks and the longitudinal joint between the traffic lanes are modeled directly. The effects of different shoulder types are modeled indirectly by increasing LTE of transverse cracks.

Design Inputs

The following factors affect the magnitude of bending stresses at the top surface of the PCC slab leading to punchout development:

- PCC thickness.
- PCC modulus of elasticity.
- PCC Poisson's ratio.
- PCC unit weight.

- PCC coefficient of thermal expansion.
- Base thickness.
- Base modulus of elasticity.
- Crack spacing.
- Subgrade stiffness (k value backcalculated from layer resilient moduli).
- Loss of support beneath the slab.
- Transverse crack LTE.
- Difference in top and bottom PCC slab surface temperature.
- Axle type (single, tandem, tridem, quad).
- Axle weight.
- Axle position (distance from the critical slab edge) – varied between 0 and 18 in from the longitudinal edge.

Calculation Procedure

The design of CRCP involves selecting design features that ensure the pavement will meet all performance criteria at an acceptable level of reliability. The method for predicting CRCP performance is based on the process associated with the development of punchout distress. Development of punchout distress is directly related to the formation of a longitudinal fatigue crack between two adjacent closely spaced transverse cracks. This crack initiates at about 3 to 5 feet from pavement edge at the top of the slab and propagates downward through the CRCP. The development of the longitudinal crack is in turn related to the accumulated fatigue damage caused by a slab bending in the transverse direction. Therefore, the prediction of punchout distress in the design process is considered in terms of the accumulated fatigue damage associated with the formation of longitudinal cracks (*2-7*) based on a sequence of events related to crack width, loss of load transfer, and foundation support changes.

Flowchart of the CRCP design procedure implemented in the 2002 Design Guide is provided in Figure 4.

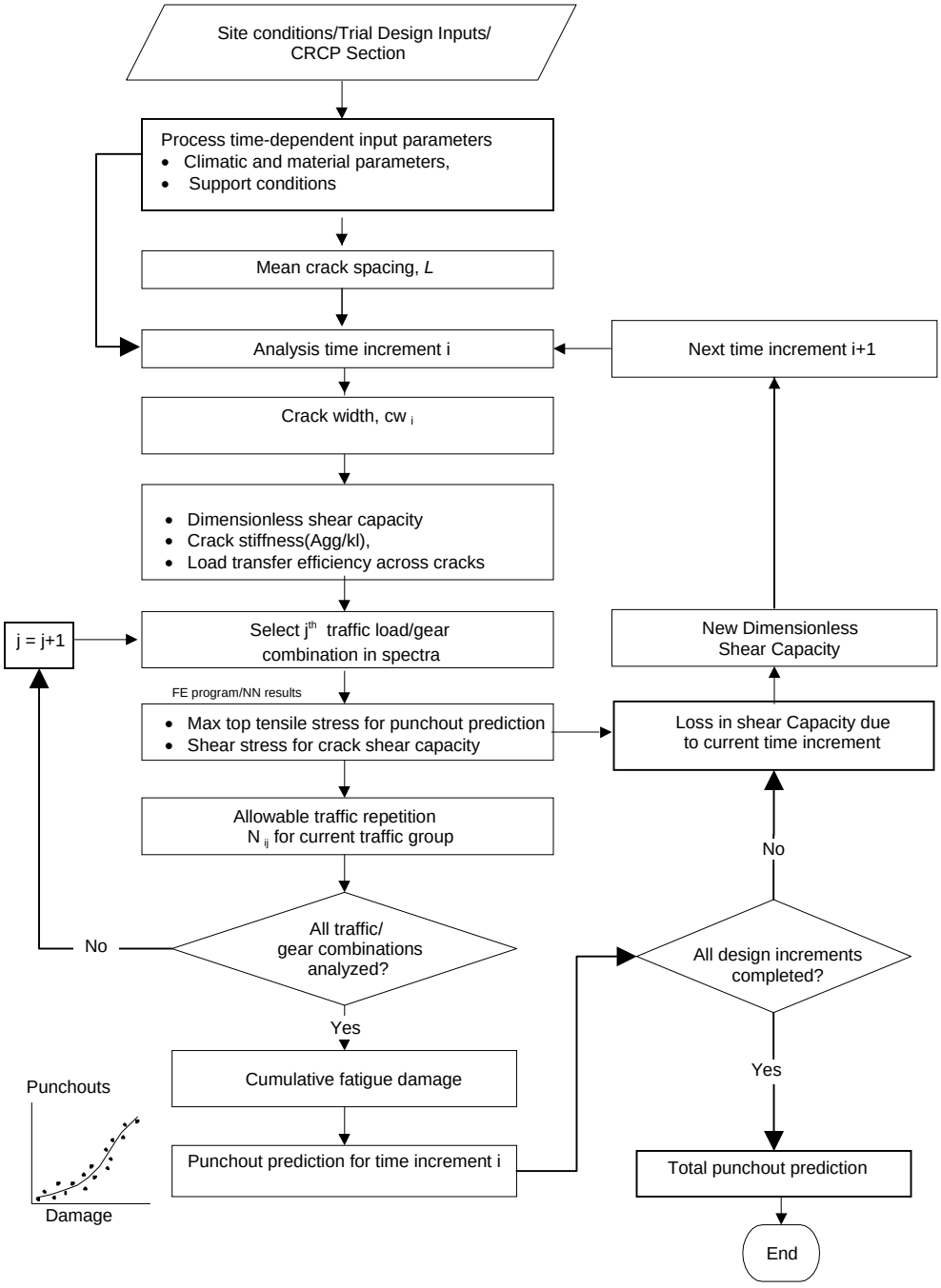

Figure 4. Punchout prediction algorithm for CRCP.

STEP-BY-STEP CRCP PUNCHOUT PREDICTION PROCEDURE

This section describes a detailed step-by-step procedure used to predict CRCP structural performance. The description of the computation steps is grouped in seven modules:

- Module 1: Process time-dependent input parameters.
- Module 2: Determine mean crack spacing.
- Module 3: Determine mean crack width for each design increment.
- Module 4: Determine load transfer efficiency for each design increment.
- Module 5: Determine traffic parameters for damage and shear loss computation.
- Module 6: Determine damage for each design increment.
- Module 7: Determine number of punchouts per mile at the end of each design increment.

A detailed list of input parameters is presented below followed by computational procedures.

DETAILED DESIGN INPUTS

Parameter	Symbol	Units
PCC 28 day compressive strength	f'_{c28}	psi
PCC elastic modulus	$E_{PCC\ i}$	psi
PCC 28 day tensile strength	$f_{t\ i}$	psi
PCC Modulus of Rupture	MR_i	psi
PCC slab thickness	h_{PCC}	inch
PCC Unit weight	γ_{PCC}	lbf/in3
PCC Water/cement ratio	w/c	fraction
PCC coefficient of thermal expansion	α_{PCC}	1/°F
PCC Poisson's ratio	μ_{PCC}	unit less
Ultimate shrinkage	ε_∞	unit less
Depth to steel	ζ	inch
Percent steel as fraction	P_b	fraction
Steel bar diameter	d_b	inch
Mean crack spacing	$\overline{L}$	inch
Shoulder joint stiffness	Js	unit less
LTE of base (alone)	LTE_{Base}	%
Base/Subbase Erodibility index	EROD	unit less
Base thickness	h_{Base}	inch
Base elastic modulus	$E_{Base\ i}$	psi
Slab/Base friction coefficient	f	unit less
Percent subgrade passing the No. 200 sieve	P_{200}	%
Mean annual precipitation	PRECIP	inch/year
Raw annual axle load spectra for design lane (base year)	n_j	unit less
Annual truck growth factor	GF_y	unit less
Monthly truck adjustment coefficients	MF_m	unit less
Hourly temperature adjustment coefficients	HF_h	unit less
Mean truck wheelpath	μ_{wp}	inch
Wheelpath lateral standard deviation	σ_{wp}	inch
PCC temperature at set time	T_{set}	°F
Built-in temperature differential	DT_{built}	°F
Average annual ambient relative humidity	Rha_{annual}	%
Average monthly ambient relative humidity	$Rha_{monthly}$	%
Average monthly ambient temperature values	Ta_m	°F
Average nightly monthly temperature at steel depth	$T_{steel\ m}$	°F
Night-time temperature differential	$DT_{night\ mh}$	°F
Axle load level for single and tandem axles	P_j	lb
Subgrade k-value	k_i	pci
Drying time (days from placement)	t_i	days

MODULE 1: PROCESS TIME-DEPENDENT INPUT PARAMATERS

Definitions:

Month *m* – used in reference to the variables that change cyclically during the year (12 monthly values).

Monthly increment *i* – used in reference to the variables that change continuously during design life and predicted for each monthly analysis increment.

Step 1. Determine PCC Modulus of Elasticity $E_{PCC\ i}$, MR_i, $f_{t\ i}$, $f_c'_i$ for Each Monthly Time Increment *i* Based on Level of User Inputs

Call the materials module to get E_i, MR_i, f_t, f_c' for each month throughout the design period.

NOTE: CRCP design procedure accepts the following ranges of PCC material inputs. If any of the user inputs are outside this range, prompt the user to adjust inputs.

PCC Material Characteristic	Variable	Input Range (all ages)
PCC elastic modulus, 28 days	E_{PCC}	1,000,000 to 7,000,000 psi
Modulus of Rupture, 28 days	MR	300 to 1000 psi
Tensile Strength, 28 days	f_t	200 to 1000 psi

Step 2. Determine PCC Relative Humidity for each Month.

Relative humidity in the PCC (rh_{PCC}) is a function of time, ambient humidity, and depth below the pavement surface.

General formula:

$$rh_{PCC} = rh_a + (100\text{-}rh_a)f(t) \quad (15)$$

Incremental formula:

$$rh_{PCC\ i} = 0.5(rh_{PCC\ annual} + rh_{PCC\ monthly}) \quad (16)$$

Where

$rh_{PCC\ i}$ = relative humidity in the concrete at steel depth for each month *i*.

rh_a = average ambient relative humidity annual ($rh_{a\ annual}$) or monthly ($rh_{a\ monthly}$), %

$$f(t) = 1/(1+ t/b) \quad (17)$$

t = drying time, days

$$b = 35*(25.4*\zeta)^{1.35}(w/c\text{-}0.19)/4 \quad (18)$$

ζ = depth to steel, inches

w/c = water/cement ratio

Step 3. Determine PCC Drying Shrinkage for each Month.

Drying shrinkage is a primary contributor to early crack initiation in CRCP. The amount of drying shrinkage that takes place depends greatly on the amount of evaporation, the quality of curing, and the water/cement ratio used to place the concrete pavement.

$$\varepsilon_{shr\,i} = \varepsilon_{\infty}\,(1 - rh^{3}{}_{PCC})\zeta \tag{19}$$

$\varepsilon_{shr\,I}$ = Unrestrained concrete drying shrinkage at the steel depth (ζ for month *i*, microstrains).

NOTE: this value needs to be divided by 10^6 to convert to actual "strain".

ε_{∞} = PCC ultimate shrinkage.

Step 4. Calculate Bond Slip Coefficient k_1 based on 28 days PCC compressive strength

Bond slip coefficient k_1 represents the slope of the bond slip versus the bond stress – it is a function of the compressive strength.

$$k_1 = 0.1172 * f'_{c28} * 1000 \tag{20}$$

k_1 = Bond slip coefficient
$f'_{c\,28}$ = 28 day PCC compressive strength, psi

Step 5. Calculate Peak Bond Stress based on 28 day PCC compressive strength

$$U_m = 0.0020k_1 \tag{21}$$

U_m = Peak Bond Stress, psi
k_1 = Bond slip coefficient.

Step 6. Calculate Drop in Temperature at the Depth of the Steel for Each Cyclic Month m

$$\text{IF } T_{steel\,m} > T_{\text{set}},\ \Delta T_{\zeta\,m} = 0$$
$$\text{ELSE } \Delta T_{\zeta m} = T_{set} - T_{steel\,m} \tag{22}$$

Where
$\Delta T_{\zeta\,m}$ = Drop in PCC temperature at the depth of the steel for month *m*, °F.
T_{set} = PCC temperature at set time at the depth of the steel, °F.
$T_{steel\,m}$ = Average seasonal temperature at the depth of the steel for month *m*, °F.

Step 7. Determine Base Modulus of Elasticity $E_{base\,i}$ for Each Month m

Call base properties module.

Step 8. Determine Subgrade k-value for Each Month m

$$k_m = f(E_{\text{subgrade m}}, \text{environment per season } m), \text{ psi/in.}$$

Call E-to-K backcalculation module.

Step 7. Determine Radius of Relative Stiffness for Each Monthly Time Increment i

$$\ell_i = [(E_{PCC\,i} * h_{PCC}^3)/(12*(1-\mu_{PCC}^2)*k_m)]^{1/4} \quad (23)$$

ℓ_i = radius of relative stiffness based on the 'simple' slab thickness for monthly increment *i*, inches
$E_{PCC\,i}$ = Elastic modulus of PCC for monthly increment *i* from Step 1 Part 2, psi
h_{PCC} = Slab thickness, in.
μ_{PCC} = Poisson's ratio for PCC.
k_m = Modulus of subgrade reaction (k-value) for season *m* from Step 3 Part 2, pci.

Step 8. Estimate Base Erodobility for Each Annual Increment i

IF $i = 1$
$VOID_i = 0$
ELSE IF $i/12$ = Integer
$VOID_i = VOID_{i-1} + RE_i$
ELSE
$VOID_i = VOID_{i-1}$

Where

$$RE_i = (-0.37 + 0.0171P_{200} + 0.0779EROD + 0.0117PRECIP)/12 \quad (24)$$
(if E < 0, set e = 0)

RE_i = monthly rate of base erosion from the slab edge, in/month
P_{200} = percent subgrade passing the no. 200 sieve
PRECIP = mean annual precipitation, inch
EROD = erodibility index from Table 1

Table 1. Recommendations for erosion potential of base/subbase material.

EROD	Material Description*
1	Lean concrete with 8 percent cement; asphalt concrete with 6 percent asphalt cement, or a permeable drainage layer.
2	Cement treated granular material with 5 percent cement manufactured in plant; asphalt treated granular material with 4 percent asphalt cement.
3	Cement-treated granular material with 3.5 percent cement manufactured in plant; asphalt treated granular material with 3 percent asphalt cement.
4	Granular material treated in place with 2.5 percent cement, treated soils.
5	Untreated granular material.

* Modified from original PIARC recommendations.

MODULE 2: DETERMINE MEAN CRACK SPACING

Assumptions used for determination of mean crack spacing:

Knowledge of mean crack spacing is required for the determination of crack opening and for prediction of the critical tensile stresses for fatigue accumulation prediction. Crack spacing may be determined using several methods based on the construction method. External software like CRCP8 or the procedure presented herein can be used. Mean crack spacing is predicted for the final constant transverse crack spacing pattern using time dependent parameters listed in Table 2.

Table 2. Time-Dependent Parameters Used in Computation of mean crack spacing $\overline{L}$.

Time-Dependent Parameter	Time
PCC compressive strength	28 day
PCC elastic modulus	28 day
PCC tensile strength	28 day
PCC relative humidity at steel depth	After 1 year
Ambient relative humidity	Average annual
Ambient temperature	Minimum in any given year
Drop in PCC temperature at the steel depth	Maximum in any given year
Subgrade k-value	Average annual
Base Elastic modulus	Average annual

Step 1. Determine Mean Crack Spacing.
To predict the mean crack spacing, the following is used:

$$\overline{L} = \frac{\left\{ f_{t28} - C\sigma_0 \left(1 - \frac{2\zeta}{h_{PCC}} \right) \right\}}{\frac{f}{2} + \frac{U_m P_b}{c_1 \, d_b} + LC} \tag{25}$$

where,

$\overline{L}$ = mean crack spacing, in

f_{t28} = concrete tensile strength at 28 days, psi

C = Bradbury's curling/warping stress coefficient

σ_0 = Westergaard's nominal stress factor

$$\sigma_0 = \frac{E_{PCC28}\varepsilon_{tot-\Delta max}}{2(1-\mu_{PCC})} \quad (26)$$

E_{PCC28} = Concrete modulus of elasticity at 28 days, psi

μ_{PCC} = Poisson's ratio

$\varepsilon_{tot-\Delta\,max}$ = Maximum equivalent total strain between the pavement surface and slab bottom.

$$\varepsilon_{tot-\Delta} = \alpha_{PCC}\Delta t_{eqv\,m} + \varepsilon_{\infty}\Delta(1 - rh_{PCC}^{3})_{eqv} \quad (27)$$

α_{PCC} = PCC coefficient of thermal expansion, $1/^{o}F$

$$\Delta t_{eqv} = \frac{R_{o\,m}}{2CF}\left(1 - e^{-\frac{h_{PCC}}{12}\sqrt{\frac{2\pi}{\gamma^2}}}\right) \quad (28)$$

Δt_{eqv} = Equivalent temperature Δt_{eqv} determined as:

$R_{o\,m}$ = Effective range obtained using minimum seasonal temperature from the Table 3

Table 3. Effective Temperature Ranges.

Minimum monthly ambient temperature, F	**Effective Range in Temperature (R_o)**
Less than 40	21.5
40 to 60	23.4
60 to 80	25.7
More than 80	30.1

$$CF = 1.000 - 0.565h_{pcc} + 0.116\,h_{pcc} * h_{pcc}^{1/2} + 0.685 * h_{pcc}^{1/2} \quad (29)$$

γ = Concrete thermal diffusivity (ft^2 per day), as defined in ACI 207, depends upon the coarse aggregate type used in the concrete from Table 4.

Table 4. Concrete Thermal Diffusivity.

Coarse Aggregate Type	Concrete Thermal Diffusivity of (ft^2/day)
Quartzite	1.39
Limestone	1.22
Dolomite	1.2
Granite	1.03
Rhyolite	0.84
Basalt	0.77
Syenite	1.00
Gabbro	1.0
Chert	1.39

$\Delta(1\text{-}rh_{PCC}^3)_{eqv}$ = equivalent relative humidity coefficient (difference between the pavement surface and bottom) from Table 5.

Table 5. Coefficients of equivalent relative humidity.

Climatic zone and minimum ambient humidity range	**CF**	**$\Delta(1 - rh^3)_{eqv}$**
DNF, 10 to 50%	0.5	= CF*($0.0008h_{pcc}^2$ - $0.0327h_{pcc}$ + 0.3754)
WF, WNF 50 to 95%	0.2	= CF*($0.0028h_{pcc}^2$ - $0.107h_{pcc}$ + 1.4292
DF 0 to 95%	N/A	= Average of case 1 and 2 above

ζ = depth to steel layer, inch
h_{PCC} = slab thickness, inch
f = base friction coefficient from Table 6 based on base type

Table 6. Slab/Base friction coefficients to produce proper CRCP crack spacing.

Subbase/Base type	**Friction Coefficient (low – mean – high)**
Fine grained soil	0.5 – 1.1 – 2
Sand**	0.5 – 0.8 – 1
Aggregate	0.5 – 2.5 – 4.0
Lime-stabilized clay**	3 – 4.1 - 5.3
ATB	2.5 – 7.5 – 15
CTB	3.5 - 8.9 - 13
Soil cement	6.0 - 7.9* - 23
LCB	1.0 – 6.6* - 20
LCB not cured**	> 36 (higher than LCB cured)

* Trimmed mean from values used in the calibration.
** Base type did not exist or not considered in calibration sections.

U_m = peak bond stress, psi
P_b = percent steel, fraction equal to area of steel reinforcement (A_s) per area of concrete (A_c) in percent,

$$P_b = A_s/A_c \tag{30}$$

d_b = reinforcing steel bar diameter, in
c_1 = first bond stress coefficient computed iteratively based on seed crack spacing L_{seed}.

$c_1 = c_{1\ seed}$ IF $\bar{L} - L_{seed} < 0.01$

$$c_{1\ seed} = 0.577 - 9.499\text{e-}09 \frac{\ln \varepsilon_{tot-\varsigma max}}{\left(\varepsilon_{tot-\varsigma max}\right)^2} + 0.00502 L_{seed} * (\ln L_{seed}) \tag{31}$$

$\varepsilon_{tot-\varsigma max}$= Total maximum strain at the depth of the steel expressed in "strains"

$$\varepsilon_{tot-\varsigma max} = \Delta T_{\varsigma max} \alpha_{PCC} + \varepsilon_{shr} \tag{32}$$

$\Delta T_{\zeta max}$ = Maximum PCC temperature difference from T_{set} temperature at the steel depth, ^oF.
ε_{shr} = Unrestrained concrete drying shrinkage at the steel depth (ζ), "strains"

MODULE 3: DETERMINE MEAN CRACK WIDTH FOR EACH DESIGN INCREMENT

Step 1. Calculate Total Strain in PCC at the Steel Depth for Each Monthly Increment i

$$\varepsilon_{tot-\varsigma i} = \Delta T_{\varsigma m} \alpha_{PCC} + \varepsilon_{shr\,i} \tag{33}$$

$\varepsilon_{tot\text{-}\zeta i}$ = Total strain at the depth of the steel for monthly increment *i* expressed in strains
$\Delta T_{\zeta m}$ = Drop in PCC temperature from steel depth $T_{zero\text{-}stress}$ temperature for each month *m*.
α_{PCC} = PCC coefficient of thermal expansion, $1/^oF$
$\varepsilon_{shr\,i}$ = Unrestrained concrete drying shrinkage at the steel depth (ζ) for monthly increment *i*, microstrains. NOTE: this value needs to be divided by 10^6 to convert to "strains".

Step 2. Calculate First Bond Slip Coefficient for Each Monthly Increment i

$$c_{1\,i} = 0.577 - 9.499\text{e-}09 \frac{\ln \varepsilon_{tot-\varsigma i}}{\left(\varepsilon_{tot-\varsigma i}\right)^2} + 0.00502 \bar{L} * (\ln \bar{L}) \tag{34}$$

$c_{1\,i}$ = First bond stress coefficient for monthly increment *i*
$\bar{L}$ = Mean crack spacing, in
$\varepsilon_{tot-\varsigma i}$ = Total strain at the depth of the steel for monthly increment *i* expressed in strains

Step 3. Calculate Second Bond Slip Coefficient for Each Monthly Increment i

$$c_{2\,i} = a_i + \frac{b_i}{k_1} + \frac{c_i}{L^2} \tag{35}$$

$c_{2\,i}$ = Second Bond stress coefficient for monthly increment *i*

$$a_i = 0.7606 + 1772.5(\varepsilon_{tot-\varsigma i}) - 2e06(\varepsilon_{tot-\varsigma i})^2 \tag{36}$$

$$b_i = 9e08(\varepsilon_{tot-\varsigma i}) + 149486) \tag{37}$$

$$c_i = 3e09(\varepsilon_{tot-\varsigma i})^2 - 5e06(\varepsilon_{tot-\varsigma i}) + 2020.4 \tag{38}$$

$\varepsilon_{tot-\varsigma i}$ = Total strain at the depth of the steel for monthly increment *i* expressed in strains

k_1 = Bond slip coefficient.

$\overline{L}$ = Mean crack spacing, in

Step 4. Calculate Environmental Tensile Stress in the PCC at the Depth of the Steel in Longitudinal Direction for Each Monthly Increment i

$$\sigma_{env\,i} = C_i \sigma_{oi}\left(1 - \frac{2\zeta}{h_{PCC}}\right) \tag{39}$$

Where

$\sigma_{env\,i}$ = environmental tensile stress in the PCC for each monthly increment *i*

h_{PCC} = PCC slab thickness, in

ζ = depth to steel, in

C_i = Bradbury's correction factor for the finite slab size

$$C_i = 1 - \frac{2\cos\lambda_i \cosh\lambda_i(\tan\lambda_i + \tanh\lambda_i)}{\sin 2\lambda_i + \sinh 2\lambda_i} \tag{40}$$

$$\lambda_i = \frac{ELC}{\sqrt{8}\,\ell_i} \tag{41}$$

ELC = 144 in, effective slab length calibration factor

ℓ_i = radius of relative stiffness for each monthly increment *i*

$\sigma_{0\,i}$ = Westergaard nominal stress factor for each monthly increment *i*

$$\sigma_{0\,i} = \frac{E_{PCCi}\varepsilon_{tot-\Delta m}}{2(1-\mu_{PCC})} \tag{42}$$

$E_{PCC\,i}$ = Concrete modulus of elasticity for each monthly increment *i*, psi

μ_{PCC} = Poisson's ratio

$\varepsilon_{tot-\Delta\,m}$ = Equivalent total strain difference between the pavement surface and slab bottom (changes with cyclic seasonal increment) expressed in strains.

$$\varepsilon_{tot-\Delta\,m} = \alpha_{PCC}\Delta t_{eqv\,m} + \varepsilon_\infty \Delta(1 - rh_{PCC}^3)_{eqv} \tag{43}$$

α_{PCC} = Coefficient of Thermal Expansion of PCC / ^oF

ε_∞ = Ultimate drying shrinkage in "strains"

$\Delta t_{eqv\ m}$ = equivalent temperature $\Delta t_{eqv\ m}$ (changes cyclically for each month) determined as:

$$\Delta t_{eqv\,m} = \frac{R_{o\,m}}{2CF}\left(1 - e^{-\frac{h_{PCC}}{12}\sqrt{\frac{2\pi}{\gamma^2}}}\right) \tag{44}$$

$R_{o\,m}$ = Effective range in seasonal temperature from Table 3

$$CF = 1.000 - 0.565h_{pcc} + 0.116\ h_{pcc} * h_{pcc}^{\ 1/2} + 0.685 * h_{pcc}^{\ 1/2} \tag{45}$$

γ = Concrete thermal diffusivity (ft^2 per day), as defined in ACI 207, depends upon the coarse aggregate type used in the concrete from Table 4.

$\Delta(1\text{-}rh_{PCC}^{\ 3})_{eqv}$ = equivalent relative humidity coefficient (difference between the pavement surface and bottom) from Table 5.

Step 5. Calculate Maximum Tensile Stress in PCC at the Steel Level for Each Monthly Increment i

Reis et al. (41) suggested an equation form for the longitudinal stress in the concrete pavement (at the depth of the steel) that is a function of the bond-slip characteristics of the reinforcing steel. A modification to this form, based on the work of Westergaard and Bradbury also allows consideration of stresses due to curling and warping, as it may contribute to the stress level resulting in transverse crack development of a single layer of steel (38, 41).

$$f_{\sigma i} = \frac{\bar{L}U_m P_b}{c_{1i} d_b} + \sigma_{env\,i} + \frac{\bar{L}}{2} f \tag{46}$$

Where

$f_{\sigma i}$ = Maximum Longitudinal Tensile Stress in PCC at steel depth computed for each monthly increment *i*, psi

$\bar{L}$ = Mean crack spacing, inch

U_m = Peak Bond Stress, psi

P_b = Percent steel, fraction

d_b = Reinforcing steel bar diameter, inch

$c_{1\,i}$ = First bond stress coefficient computed for each monthly increment *i*.

$\sigma_{env\,i}$ = Environmental Tensile Stress in the PCC for each monthly increment *i*.

f = Subbase friction coefficient from Table 6 based on subbase type.

Step 6. Determine Mean Crack Width for Each Month during Design Life.

To predict the mean estimate of the opening of the transverse cracks at the level of the steel due to shrinkage, thermal contraction, and counteracted by the restraint of the reinforcing steel and the subbase friction, the following crack width formula is used in this design procedure:

$$cw_i = CC \cdot \overline{L}\left(\varepsilon_{shr\,i} + \alpha_{PCC}\Delta T_{\zeta m} - \frac{c_{2i} f_{\sigma i}}{E_{PCCi}} \right) \cdot 1000 \qquad (47)$$

If $cw_i < 0$, $cw_i = 0$

where

cw_i = average crack width at the depth of the steel for monthly increment *i*, mils

CC = local calibration constant (CC=1 is used based on global calibration)

$\overline{L}$ = mean crack spacing, inch

$\varepsilon_{shr\,i}$ = unrestrained concrete drying shrinkage at the depth of the steel for monthly increment *i*, "strains"

α_{PCC} = PCC coefficient of thermal expansion, $°F^{-1}$

$\Delta T_{\zeta m}$ = drop in PCC temperature from the concrete "set" temperature at the depth of the steel for each month *m*, °F

$c_{2\,i}$ = second bond stress coefficient for monthly increment *i*

$f_{\sigma\,i}$ = maximum longitudinal tensile stress in PCC at the steel level for monthly increment *i*

$E_{PCC\,i}$ = PCC elastic modulus for monthly increment *I*, psi

MODULE 4: DETERMINE LOAD TRANSFER EFFICIENCY FOR EACH MONTHLY INCREMENT (I)

The degree of LTE and stiffness across the transverse cracks is key to CRCP performance. The ability of the crack to transfer vertical shear loads is highly related to the crack width. Crack shear capacity varies with the crack opening and season as it affects crack LTE over the life of the pavement.

Step 1. Calculate Crack Shear Capacity $s_{0\,i}$ for Each Monthly Increment i

$$s_{0i} = 0.05 \cdot h_{PCC} \cdot e^{-0.032 cw_i} \qquad (48)$$

Where

s_{0i} = Dimensionless Seasonal Shear Capacity for each monthly increment *i*

h_{PCC} = Thickness of the slab, inch

cw_i = Crack width calculated for each monthly increment *i*, mil.

Step 2. Adjust Crack Shear Capacity s_{ki} for Each Monthly Increment i by Total Accumulated Loss in Crack Shear Capacity from Previous Increments.

$$s_i = s_{0i} - \Delta S_{i-1} \qquad (49)$$

Where

s_i = adjusted shear capacity computed for the current monthly increment *i*.
s_{0i} = Dimensionless Seasonal Shear Capacity for each monthly increment *i*
ΔS_{i-1} = Total accumulated loss in shear capacity at the end of the previous monthly increment (i-1).
NOTE: For the first time increment i=1, $\Delta S_{i-1} = 0$.

Step 3. Calculate Transverse Crack Stiffness for Each Progressive Seasonal Increment i

$$Log(J_{ci}) = ae^{-e^{-\left(\frac{J_s-b}{c}\right)}} + de^{-e^{-\left(\frac{s_i-e}{f}\right)}} + ge^{-e^{-\left(\frac{J_s-b}{c}\right)}} \cdot e^{-e^{-\left(\frac{s_i-e}{f}\right)}} \quad (50)$$

Where:

$J_{c\,i}$ = transverse crack stiffness for monthly increment i, $(AGG/kl)_c$
s_i = adjusted shear capacity computed for the current monthly increment *i*.
J_s = stiffness of the shoulder/lane joint from Table 7, $(AGG/kl)_S$.

Table 7. Stiffness of the shoulder/lane joint.

Shoulder type	**$(AGG/kl)_s$**
Granular	0.04
Asphalt	0.04
Tied PCC	4

Regression constants:

a = -2.20;
b = -11.26;
c = 7.56;
d = -28.85;
e = 0.35;
f = 0.38;
g = 49.80;

Step 4. Calculate Transverse Crack LTE_c due to Aggregate Interlock to Be Used in Crack Shear Deterioration Routine for Each Monthly Increment i.

$$LTE_{c\,i} = \frac{100}{1+\log^{-1}\left[\frac{0.214-0.183\frac{a}{\ell_i}-\log(J_{ci})}{1.18}\right]} \tag{51}$$

NOTE: Log^{-1} stays for 10^

$LTE_{c\,i}$ = transverse crack load transfer efficiency due to aggregate interlock for monthly increment *i*, %
ℓ_i = radius of relative stiffness computed for monthly increment *i*, inch
$J_{c\,i}$ = Transverse crack stiffness computed for monthly increment *i*.
a = Typical radius for a loaded area (6 inches).

Step 5. Obtain from NN Corner Shear Stress on Transverse Crack for Each Corner Load j for Monthly Increment i

$$\tau_{ij} = \text{f}(L\text{=2feet}, \ell_{eff\,i}, \text{VOID}_y, \text{LTE}_{c\,i}, \phi_i^*, \text{q}_{ij}^*, \text{OFFSET=0 inch}) \tag{52}$$

It is assumed that all the loads are applied at corner location (number of loads will be adjusted based on ESR).

Step 6. Compute Reference Shear Stress Derived from PCA Test Results for Each Monthly Increment i

$$\tau_{ref\,i} = 111.1 * s_{pca} = 111.1 * \left(e^{-e^{X'}}\right) \tag{53}$$

Where

$\tau_{ref\,i}$ = Reference shear stress derived from the PCA test results for monthly increment i

$$X' = \alpha e^{-(\lambda Ln J_{ci})^{\gamma}} = 0.9988 \cdot e^{-(0.1089 \cdot Ln(J_{ci}))^{1.0}} \tag{54}$$

$J_{c\,i}$ = Transverse crack stiffness computed for monthly increment *i*.

Step 7. Determine Shear Capacity Loss due to Aggregate Wear-Out during Monthly Increment i

As the concrete slab is subjected to axle load applications, vertical crack surfaces are subjected to repetitious shear loading between the two sides of the crack that leads to aggregate wear-out and decreases crack load transferring capacity. Crack shear capacity shows sufficient deterioration potential if the crack width-to-PCC thickness ratio is 0.0038 or greater (crack width and PCC thickness are expressed in the same units).

Select appropriate formula for shear loss Δs_i based on $\frac{cw_i}{h_{PCC}}$ value as following:

$\frac{cw_i}{h_{PCC}}$	Δs_i
If < 3.8	$\Delta s_i = \sum_j \left(\frac{0.005}{1+1\cdot\left(\frac{cw_i}{h_{PCC}}\right)^{-5.7}} \right) \left(\frac{n_{ji}}{10^6}\right)\left(\frac{\tau_{ij}}{\tau_{ref\,i}}\right) ESR_i$ (55a)
otherwise	$\Delta s_i = \sum_j \left(0.004 + \frac{0.068}{1+6\cdot\left(\frac{cw_i}{h_{PCC}}-3\right)^{-1.98}} \right) \left(\frac{n_{ji}}{10^6}\right)\left(\frac{\tau_{ij}}{\tau_{ref\,i}}\right) \cdot ESR_i$ (55b)

Where:

Δs_i = loss in shear capacity during monthly increment *i* due all load applications *j*

cw_i = Crack width calculated for each monthly increment *i*, mil.

h_{PCC} = PCC thickness, in

n_{ji} = Number of efficient axle load applications for monthly increment (*i*) and load level (*j*) (no traffic wander).

τ_{ij} = NN corner shear stress on the transverse crack due to load level (*j*) during monthly increment (*i*)

τref i = Reference shear stress derived from the PCA test results for monthly increment i

ESR_i = equivalent shear ratio that is an adjustment factor for lateral traffic wander.

$$ESR_i = a + \frac{b}{\frac{L}{\ell_i}} + C\frac{LTE_{ci}}{100}$$

$$a = 0.0026\mu_{wp}{}^2 - 0.1779\mu_{wp} + 3.2206 \quad (56)$$

$$b = 0.1309Ln(\mu_{wp}) - 0.4627$$

$$c = 0.5798Ln(\mu_{wp}) - 2.061$$

where

L = 24 inches (2 feet) crack spacing, in

ℓ_i = Radius of relative stiffness, in

$LTE_{c\,i}$ = Transverse crack load transfer efficiency due to aggregate interlock for monthly increment *i*, %

μ_{wp} = Mean wheelpath, in

Step 8. Determine Accumulated Loss in Aggregate Shear Capacity from All Previous Progressive Seasonal Time Increments

$$\Delta S_i = \sum_{i=1}^{i=current} \Delta s_i = \Delta S_{i-1} + \Delta s_i \qquad (57)$$

NOTE: At the beginning of the first time increment i=1, $\triangle S_i = 0$.

Where:

ΔS_i = Total accumulated loss in shear capacity from all increments *i*

Δs_i = Loss in shear capacity during current monthly increment *i* due all load applications *j*

ΔS_{i-1} = Total accumulated loss in shear capacity computed at the end of the previous monthly increment (i-1).

Step 9. [For Damage Prediction] Calculate Total LTE due to Aggregate Interlock, Steel Reinforcement, and Base Layer for Each Monthly Increment i.

$$LTE_{TOT\,i} = 100 * \left(1 - \left(1 - \frac{1}{1 + \log^{-1}\left[(0.214 - 0.183 \frac{a}{\ell_i} - \log(J_{ci}) - R)/1.18 \right]} \right) \left(1 - \frac{LTE_{Base}}{100} \right) \right) \qquad (58)$$

NOTE: Log^{-1} stands for 10^

$LTE_{TOT\,i}$ = transverse crack load transfer efficiency due to aggregate interlock, reinforcement, and base for monthly increment *i*, %

ℓ_i = radius of relative stiffness computed for monthly increment *i*, inch

$J_{c\,i}$ = Transverse crack stiffness computed for monthly increment *i*.

a = Typical radius for a loaded area (6 inches).

R = Residual factor to account for residual load transfer provided by the steel reinforcement.

$$R = 500 P_b - 3$$

P_b = Percent of longitudinal reinforcement expressed as a fraction

LTE_{BASE} = Load transfer efficiency contributed by the base layer from Table 8, %.

Table 8. Load transfer efficiency contributed by the base layer.

Base type	LTE_{Base}
aggregate base	20%
ATB or CTB base	30%
LCB base	40%

MODULE 5: DETERMINE TRAFFIC PARAMETERS FOR DAMAGE AND SHEAR LOSS COMPUTATION

For every time increment, the number of applied traffic loads (n_{ij}) in the traffic lane are computed using input traffic data for the analysis period. Traffic load spectra is estimated and axle load distributions developed for each axle type (single, tandem, tridem, quad). Lateral offsets from the slab edge are also considered. Axle load distributions are used in the response model to compute maximum top of slab transverse tensile stresses for each time increment.

Step 1. Adjust Base Annual Number of Axle Load Counts n_j to Efficient Number of Single and Tandem Axle Loads n_j for Each Load Level/Axle Type j.

As a result of this step, all applied loads will be converted to either (1) single axle loads or to (2) tandem axle loads. Adjusted counts of single and tandem axle load applications will be obtained for n_j.

n_j = efficient base annual number of axle load applications of the jth magnitude.

- For single axles J = 1 to 40
- For tandem axles J = 41 to 80.

Table 9. Traffic Loading Conversion Rules For CRCP Response Model

Axle Type	**Efficient number of passes**
Single	1 pass
Tandem	1 pass of tandem axle segments plus 1 pass of single axle loaded to ½ tandem axle load magnitude
Tridem	2 passes of tandem axle loaded to 2/3 tridem axle load magnitude plus 1 pass of single axles loaded to 1/3 of tridem axle load magnitude
Quadruple	3 passes of tandem axles loaded to ½ of quad axle load magnitude plus 1 pass of single axles loaded to 1/4 quad axle load magnitude

These efficient base annual single and tandem axle loads will be stored in 2 axle load spectra.

Step 2. Adjust Efficient Base Annual Single and Tandem Annual Axle Load Spectra for Within-Year Variations.

(A). For Damage model, adjust traffic for each with-in 24 hours probability of temperature gradients occurrence, seasonal cycle, and annual traffic growth:

$$n_{ji} = n_j * P(TG)_h * MF_m * GF_y \quad (59)$$

n_{ji} = Efficient number applied annual axle loads of the *j*th magnitude evaluated based on probability of temperature gradient occurrence *h*, for month *m* and year *y*.
n_j = Efficient base annual number of axle load applications of the *j*th magnitude.
$P(TG)_h$ = Probability of temperature gradient occurrence
MF_m = Monthly adjustment coefficients
GF_y = Growth Factor for year *y*

(B). For Shear Loss Model, adjust traffic for each seasonal cycle and annual traffic growth:

$$n_{ji} = n_j * MF_m * GF_y \quad (60)$$

n_{ji} = Efficient number of applied annual axle load applications of the *j*th magnitude evaluated for month *m* and year *y*.
n_j = Efficient base annual number of axle load applications of the *j*th magnitude.
MF_m = Monthly adjustment coefficients
GF_y = Growth Factor for year *y*

Step 3. For Damage Model, Determine P(cov) at Gaussian Points to Account for Traffic Wander

The probability of coverage, including probability of traffic to be partially off the pavement is determined using the following formula:

$$P_g(cov) = NORMDIST(g) + NORMDIST(-g) \quad (61)$$

Where:

$P_g(cov)$ = Probability of traffic (outer edge of the wheel) passing through point placed *g* inches away from the pavement edge.
NORMDIST (g) = Probability that the outer edge of the wheel will pass through the point located *g* inches inside of the pavement edge.
NORMDIST (-g) = Probability that the outer edge of the wheel will pass through the point located *g* inches off the pavement edge.

$$NORMDIST(g) = \frac{1}{\sigma_{wp}\sqrt{2\pi}} e^{-\frac{1}{2}\left(\frac{g-\mu_{wp}}{\sigma_{wp}}\right)^2} \quad (62)$$

Where:

NORMDIST = normal distribution density function.
μ_{wp} = Mean wheelpath from the lane-shoulder to the outer wheel edge (18 in).
σ_{wp} = Standard deviation (10 in).
g = Wheel location at Gauss point from the table below

Gauss Point number	Location of Gauss Point *g*, inch
1	0.5555
2	2.6401
3	5.3599
4	7.4445
5	10.1132
6	15.8868

Step 4. For Damage Model, Determine Number of Axle Load Applications at Each Gaussian Point Based on Probability of Coverage function.

$$n_{jig} = n_{ji} * P_g(cov) \quad (63)$$

where
n_{jig} = Efficient number of single and tandem axle loads of the *j*th magnitude applied at Gaussian point *g* for each month *m*, temperature cycle *h*, and year *y*.
n_{ji} = Efficient number of applied annual axle load of the *j*th magnitude evaluated based on probability of temperature gradient occurrence *h*, for each month *m* and year *y*.
$P_g(cov)$ = Probability of traffic passing through point placed *g* inches away from the pavement edge.

MODULE 6: DETERMINE DAMAGE FOR EACH LOAD INCREMENT (J) AND TIME INCREMENT (I)

To evaluate accumulated fatigue damage due to slab bending in the transverse direction, an incremental analysis is used in this procedure. The analysis period is subdivided into time increments based on pavement design life, concrete strength gain, subgrade support, and climatic conditions relative to their effect on crack width and load transfer. Depending on the site climatic conditions and the level of desired accuracy, a separate analysis is carried out in steps for every monthly increment. When the time of day makes a dramatic difference on the pavement structural response (i.e., thermal stress contribution to maximum tensile stress in CRCP as in the case of extreme nighttime temperature gradients), the analysis increment is further refined. Total fatigue damage is computed as a summation of fatigue damages developed during each analysis increment. Several input parameters are adjusted for different time increments, as shown in Table 10.

Table 10. Input parameters that change with analysis period increment.

Input Parameter	Basis for Change
Number of load applications	Traffic growth through design period, monthly variation, hourly variation
Temperature gradient	Day and night, monthly variation
Ambient temperature and humidity	Monthly variation
Subgrade modulus	Monthly variation
Pavement edge support conditions	Possibility of loss of edge support through design period (monthly)
Crack LTE	Incremental wear out of crack aggregate interlock (monthly)
Concrete strength	Incremental strength gain through design period (average monthly strength)
Transverse crack width	(1) Incremental opening over time due to continuous drying shrinkage (2) Monthly variation (as function temperature and moisture)

Step 1. Obtain Top Bending Stress from NN at Critical Point Using Specified Load Offset Positions g for Each Load Level j, Progressive Monthly and Cyclic Hourly Increment i

Assumptions:

- Bending stresses are obtained based on FE model with 2 ft transverse crack spacing.
- Mean crack LTE is predicted based on mean crack spacing.
- Bending stresses are obtained at "critical" point @ 48 inches from pavement edge.
- Loads are applied at 6 Gaussian integration points

$$\sigma_{tot\ ijg} = f(\text{Load } j, \text{OFFSET}_g, \ell_{eff\,i}, \text{VOID}_i, \text{LTE}_{TOT\,i}, \phi_i^*, q_{ij}^*) \quad (64)$$

where

$\sigma_{tot\ ijg}$ = Total bending stress at critical point for monthly and hourly time increment *i* due to load of magnitude *j* applied at Gaussian point *g* with associated temperature gradient ϕ^*_i

$\ell_{eff\,i}$ = Radius of relative stiffness for monthly increment *i* based on effective slab thickness, inch.

VOID_i = Extension of erosion from the slab edge for monthly increment *i*, inch

$\text{LTE}_{TOT\,i}$ = Load transfer efficiency for monthly increment *i*, %

ϕ^*_i = Non-dimensional temperature gradient for monthly and hourly increment *i*

q_{ij}^* = Adjusted load/pavement weigh ratio for load level *j* for progressive seasonal time increment *i*, ft^{-2}

$OFFSET_g$ = Gaussian integration point locations.

NOTE: for each time increment and each load level and axle type, 6 stress values are obtained from NN (for loads at 6 Gaussian points).

Step 2. Calculate Number of Allowable Axle Load Applications for Each Cyclic Hourly and Progressive Seasonal Increment I

The maximum bending stresses (σ_{totij}) and bending strength (MR_i) are used to compute the number of allowable axle load applications (N_{ij}) and aggregate interlock wear due to each design wheel load *(j)* for each time increment *(i)* using the following relation:

$$Log\ N_{ijg} = 2.2*(MR_i/\sigma_{tot\ ijg})^{1.22} + a \quad (65)$$

where,

N_{ijg} = number of allowable load applications at Gaussian point *g* during monthly and hourly increment *i* at load magnitude *j*

MR = PCC modulus of rupture for monthly increment *i*

$\sigma_{tot\ ijg}$ = Total bending stress at critical point for monthly and hourly time increment *i* due to load of magnitude *j* applied at Gaussian point *g* with associated temperature gradient ϕ^*_i

a = calibration shift factor (-1)

Step 3. Calculate Fatigue Damage at Critical Points l due to Axle Load Level j for Progressive Monthly and Cyclic Hourly Increment i at Gauss Point g

$$D_{lijg} = n_{ijg} / N_{lijg} \quad (66)$$

Where

D_{lijg} = Damage computed for progressive monthly and cyclic hourly increment *i* due to number of applied axle load applications n_{ijg} of the *j*th magnitude applied at Gaussian point *g*.

n_{ijg} = Number of efficient axle loads of the *j*th magnitude applied at Gaussian point *g* during progressive seasonal and cyclic hourly increment *i*.

N_{ijg} = number of allowable load applications at Gaussian point *g* during monthly and hourly increment *i* at load magnitude *j*.

Step 4. Use Gaussian Numerical Integration to Calculate Fatigue Damage at Critical Point due to Axle Load Level j for Progressive Monthly and Cyclic Hourly Increment i Accounting for Traffic Wander

In this step, stresses computed at 6 Gaussian points *g* are used to obtain fatigue damage for a given time increment (*i*) and load level (*j*) using Gaussian integration scheme.

$$D_{ij} = 4*(0.384259*D_{ijg=1} + 0.615741*D_{ijg=2} + 0.615741*D_{ijg=3} + 0.384259*D_{ijg=4}) + + 5*(1*D_{ijg=5} + 1*D_{ijg=6}) \quad (67)$$

D_{ij} = Damage accumulated at critical point during progressive monthly and cyclic hourly time increment i due to number of applied axle load applications n_{ij} of the jth magnitude

D_{ijg} = Damage computed for progressive monthly and cyclic hourly increment i due to number of applied axle load applications n_{ijg} of the jth magnitude applied at Gaussian point g.

Step 5. Accumulate Damage for Each Progressive Monthly and Cyclic Hourly Increment i over All Axle Load Level j

$$D_i = \sum_{j}^{j=80} D_{ij} \quad (68)$$

D_i = Accumulated fatigue damage during progressive seasonal and cyclic hourly time increment i

D_{ij} = Damage accumulated at critical point during progressive monthly and cyclic hourly time increment i due to number of applied axle load applications n_{ij} of the jth magnitude

MODULE 7: DETERMINE NUMBER OF PUNCHOUTS PER MILE AT THE END OF MONTHLY INCREMENT (I)

Step 1. Accumulate Damage at the End of Each Progressive Monthly Increment i Considering All Hourly Increments

$$D_i = \sum_{h=1}^{h=24} D_{hi} \cdot m\_days_i \quad (69)$$

D_i = Accumulated fatigue damage during monthly increment i

D_{hi} = Damage accumulated at critical point during progressive monthly increment i and cyclic hourly increment h due to all applied loads n_{hi}

m_days_i = Number of days in monthly increment i

Step 2. Accumulate Fatigue Damage from All Previous Monthly Increments i.

IF (i corresponds to end of year y) = TRUE THEN

$$FD_i = D_i + \sum_{i=1}^{i-1} D_i \quad (70)$$

FD_i = Accumulated fatigue damage at the end of the i^{th} increment.
D_i = Accumulated fatigue damage during monthly increment i

After total damage is computed, the mean number of punchouts per mile or kilometer will be predicted using a model calibrated with respect to field data.

Step 3. Calculate Number of Punchouts per Mile from Calibrated Curves.

A calibrated model for punchout prediction as a function of accumulated fatigue damage due to slab bending in the transverse direction is used in this design procedure. The nationally calibrated model is provided as follows:

$$PO_i = \sum_{i=1}^{Life} \frac{a}{1 + b \cdot D_i^c} \quad (71)$$

where,
PO_i = total predicted number of punchouts per mile at the end of i^{th} monthly increment
D_i = accumulated fatigue damage (due to slab bending in the transverse direction) at the end of i^{th} monthly increment
a, b, c = calibration constants for the nationally calibrated model (105.26, 4.0, -0.38)

CALIBRATION OF NCHRP 1-37A PUNCHOUT MODEL

CRCP Database

Three sources were used to obtain data for calibration of CRCP punchout prediction model:

- LTPP GPS-5 Experiment (Main CRCP data source from 22 States)
- Vandalia experimental CRCP sections (US 40)
- Illinois heavily trafficked CRCP sections on I-80 and I-94 (Edans expressway)

The following sections provide an overview of main data characteristics for the sections used in calibration.

Characteristics of LTPP GPS-5 Data

The main source of data for calibration of punchout prediction model was LTPP database. Experimental research data were obtained from the General Pavement Experiment Study number 5 (GPS-5) maintained under the FHWA LTPP program. Pavements monitored under the GPS-5 experiment are the continuously reinforced Portland cement concrete (PCC) slabs placed over different types of base layer.

All the pavement design and performance data available in the database were reviewed for data reasonableness and data competence. Based on data availability and data reasonableness evaluation, 58 CRC pavement sections located in four climatic regions and 22 different states throughout the United States were selected for calibration.

Major LTPP and other section characteristics are summarized in Table 11. In addition to the LTPP sections, this table also contains IL sections outside LTPP program used in calibration of CRCP design equations. Detailed data for each section are provided in Appendix FF.

Table 11. Major characteristics of LTPP and other CRCP sections used in calibration.

Section	State	28-day MR, psi	PCC Thickness, in	% Steel	Base Type	Shoulder Type	Climatic region	Cumulative ESAL, millions
1_5008	AL	745	9.2	0.66	ATB	TIED	WNF	29.4
5_5803	AR	735	8	0.61	ATB	ASPHALT	WNF	1.2
5_5805	AR	655	8	0.61	ATB	TIED	WNF	4.1
4_7079	AZ	741	9	0.57	ATB	TIED	DNF	1.2
6_7455	CA	756	8.9	0.54	CTB	ASPHALT	DNF	10
16_5025	ID	733	8.3	0.59	CTB	ASPHALT	DF	3.1
17_5020	IL	734	8.6	0.68	CTB	ASPHALT	WF	0.5
17_5843	IL	846	10.4	0.68	CTB	ASPHALT	WF	22.1
17_5849	IL	777	7.2	0.70	ATB	ASPHALT	WF	15.7
17_5854	IL	784	10	0.65	CTB	ASPHALT	WF	1.3
17_5869	IL	840	8.9	0.60	CTB	ASPHALT	WF	1.9
17_5908	IL	840	8.8	0.54	ATB	ASPHALT	WF	1.9
17_9267	IL	809	8.5	0.56	ATB	GRANULAR	WF	36.6
18_5022	IN	742	9.8	0.60	ATB	ASPHALT	WF	39.8
18_5043	IN	770	7.5	0.60	ATB	ASPHALT	WF	0.5
18_5518	IN	697	9.3	0.61	GB	ASPHALT	WF	22.9
19_5042	IO	781	8	0.65	ATB	ASPHALT	WF	9.2
19_9116	IO	722	7.8	0.66	ATB	ASPHALT	WF	8.8
29_5047	MO	642	8.3	0.60	GB	GRANULAR	WF	11.6
28_3099	MS	861	8	0.61	CTB	GRANULAR	WNF	10.9
28_5006	MS	841	8.2	0.59	CTB	GRANULAR	WNF	8.1
28_5025	MS	803	8.3	0.56	ATB	GRANULAR	WNF	3.7
28_5803	MS	766	7.9	0.61	CTB	GRANULAR	WNF	15
28_5805	MS	921	8.2	0.59	ATB	ASPHALT	WNF	8.8
37_5037	NC	776	7.8	0.65	GB	ASPHALT	WNF	14.6
37_5827	NC	698	8.1	0.63	GB	ASPHALT	WNF	5.6
38_5002	ND	635	8	0.60	ATB	TIED	WF	1.3
31_5052	NE	658	7.6	0.75	CTB	ASPHALT	WF	9.5
39_5003	OH	764	9.7	0.88	ATB	TIED	WF	3.7
39_5010	OH	784	8.8	0.54	CTB	ASPHALT	WF	3.2
40_4158	OK	702	10.3	0.59	ATB	TIED	WNF	1.2
40_4166	OK	779	10.1	0.67	CTB	ASPHALT	WNF	4.3

Section	State	28-day MR, psi	PCC Thickness, in	% Steel	Base Type	Shoulder Type	Climatic region	Cumulative ESAL, millions
40_5021	OK	728	9.5	0.57	ATB	TIED	WNF	2.4
41_5005	OR	819	11.5	0.66	CTB	ASPHALT	WNF	26.4
41_5006	OR	698	8	0.60	CTB	ASPHALT	DF	19.1
41_5008	OR	713	8.1	0.59	CTB	ASPHALT	DF	15.3
41_5021	OR	710	10.8	0.63	CTB	ASPHALT	WNF	19.3
41_5022	OR	770	12.8	0.72	GB	ASPHALT	WNF	24.7
41_7081	OR	743	10.4	0.65	CTB	ASPHALT	DF	7.1
42_5020	PA	729	9.3	0.59	GB	ASPHALT	WF	12.3
45_5017	SC	700	8.9	0.57	CTB	ASPHALT	WNF	7.9
45_5034	SC	718	8.3	0.64	CTB	ASPHALT	WNF	11.2
45_5035	SC	743	7.7	0.67	CTB	ASPHALT	WNF	9.3
46_5020	SD	765	7.9	0.57	ATB	ASPHALT	DF	1.1
46_5025	SD	786	8.1	0.59	GB	ASPHALT	DF	1
48_3779	TX	666	8.4	0.49	ATB	ASPHALT	DNF	1.6
48_5024	TX	759	11.1	0.55	ATB	TIED	WNF	2.5
48_5026	TX	837	10.2	0.56	ATB	TIED	WNF	0.4
48_5154	TX	707	8.2	0.52	ATB	ASPHALT	WNF	20.9
48_5278	TX	769	6.2	0.59	ATB	ASPHALT	DNF	0.4
48_5328	TX	741	8	0.61	ATB	ASPHALT	WNF	12
48_5334	TX	716	8	0.51	ATB	GRANULAR	WNF	8.6
48_5336	TX	713	9	0.61	ATB	ASPHALT	WNF	4.6
51_2564	VA	747	7.9	0.66	CTB	ASPHALT	WNF	19.9
51_5010	VA	671	9.1	0.65	CTB	TIED	WNF	12.3
55_5037	WI	802	8.2	0.61	GB	ASPHALT	WF	1.3
55_5040	WI	776	8.4	0.62	GB	TIED	WF	11.1
I80_EB_137.65	IL	784	9	0.6	ATB	ASPHALT	WF	33.2
I80_EB_143.79	IL	784	9	0.6	ATB	ASPHALT	WF	33.7
I80_EB_151.12	IL	784	9	0.6	ATB	ASPHALT	WF	35.6
I80_EB_152.33	IL	784	9	0.6	ATB	ASPHALT	WF	36.0
I80_WB_137.65	IL	784	9	0.6	ATB	ASPHALT	WF	33.2
I80_WB_143.79	IL	784	9	0.6	ATB	ASPHALT	WF	33.7
I80_WB_148.39	IL	784	9	0.6	ATB	ASPHALT	WF	33.7
I80_WB_152.33	IL	784	9	0.6	ATB	ASPHALT	WF	36.0
I94_Edens_28.46	IL	784	10	0.75	ATB	ASPHALT	WF	27
I94_Edens_30.11	IL	784	10	0.75	ATB	ASPHALT	WF	32
I94_Edens_32.90	IL	784	10	0.75	ATB	ASPHALT	WF	35
Vandalia 1	IL	800	7	1	GB	GRANULAR	WF	4.3
Vandalia 3	IL	800	7	0.5	GB	GRANULAR	WF	4.3
Vandalia 4	IL	800	7	0.7	GB	GRANULAR	WF	4.3
Vandalia 5	IL	800	8	1	GB	GRANULAR	WF	4.3
Vandalia 7	IL	800	8	0.5	GB	GRANULAR	WF	4.3
Vandalia 8	IL	800	8	0.7	GB	GRANULAR	WF	4.3

Site Locations

Map of the States with LTPP sections used in CRCP punchout calibration is shown in Figure 5. Numbers in brackets indicate number of LTPP sites per state used in calibration.

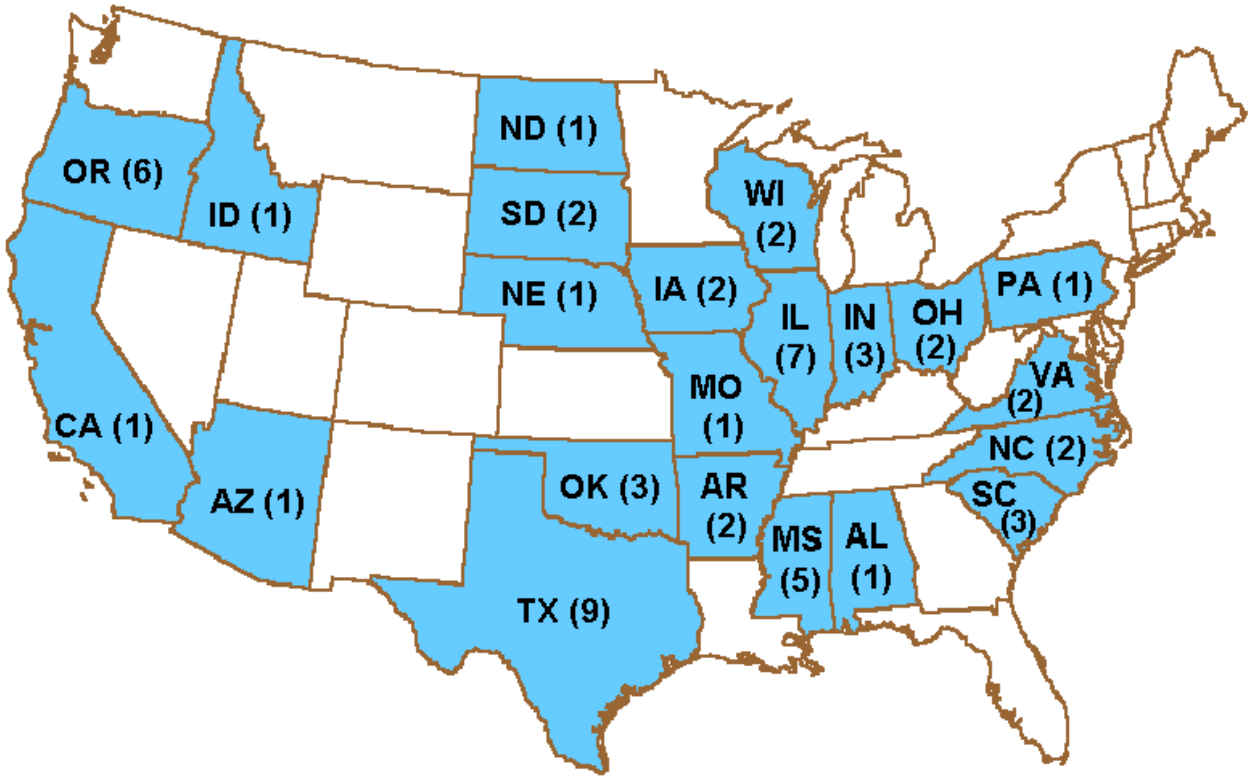

Figure 5. Map of the States with LTPP sites used in calibration of CRCP design procedure.

Age Distribution

Each section used in calibration procedure had distress data collected at up to 7 different times during its service life. As a result, data for 212 calibration points were used to derive the calibrated punchout prediction curve. The histogram in Figure 6 provides statistics about number of distress surveys per section. Most of the sections had at least 3 distress surveys during service life. Distribution of calibration data points by age is shown in Figure 7.

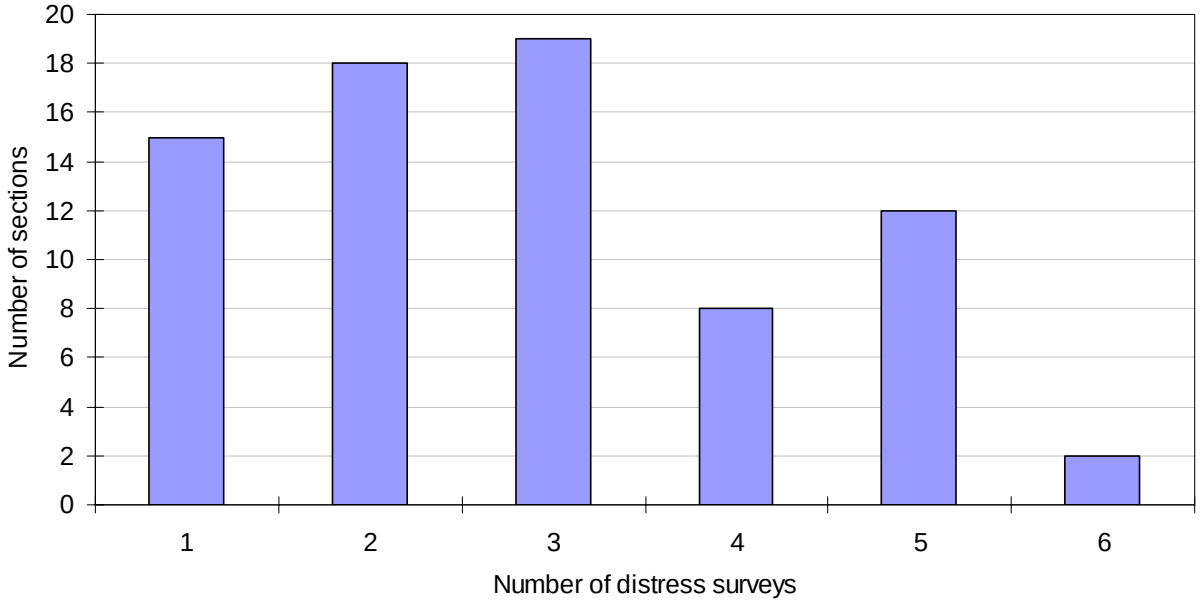

Figure 6. Distribution of LTPP sections used for calibration by number of distress surveys.

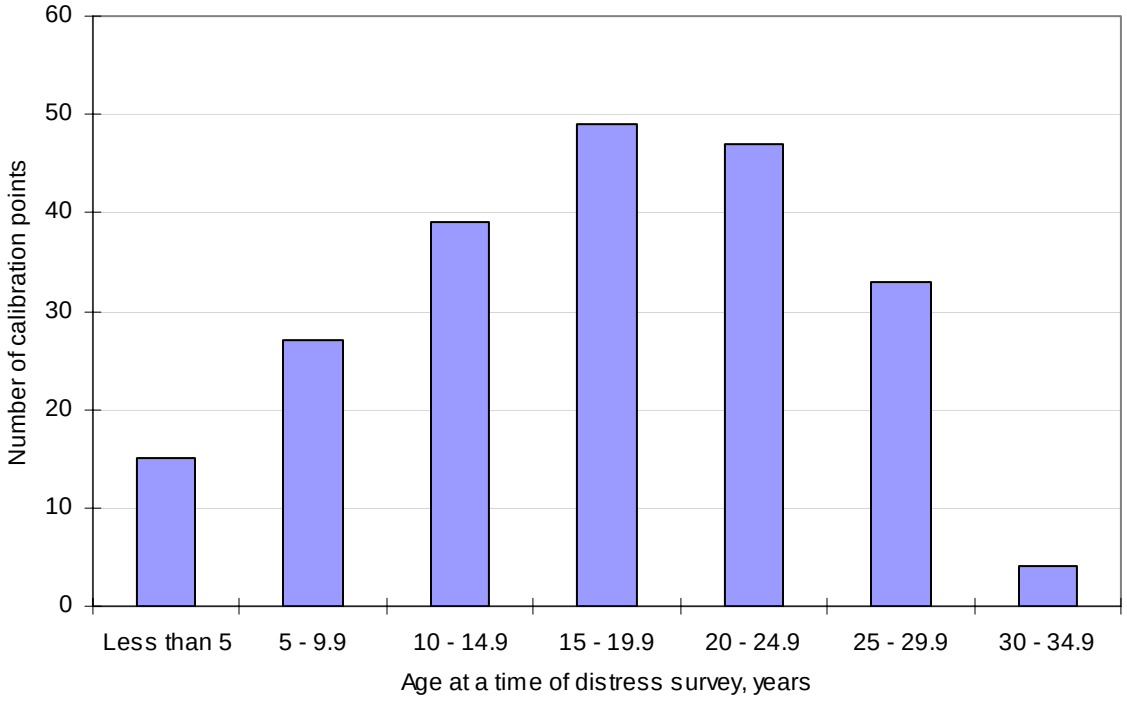

Figure 7. Distribution of data points used for calibration by age for LTPP data.

Traffic Distribution

ESAL values were used as a traffic summary statistic to summarize calibration points by traffic load levels at a time of distress surveys. Distribution of calibration data points by ESAL values is shown in Figure 8.

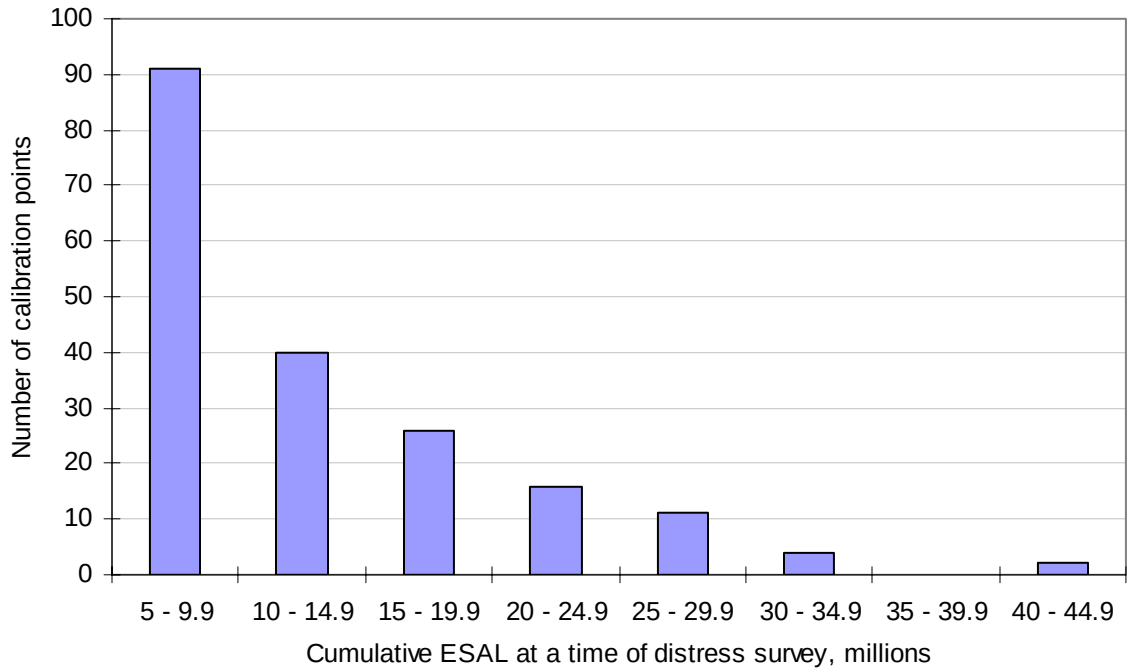

Figure 8. Distribution of data points used for calibration by cumulative ESAL numbers for LTPP CRCP data.

PCC Thickness

PCC slab thicknesses of the LTPP sections used in calibration varied from 6.2 to 12.8 inches. Distribution of sections by PCC thickness ranges is shown in Figure 9.

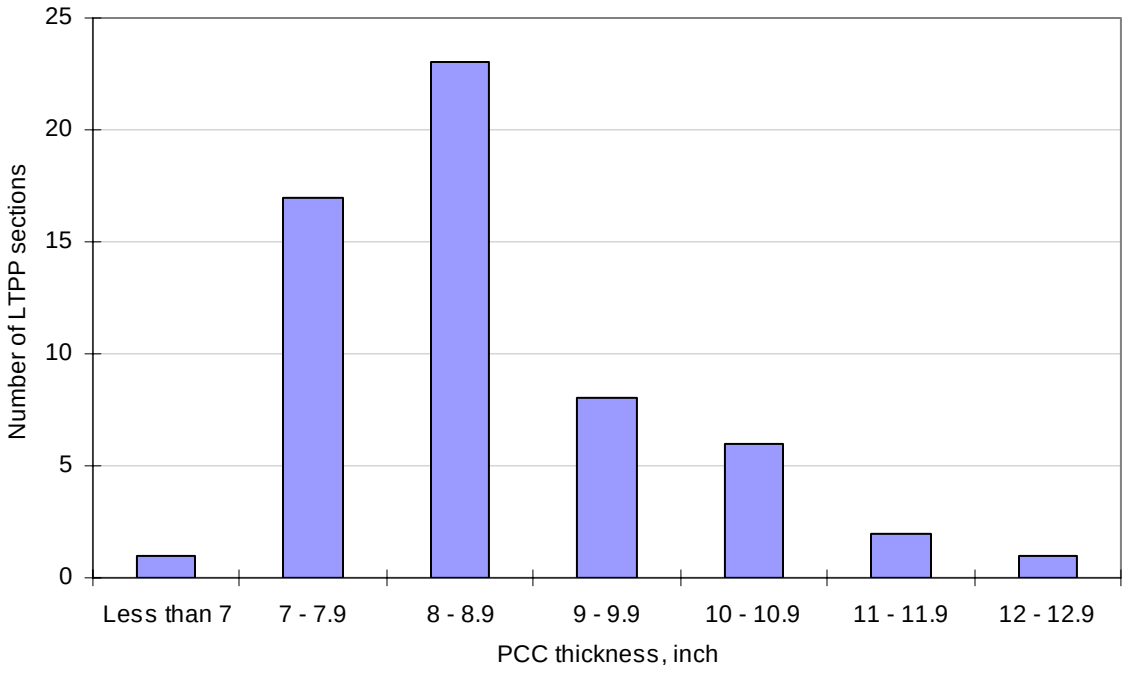

Figure 9. Distribution of LTPP CRCP sections used for calibration by PCC thickness.

PCC Modulus of Rupture

PCC modulus of rupture (MR) characterizes PCC flexural strength. This is an important PCC material property that affects the rate of fatigue damage accumulation in concrete. PCC mean modulus of rupture of the LTPP sections was predicted from long-term PCC compressive strength of cores and then adjusted to a 28-day value. Backcasted MR 28-day values used in the calibration varied from 635 psi to 921 psi. Distribution of sections by PCC modulus of rupture ranges is shown in Figure 10. It is important to note that these are mean values for each section. The designer must use mean expected MR for the project, and certainly not the minimum construction specification limit. It would be erroneous to use the construction specification minimum MR for design purposes commonly used in the previous versions of the AASHTO Guide.

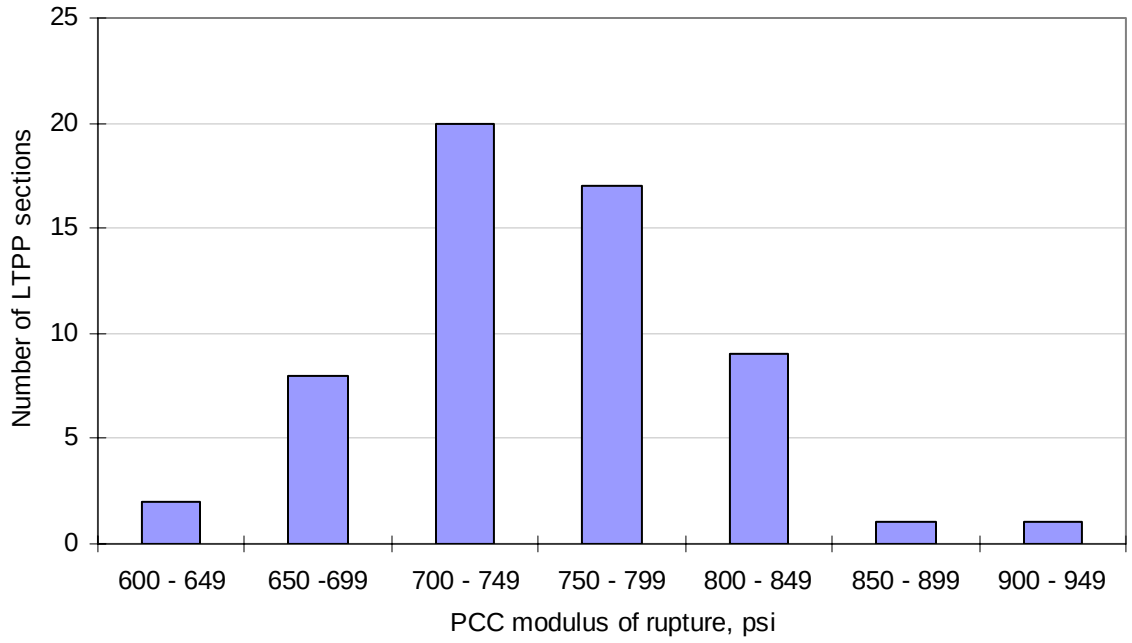

Figure 10. Distribution of LTPP CRCP sections used for calibration by PCC modulus of rupture.

Percent Longitudinal Reinforcement

Percent of longitudinal reinforcement of the LTPP sections used in calibration varied from 0.49% to 0.88%. Distribution of sections by percent of longitudinal reinforcement ranges is shown in Figure 11.

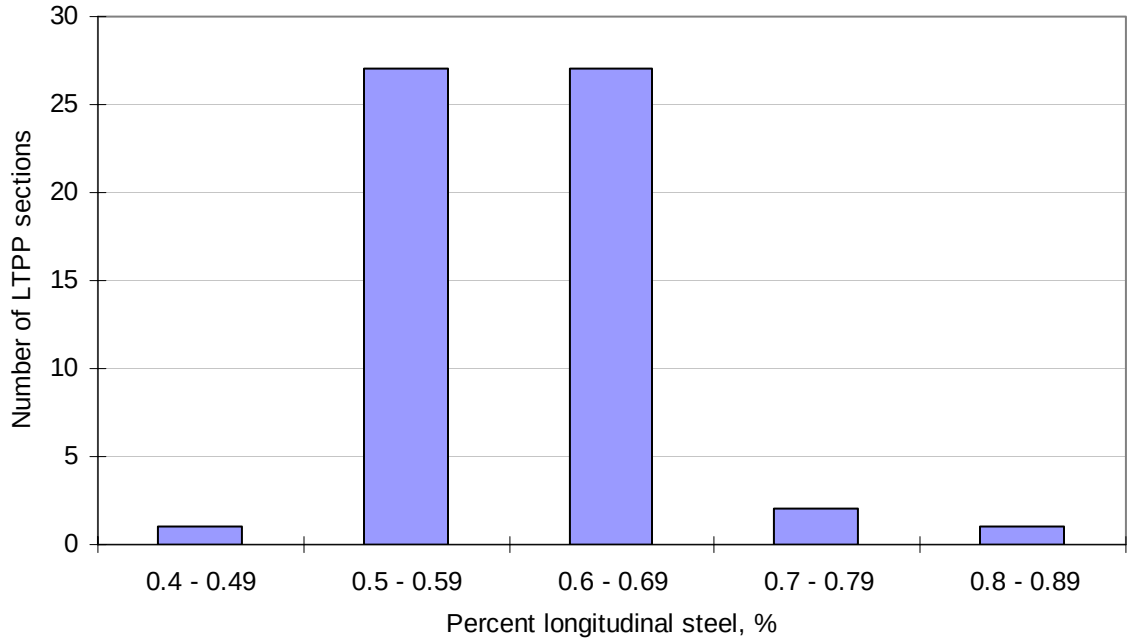

Figure 11. Distribution of LTPP sections used for calibration by percent of longitudinal reinforcement.

Base Material and Friction

Four different base types were used for LTPP CRCP sections:

- ATB – Asphalt-Treated Base
- CTB – Cement-Treated Base
- LCB – Lean Concrete Base
- GB – Granular Base

Distribution of the LTPP sections used in calibration by base type is shown in Figure 12.

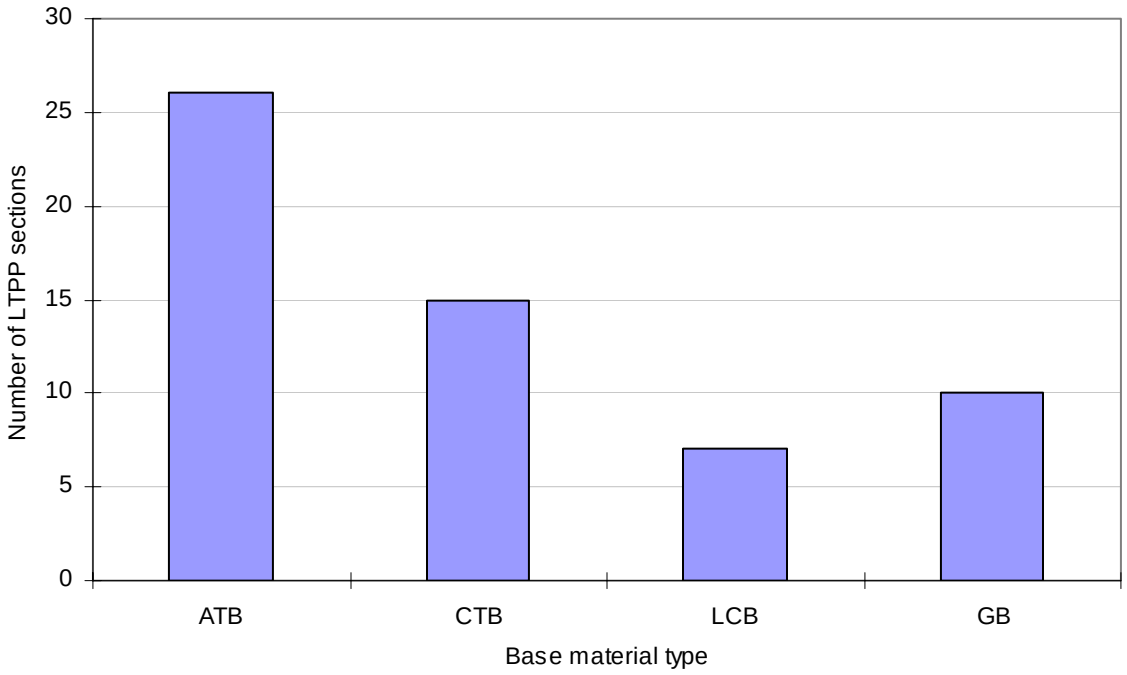

Figure 12. Distribution of LTPP sections used for calibration by base material type.

Base friction is an important property affecting formation and distribution of the transverse cracking in CRCP and, to some degree, transverse crack opening. Base friction values for the LTPP sections were unknown. These values were backcalculated based on

- Known (measured) mean crack spacing for each section
- AASHTO guidelines for selection of friction values for different base types.

The following Table 12 provides descriptive statistics of the backcalculated friction values for each base type.

Table 12. Descriptive statistics of backcalculated friction values used in calibration to match observed crack spacing.

Base Type	Number of sections	Mean friction	Minimum friction	Maximum friction
ATB	36	7.6	2.5	15.0
CTB (including soil cement)	15	9.5	3.5	23.0
LCB	7	8.5	3.0	20.0
GB	10	2.5	0.5	4.0
Fine grained soils	6	1.15	0.5	2.0

Climatic regions

Four different climatic zones were identified for LTPP CRCP sections:

- Dry $\leq$ 20 in/yr
- Wet > 20 in/yr
- Freeze > 150 oF-days/yr
- Non-freeze $\leq$ 150 oF-days/yr

Distribution of the LTPP sections used in calibration by climatic zone is shown in Figure 13.

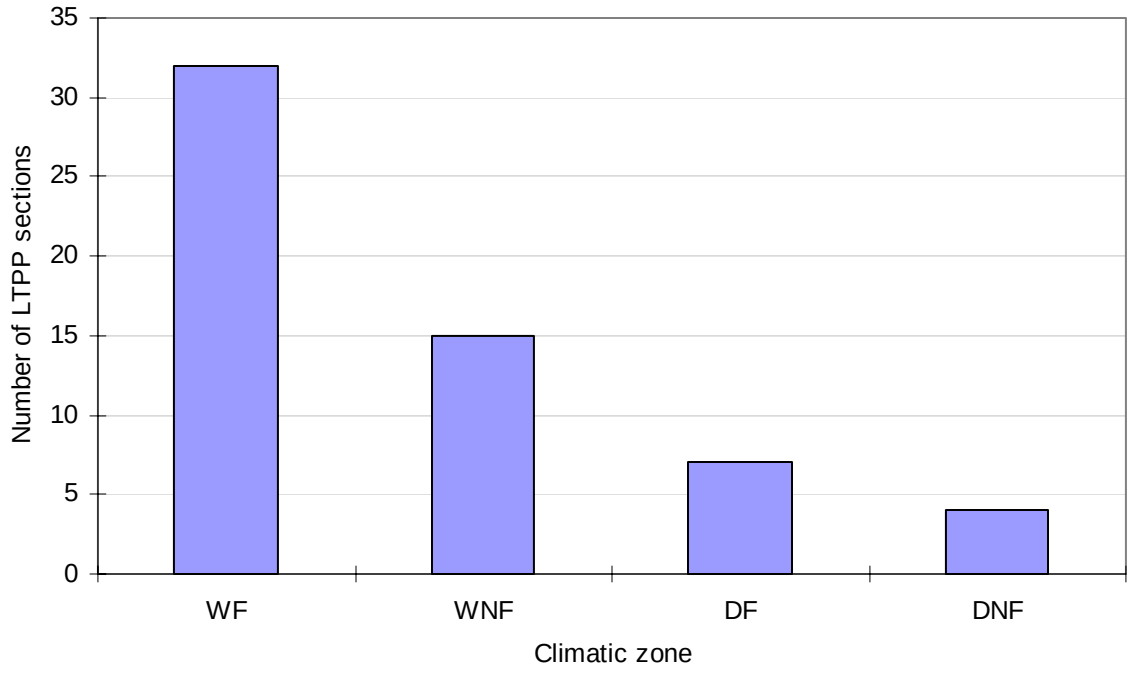

Figure 13. Distribution of LTPP sections used for calibration by climatic zone.

Transverse Crack Spacing

Transverse crack spacing is an important characteristic affecting CRCP performance. Using crack spacing measurements along the section obtained from the CRCP distress maps, descriptive statistical measures such as mean, standard deviation, coefficient of variation (COV), were computed for each LTPP section used in calibration.

The LTPP CRCP sections show a spectrum of transverse cracking varying from 0.1 to 3 m (0.25 to 10 feet). Mean crack spacing varies between 0.3 and 2.3 m (1 and 7.5 feet). The relationship between mean crack spacing and standard deviation of crack spacing was analyzed. The analysis indicates that LTPP CRCP sections with larger crack spacing usually have a larger standard deviation of crack spacing, as shown in Figure 14. The coefficient of variation obtained using all the LTPP sections with crack spacing information was found to be fairly stable, with an average value of 56%. This means that the standard deviation of the crack spacing is roughly half of the mean crack spacing.

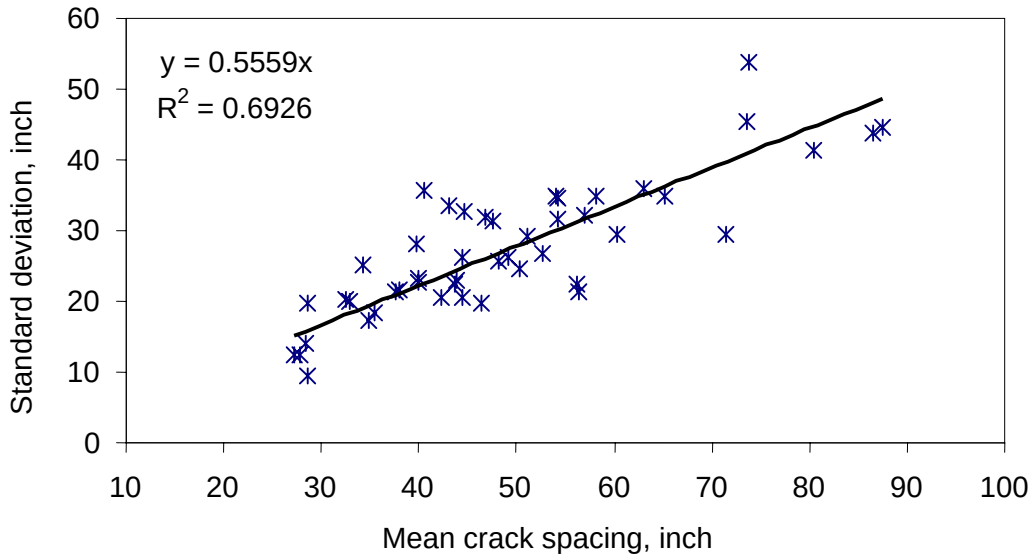

Figure 14. Comparison between mean crack spacing and standard deviation computed for LTPP GPS 5 CRCP sections.

The CRC pavement surface condition (distress) maps based on manual and automatic surveys were obtained and used in the analysis. LTPP distress data were collected at different times during the program.

Available punchout data were then correlated with transverse crack spacing information. The results of the analysis, presented in Figure 15, show that the majority of punchouts develop on CRCP panels that are approximately 1 to 2 ft in width.

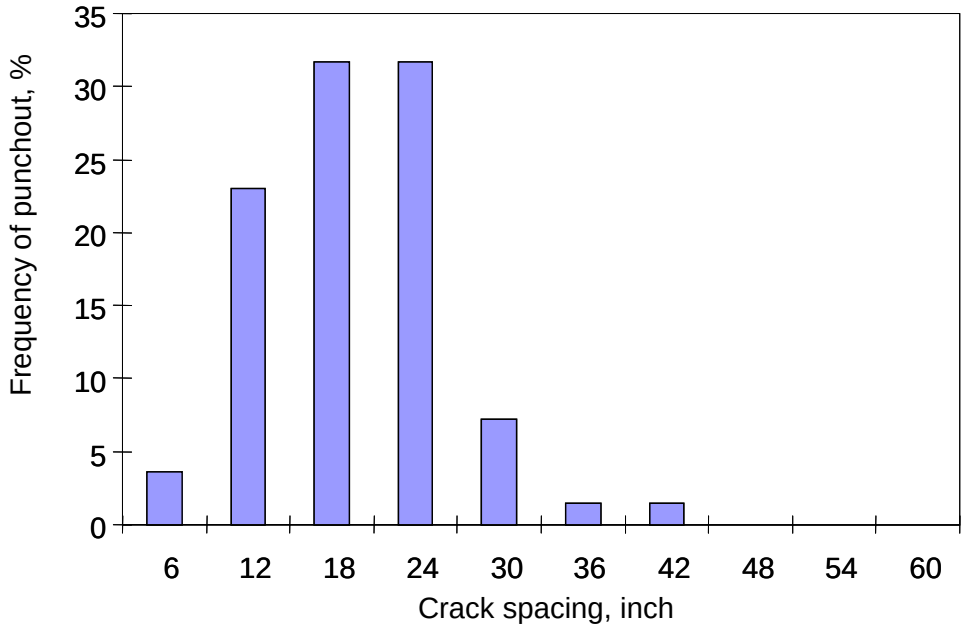

Figure 15. Punchout frequency on narrow segments for the LTPP GPS-5 experiment sections.

Observed Punchouts

LTPP CRCP distress data were used as a main source of data for calibration of the CRCP punchout prediction model. The actual field survey data sheets were reviewed for every CRCP section to verify the punchout count. The following criteria were used to interpret punchout data:

- Only outer lane/shoulder edge punchout and patches were considered in calibration.
- Y-cracks and inner lane punchouts were excluded due to a different mechanism of punchout development than the one used in the design model.
- Clustered punchouts formed by the same longitudinal crack propagating over several transverse crack segments were counted as one punchout.

LTPP includes three levels of punchout severity which were all included in the counting of punchouts:

- *Low:* Longitudinal and transverse cracks are tight and may have spalling less than 3 inches or faulting less than 0.25 inches.
- *Medium:* Longitudinal and transverse cracks have spalling 3 to 6 inches or faulting between 0.25 and 0.5 inches.
- *High:* Longitudinal and transverse cracks have spalling over 6 inches and concrete within the punchout is settled or loose and moves under traffic.

Over 90% of LTPP punchout data used for calibration were of "low severity". Therefore, when considering the critical CRCP punchout situation for design, if say 10 punchouts per mile were

selected, this would mean that at least 9 of them were defined as Low above. Over time, some of these areas will develop into higher levels of severity and require repair, but not all.

Another aspect is that LTPP sections were only 500 ft long and this resulted in a "step" function of punchouts. For example, if a section included 0 punchouts, this translated to 0 per mile. If a section included 1 punchout, this translated to 10 per mile. If 2 punchouts this translated to 20 per mile and so on.

Vandalia US 40 Experimental Sections

Data from the Vandalia experimental sections were used in the calibration since they added additional range of reinforcement content and measurements of crack width. Eight experimental sections were built on US 40 west of Vandalia, Illinois in 1947-48. These sections were monitored over the next 20 years until 1967 when I-70, which paralleled US 40, was opened to traffic. All sections are located in Wet-Freeze (WF) climatic region and were exposed to the same amount of traffic (4.3 million ESAL).

General design characteristics for the Vandalia sections are give in table 11. The experimental design of these eight sections included a 2 by 4 factorial as follows:

- Slab thickness of 7 and 8 inches
- Steel content of 0.3, 0.5, 0.7 and 1.0 percent (0.3 percent sections were not used in the 2002 Design Guide calibration)

Average daily traffic volumes for major truck classes and ESAL data were available for these sections. These traffic data were used to create axle load spectra based on regional axle load factors. Condition measurements were taken on these sections at 5, 10, 15, and 20 years after construction included crack spacing, crack width, smoothness, patched areas, steel ruptures. Punchouts were estimated from the distress maps and patching.

Crack Spacing and Width

Data from Vandalia experiment were used to help validate crack width prediction model utilized in CRCP punchout procedure. To test the crack width model, predicted crack spacing was compared to the crack spacing measured after the sections have been in service for 20 years. Since there were several unknowns regarding factors affecting crack spacing it was decided to adjust either the zero-stress temperature or the slab/base friction factor until crack spacing was similar to the 20 year measured mean crack spacing. The following Table 13 summarizes the crack spacing and the mean crack width at 20 years in the month of August when it was measured. The crack spacing is matched fairly well (as calibrated) and the crack widths are generally in good agreement but mostly lower. This is logical since the measured crack widths were at the surface and the predicted were at the depth of the reinforcement.

Table 13. Comparison between predicted and measured mean crack spacing and the mean crack width at 20 years for Vandalia, IL US 40 sections.

CRCP Slab, in	Rein-forcement %	Mean Measured Crack Spacing, in	Mean Predicted Crack Spacing, in	Mean Measured Surface Crack Width, mils*	Mean Predicted Steel Level Crack Width, mils**
7	0.3	122	112	35	34
	0.5	78	79	20	19
	0.7	68	72	16	13
	1.0	60	54	12	10
8	0.3	120	135	42	30
	0.5	90	91	28	17
	0.7	72	70	21	13
	1.0	60	56	11	9
Mean		84	84	23	18

* Reported crack width measured at the surface.
**Predicted crack width is at reinforcement level.

Illinois I-80 and I-94 Database Sections

Several sections of CRCP that were subjected to heavy traffic were obtained from the Illinois CRCP database. These sections are 9 and 10 in CRCP located along I-80 near Chicago and along I-94 (Edens expressway) in Chicago and provide some heavier trafficked sections that were left in service over long time periods. They essentially fill in some of the missing factor space of the LTPP sections. Table 11 shows a summary of design characteristics for these sections.

Calibration Database Summary

All the selected sections (58 LTPP, 6 Vandalia, and 7 Illinois) with available pavement design, performance, and traffic data were categorized in several groups using the following criteria:

- Slab thickness:
  - Low $\leq$ 9 in,
  - High > 9 in
- Percent steel:
  - Low $\leq$ 0.6 %,
  - High > 0.6 %
- Base type:
  - GB = Granular base
  - ATB = Asphalt treated base
  - CTB = Cement treated base

- Climate:
  - Dry ≤ 20 in/yr
  - Wet > 20 in/yr
  - Freeze > 150 oF-days/yr
  - Non-freeze ≤ 150 oF-days/yr

The number of calibration data points using data for the above mentioned sections available in each category is shown in Table 14.

Table 14. Factorial of CRCP sections used in the calibration.

Climate:		Wet						Dry					
		Freeze			No freeze			Freeze			No freeze		
Base Type:		ATB	CTB	GB	ATB	CTB	GB	ATB	CTB	GB	ATB	CTB	GB
% Steel	Thickness												
less than 0.6%	less than 9"	4	1	7	14	8	0	2	7	1	8	4	0
	9" or more	0	0	3	22	0	0	0	0	0	4	0	0
0.6% or more	less than 9"	8	5	22	10	15	7	0	0	0	0	0	0
	9" or more	31	4	2	5	12	3	0	3	0	0	0	0

Calibration Procedure

The 2002 design procedure is largely based on mechanistic engineering principles that provide a fundamental basis for the structural design of pavement structures. However, without calibration, the results of mechanistic calculations (fatigue damage) cannot be used to predict punchouts with any degree of confidence. Pavement responses (CRCP critical bending stresses) cannot be used directly to predict the rate of punchout development because the actual distress mechanisms are far more complex than we can practically model. Therefore, fatigue damage parameter obtained from the mechanistic model must be correlated with actual punchouts in the field. This is the reason why empirical factors and calibration is necessary to obtain realistic performance predictions.

The CRCP design procedures have been calibrated using design inputs and performance data largely from the national LTPP database, which includes sections located throughout significant parts of North America. As indicated earlier, the base friction values were adjusted within a reasonable range in order to match predicted crack spacings with the measured spacing. Figure 16 presents the correlation between the measured and predicted crack spacing in the sections used for calibration of the punchout model.

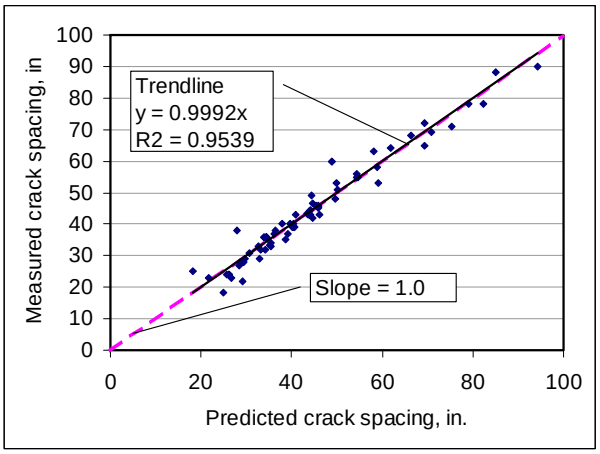

Figure 16. Predicted vs. Measured crack spacings of CRCP calibration database.

This calibration, performed using nationwide sections, resulted in a punchout prediction model with national calibration constants. The calibration curve represents "national" CRCP performance in the LTPP database. Whatever bias was included in the calibration data is naturally incorporated into the punchout prediction model.

The initial calibration was based on 80 percent of the data randomly chosen. The model was then "validated" using the remaining 20 percent of the data, which showed a similar fit. Since both models showed reasonable validation, all data were combined to obtain the final national calibration model.

Distress Prediction through Calibrated Models

The accumulated damage is a mechanistic parameter that represents what is going on within the pavement structure. The incremental damage is accumulated month by month and is converted to physical pavement distresses such as punchouts using a calibrated damage-to-distress correlation model. Each of the sections in the calibration database was run through the 2002 design software and the damage calculated from opening to traffic to the latest distress measurement data point. The results are shown in Figure 17. When "damage" is very small (e.g., 0.0001) the pavement structure would not be expected to have any significant physical distress (punchouts). As computed "damage" increases and approaches 0.1 to 1.0 or more, a significant number of punchouts is expected to occur. This plot shows 100 percent of the data and follows the above logic.

Calibrated Model

A calibrated model for punchout prediction as a function of accumulated fatigue damage due to slab bending in the transverse direction has the following functional form:

$$PO_i = \sum_{i=1}^{Life} \frac{a}{1 + b \cdot D_i^c} \tag{72}$$

where,

PO_i = total predicted number of punchouts per mile at the end of i^{th} monthly increment
D_i = accumulated fatigue damage (due to slab bending in the transverse direction) at the end of i^{th} monthly increment
a, b, c = calibration constants for punchout function

As a result of model calibration using national data set, the following calibration constants were derived:

- a = 105.26
- b = 4.00
- c = -0.38

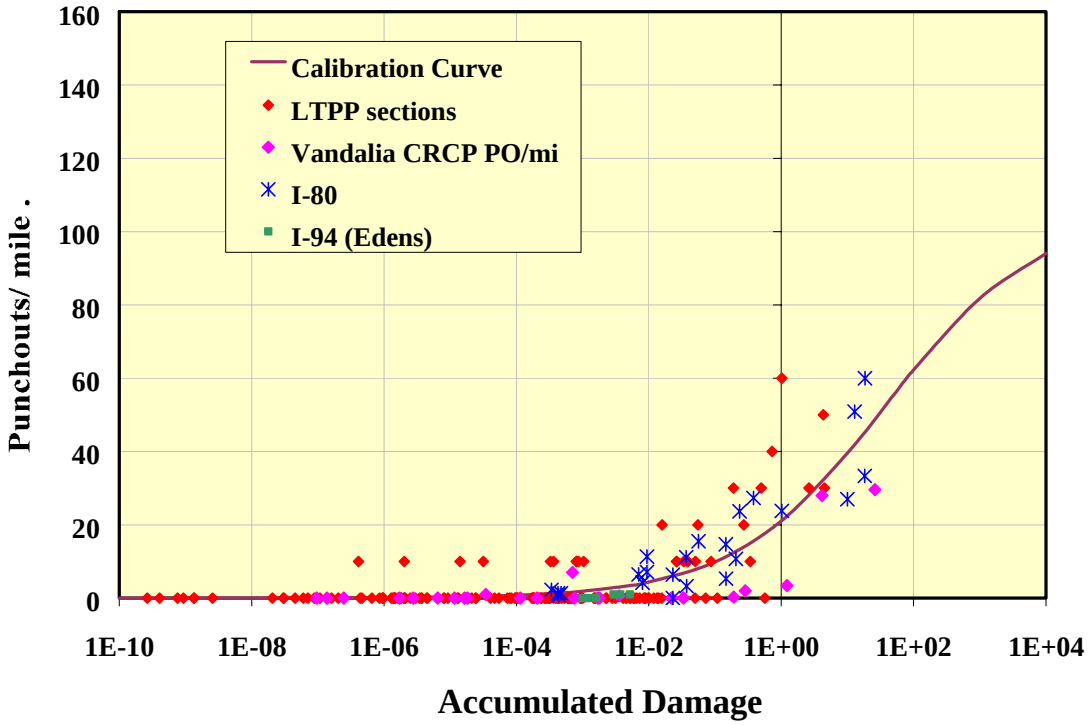

Figure 17. Relationship between computed fatigue damage and observed punchouts per mile in CRCP (100 percent of calibration database).

Predicted Vs. Measured Punchout

This data is plotted in Figure 18 showing the correlation between observed and predicted punchouts. A one-to-one line is included on the graph and the R-squared value is 68 percent, which indicates a reasonable fit to the data. The standard error of prediction will be discussed in the section on reliability analysis. The one-to-one graph shows that overall model does not have a bias towards underpredicting or overpredicting observed punchout values.

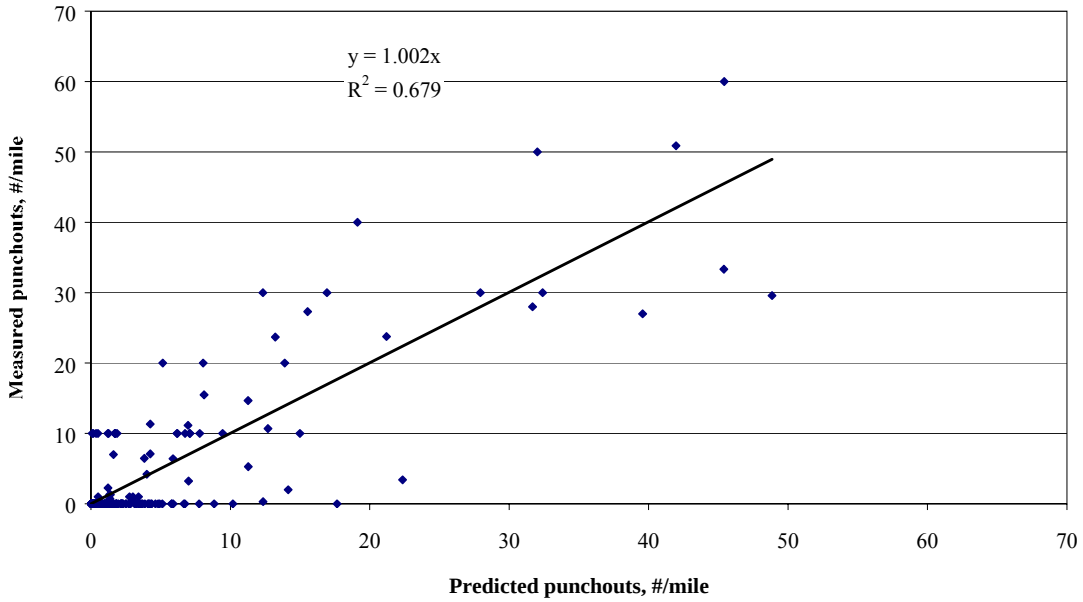

Figure 18. Predicted punchouts vs. Observed punchouts for 100 percent of CRCP calibration database.

A statistical verification was conducted to prove that the predicted and measured values for punchouts are not distinct. A two-sample paired t-test was the chosen method because the data sets contain a natural pairing of observations for each point along the timeline of the calibration sections. The t-test was performed at a confidence level of 95% (alpha value of 0.05) using the data shown in Figure 18. The t-test is performed based on the null hypothesis that there is no difference between the means of the two sets. The of t-test are presented in Table 15 and they indicate that the level of significance, or the p-value is greater than 0.05, thereby accepting the null hypothesis that the predicted and actual punchout values are not statistically different.

Table 15. Results of paired T-test statistic on measured and predicted punchouts

Statistical Quantity	Measured	Predicted
Mean	4.24	4.40
Variance	105.01	69.57
Observations	220	220
Pearson Correlation	0.82	
Hypothesized Mean Difference	0.0	
df	219.00	
t Stat	-0.41	
P(T<=t) one-tail	0.34	
t Critical one-tail	1.65	
P(T<=t) two-tail	0.69	
t Critical two-tail	1.97	

Reliability

The reliability procedure described in Appendix BB involved dividing the sections into four different groups in an optimum manner so that the mean predicted punchout closely matched the mean measured punchouts within the group. The standard deviation of each group increased as the mean predicted punchout increased. The measured standard deviation is plotted against the predicted punchouts in Figure 19 and the correlation is expressed as an exponential function, which forms the basis of the reliability incorporated in the CRCP design.

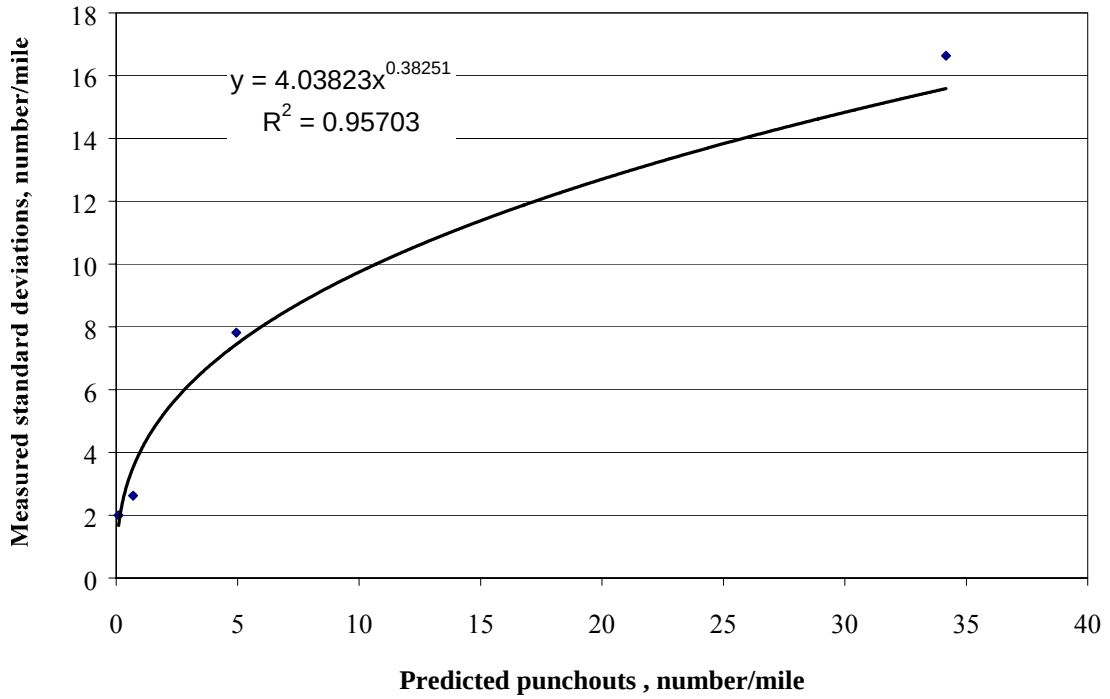

Figure 19. Standard deviation vs. mean punchouts for different groups

Limitations and recommendations for future studies

The national calibration model developed in this guide is subject to the following limitations:

- Observed punchouts included low, medium, and high, however, about 90 percent of them were of low severity (this is important to recall when selecting performance criteria for CRCP design).
- Short monitoring length (500 ft) resulted in large "steps" for observed punchouts (e.g., 1 punchout = 10 per mile, 2 = 20 per mile, 3 = 30 per mile) which obviously makes the prediction process quite difficult.
- Few CRCP sections were located in dry climatic zones.

- No field data on loss of support were available.
- No effective permanent curl/warp temperature measurements were available (nearly all sections were assumed to be -10^0 F which is the same as developed nationally for JPCP).
- No base friction measurements were available (values were assumed within the guidelines from table 12 for a given base type).
- No construction zero-stress temperatures were available (they were estimated from mean monthly temperatures during construction).
- Accuracy of construction and traffic opening dates were questionable for many sections.
- No actual 28-day PCC material properties were available (most were backcasted from long-term core tests).
- Numbers of traffic loadings were limited to about 40 million ESALs in the lane under consideration.
- Various design features were limited to those shown in the various tables of this section.

SENSITIVITY

Approach to Sensitivity Analysis

Sensitivity analyses were conducted to test the new CRCP punchout prediction procedure. This was accomplished by selecting typical design situations for different functional road types and truck traffic volume. The designs were selected to show adequate performance over the design period. The software was run and the punchouts were predicted over the design period. Then individual inputs were varied, normally one at a time (unless two or more were correlated and then two or more were varied in unison as would occur in nature such as PCC modulus of elasticity and strength) and the change in all outputs was observed. Appropriate tables and plots were prepared and the results were discussed.

Sensitivity Analysis Results

To test sensitivity of the CRCP structural performance prediction model to key input parameters, a series of sensitivity analyses were conducted. LTPP sections located in four climatic zones (WF, WNF, DF, DNF) were selected as a basis for sensitivity analysis. Two of sections located in Texas and Mississippi showed good performance over the years. These sections were exposed to medium and low truck traffic volumes and loads. One section located in Illinois had reached its performance criterion after 18 years of service. This section was exposed to high levels of track traffic volumes and loads.

The purpose of the sensitivity analysis was to see how change in different input parameters would affect CRCP performance over design life. Table 16 provides basic characteristics of the LTPP sections selected as “base” sections for sensitivity analyses.

Table 16. Basic characteristics of selected LTPP sections.

Section characteristic	LTPP Section ID			
	17-5843	**28-5006**	**38-5002**	**48-5278**
State	IL	MS	ND	TX
Slab thickness	10.4 inch	8.2 inch	8.0 inch	6.2 inch
% Steel	0.68	0.59	0.60	0.59
Base type	CTB	CTB	ATB	ATB
Climatic zone	WF	WNF	DF	DNF
ADTT (base year)	1,700	500	480	200
Avg. ESAL per truck	1.5	1.1	0.7	0.3
Compound Growth	3.6%	8.0%	5.0%	0.0%

The following input parameters and their ranges, shown in Table 17, were considered in the sensitivity analyses.

Table 17. Input parameters and ranges used in calibration.

Input parameter	Units	Range
Slab thickness	inch	7 – 11
% Steel	%	0.5 – 0.8
PCC Modulus of rupture	psi	500 – 900
PCC CTE	$x\ 10^{-6}\ {}^{o}F^{-1}$	4 – 7
Permanent curl/warp	^{o}F	-3 – -25
Climatic zone	N/A	WF, DF, WNF, DNF

The results of punchout prediction sensitivity to individual input parameters are discussed next.

Sensitivity Results for Slab Thickness

Figures 20, 21, 22, and 23 show the effect of slab thickness on punchouts for sections in four different climates. All sections show that as CRCP slab thickness increases punchouts decrease. Similar results have been obtained in several field experiments of CRCP. This is largely due to reduced critical stress levels. Note that as thickness increases over a certain level for each section, the benefit of using higher thickness diminishes.

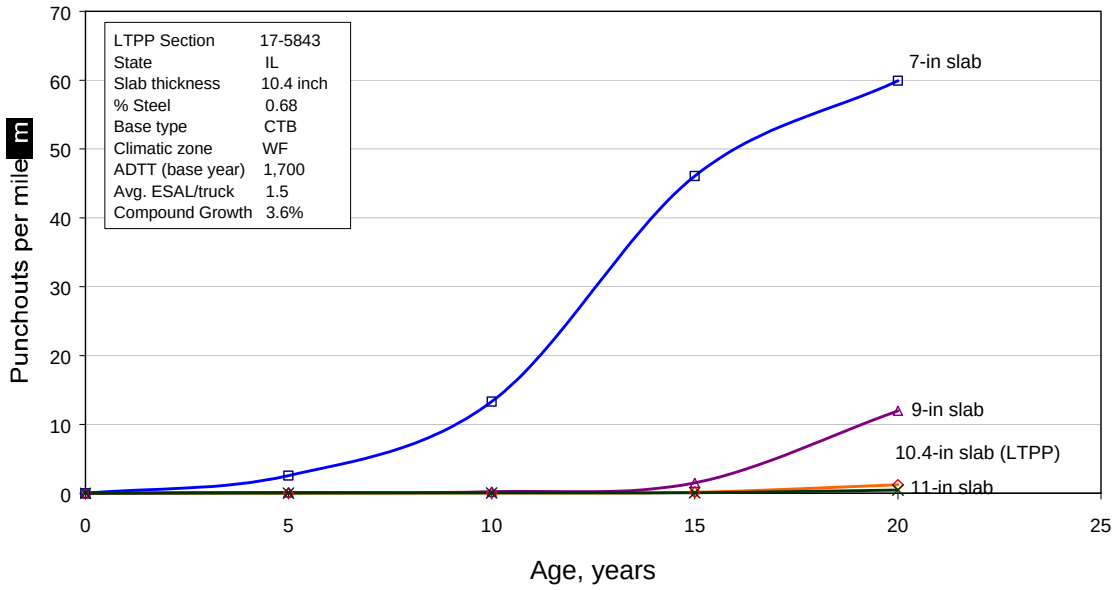

Figure 20. Predicted punchouts for various slab thickness for IL section 17-5843.

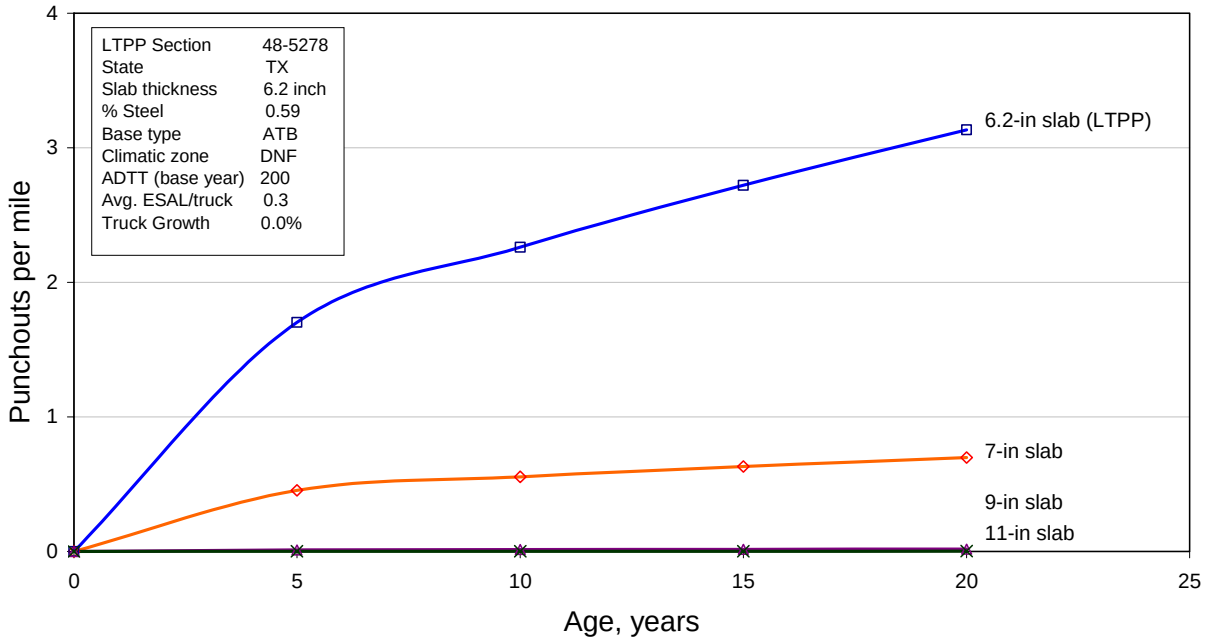

Figure 21. Predicted punchouts for various slab thickness for Texas section 48-5278.

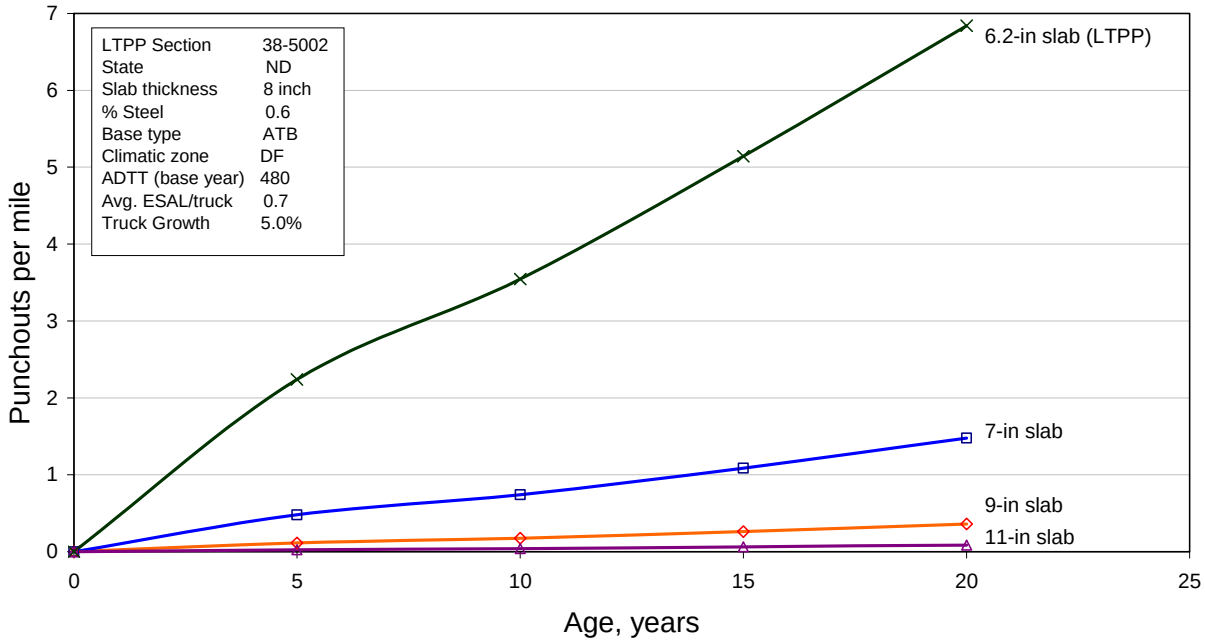

Figure 22. Predicted punchouts for various slab thickness for North Dakota section 38-5002.

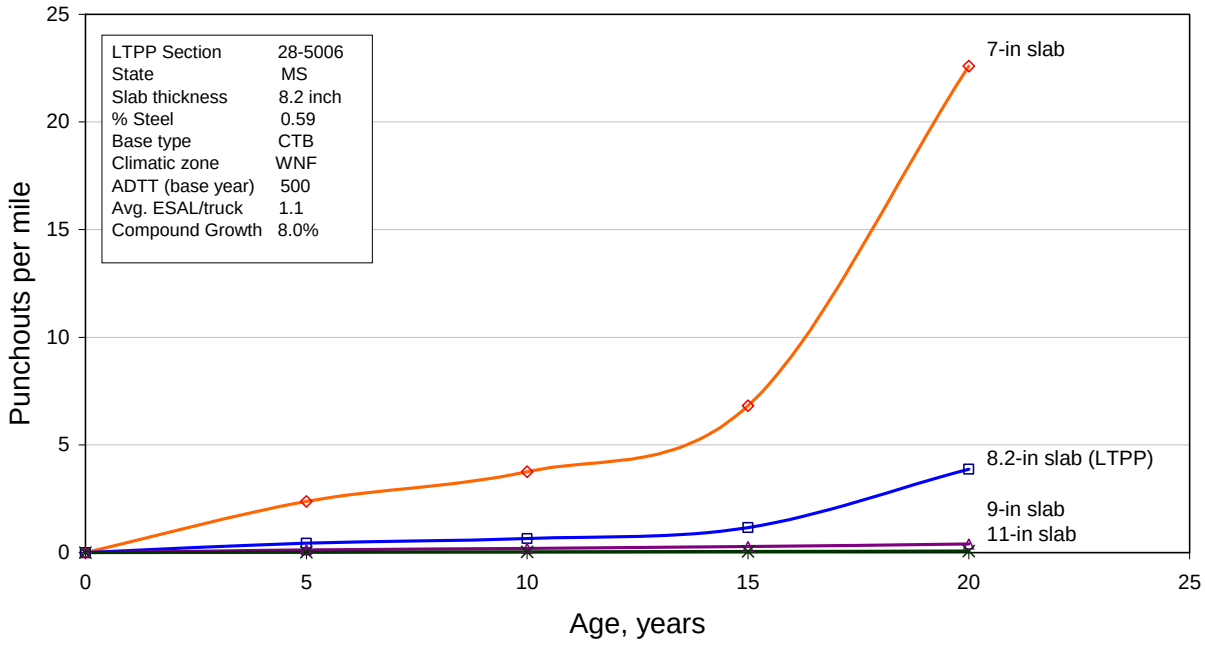

Figure 21. Predicted punchouts for various slab thickness for Mississippi section 28-5006.

Percent Reinforcement

Figures 24, 25, and 26 show the sensitivity of punchouts to the percentage of longitudinal reinforcement used in the CRCP slab. All plots show that as longitudinal reinforcement increases to 0.8 percent, the number of punchouts decrease dramatically. Similar results have been found in various field experiments. This is due to two effects. Higher reinforcement results in closer crack spacing and thus smaller crack openings. Higher reinforcement content also holds cracks much tighter together which is the key to maintaining good LTE over the life. The sensitivity shows that after a certain point (different for each section), increasing steel content does not result in any significant reduction in punchouts. Also, for the very thin Texas section in Figure 25, increasing steel content beyond 0.6 percent does not provide sufficient control of punchout development because the slab thickness is inadequate to prevent fatigue damage. Note that for the other sections with thicker slabs, the optimum steel content is higher. Thus, thickness and reinforcement content must be both considered to optimize design.

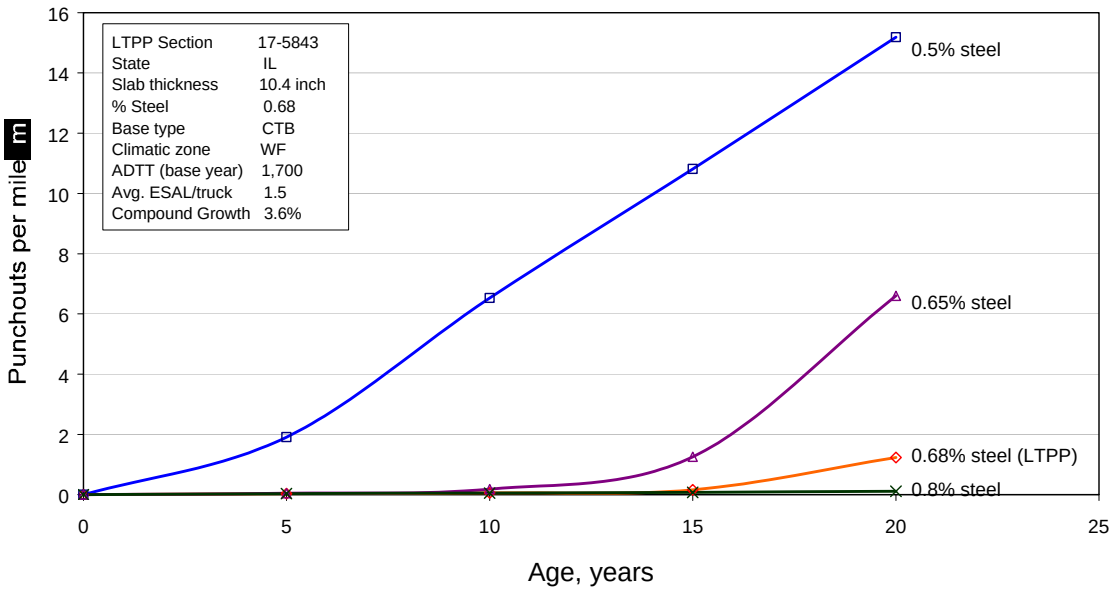

Figure 24. Predicted punchouts with various percent of longitudinal reinforcement for Illinois 17-5843.

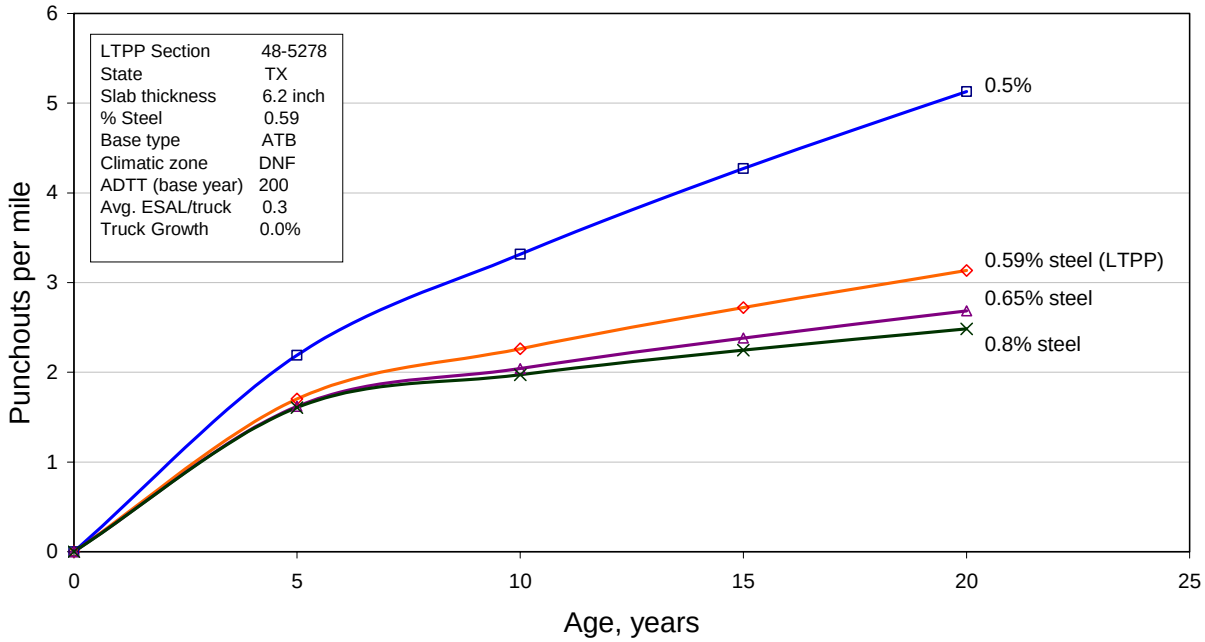

Figure 25. Predicted punchouts with various percent of longitudinal reinforcement for Texas 48-5278.

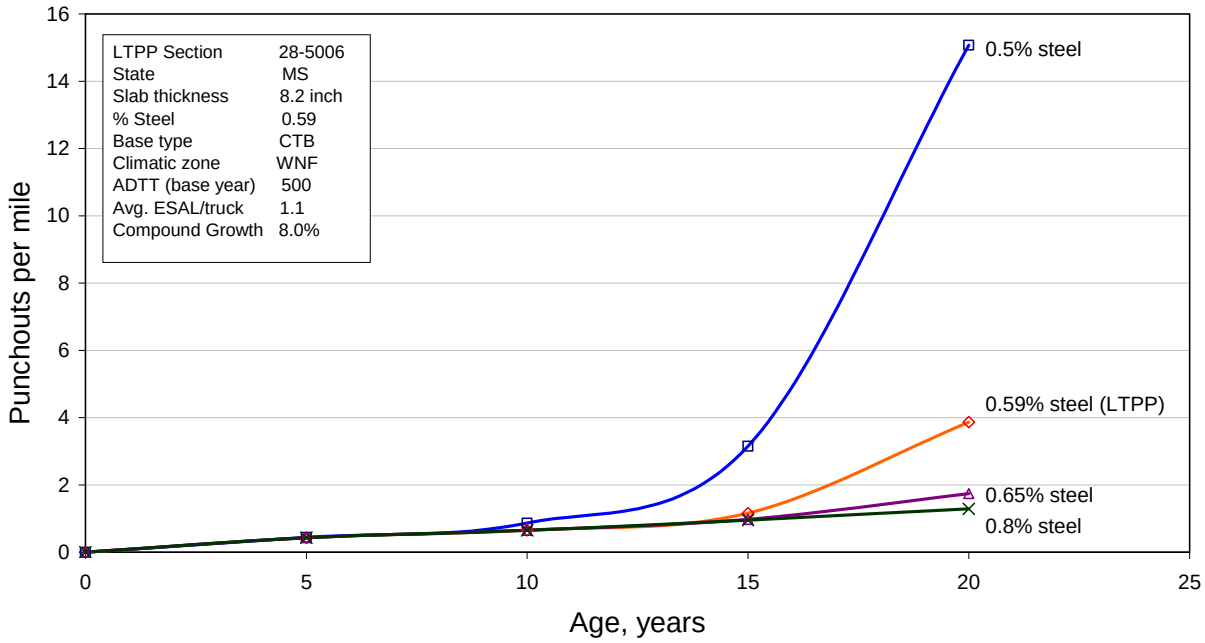

Figure 26. Predicted punchouts with various percent of longitudinal reinforcement for Mississippi 28-5006.

Reinforcement Cover

Figure 27 shows the effect of reinforcement cover on punchouts for the Illinois section. Reinforcement cover is characterized by a distance from the slab surface to the top of the longitudinal reinforcement. This example demonstrates that the deeper the reinforcement the more punchouts occur over time. This result has been observed in field performance of CRCP. It occurs because when reinforcement is higher in the slab it keeps cracks tight at the top of the slab. This reduces the amount of crack deterioration and helps maintain high LTE.

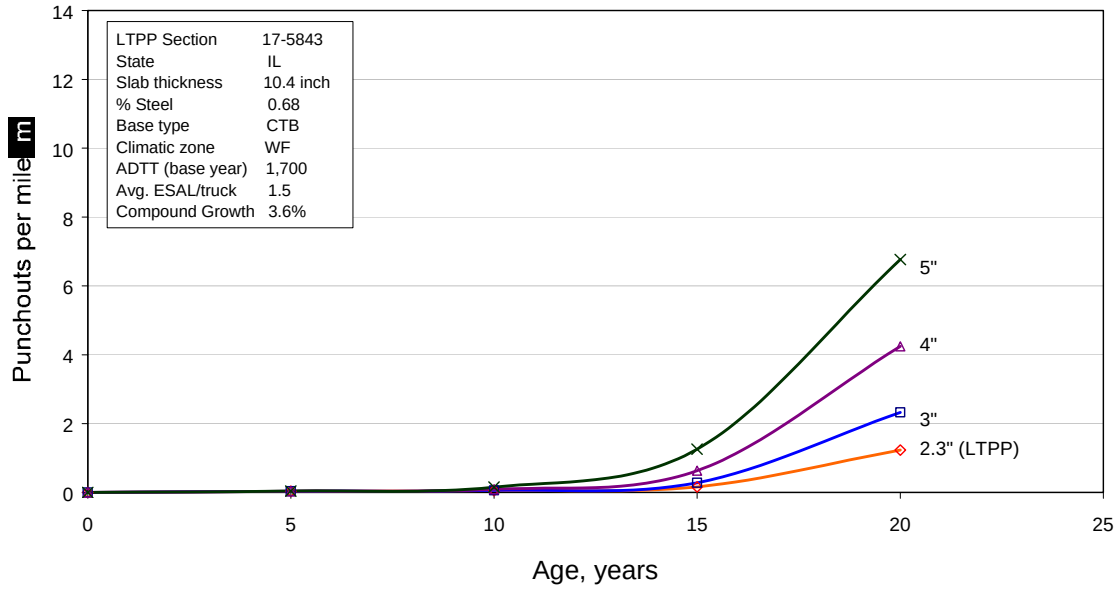

Figure 25. Predicted punchouts for sections with various reinforcement cover for Illinois 17-5843.

PCC Flexural Strength

Figures 28, 29, 30, and 31 show the effect of PCC flexural strength on punchouts development for the four sections chosen for sensitivity analysis in different climatic locations. The labels on the plot show 28-day PCC modulus of rupture. All sections show that as the modulus of rupture increases the number of punchouts decrease dramatically. This is due to lower fatigue damage with higher strength PCC. Sections with PCC modulus of rupture 700 psi or less developed greatly increased number of punchouts. There is also a point of diminishing returns where increased strength does not improve performance significantly.

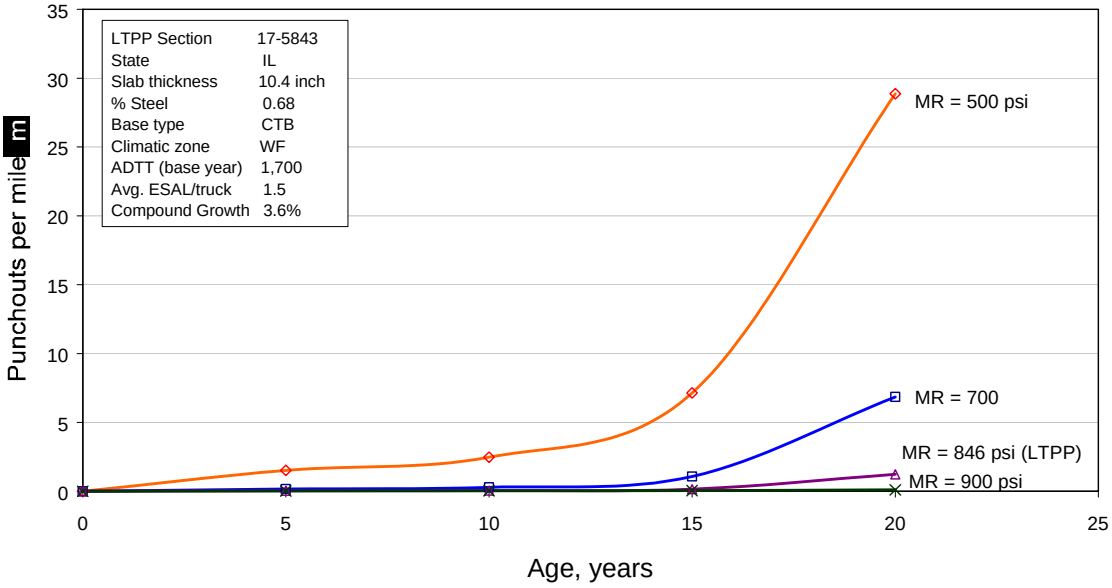

Figure 28. Predicted punchouts for sections with various PCC modulus of rupture for Illinois 17-5843.

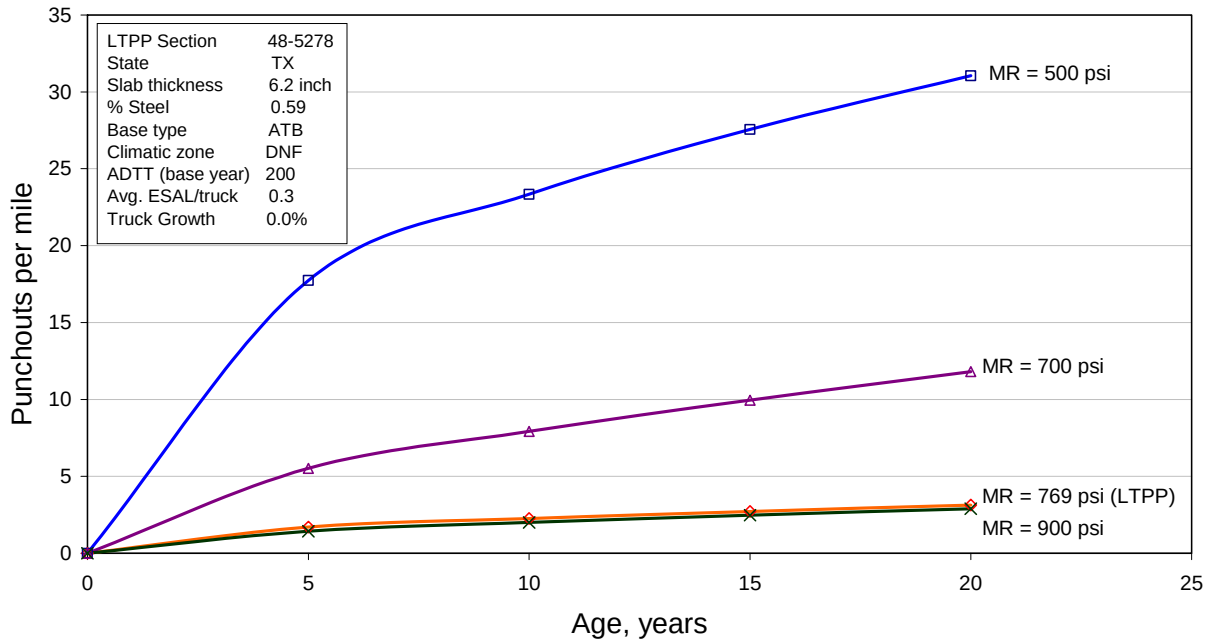

Figure 29. Predicted punchouts for sections with various PCC modulus of rupture for Texas 48-5278.

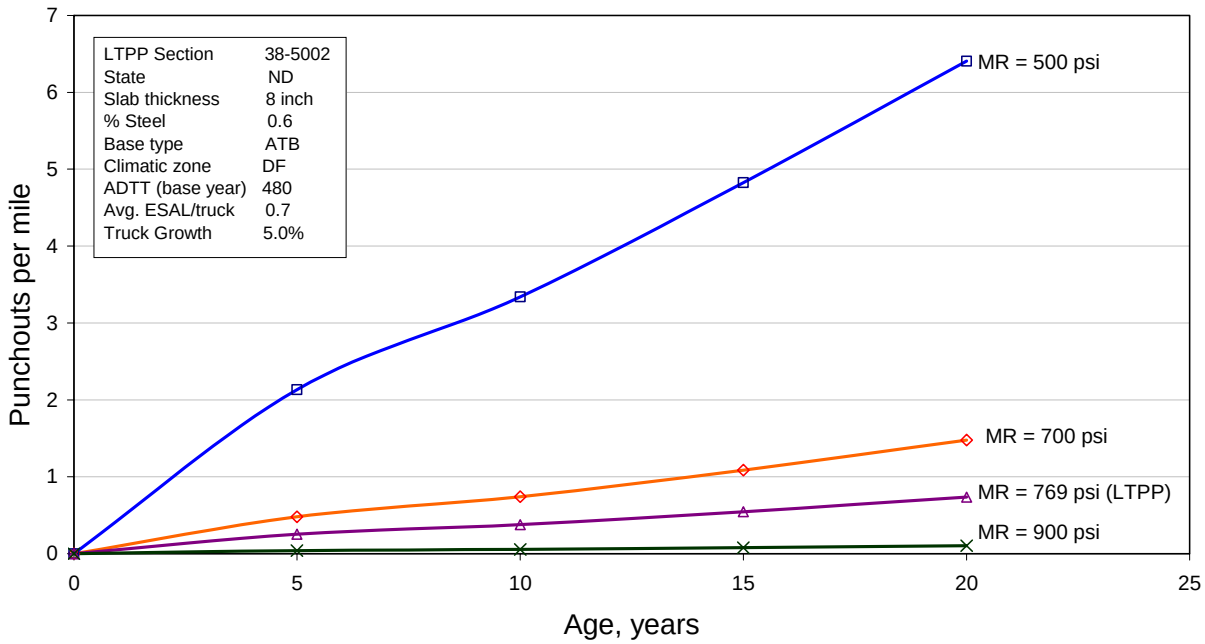

Figure 30. Predicted punchouts for sections with various PCC modulus of rupture for North Dakota 38-5002.

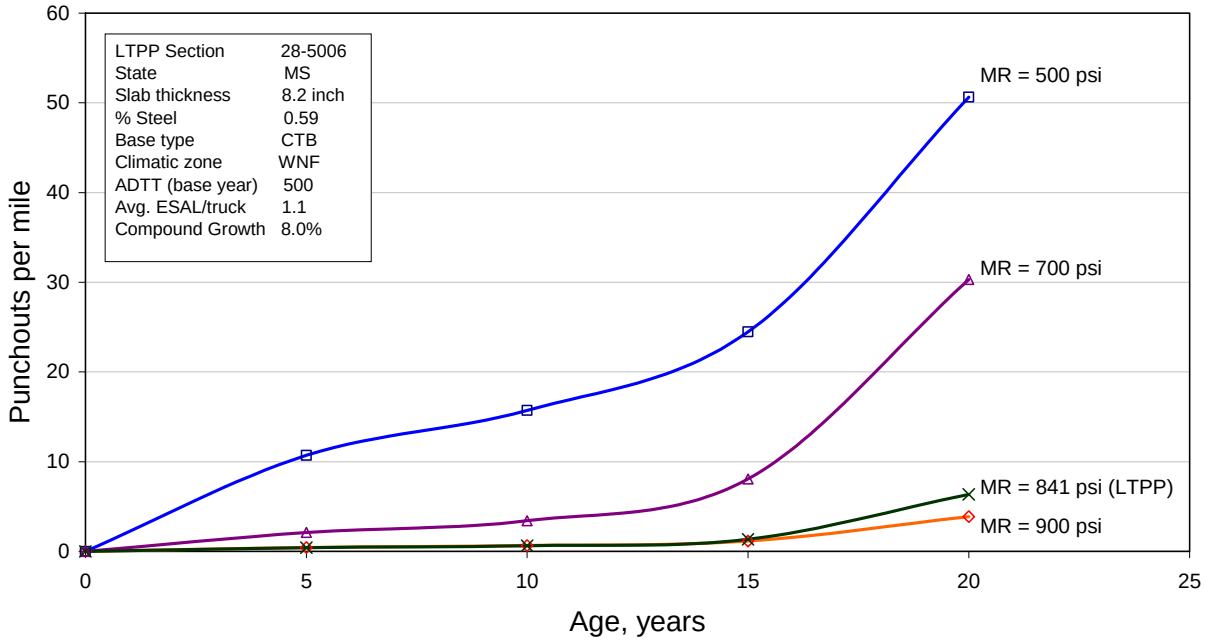

Figure 31. Predicted punchouts for sections with various PCC modulus of rupture for Mississippi 28-5006.

PCC Coefficient of Thermal Expansion (CTE)

Figures 32, 33, 34, and 35 show the effect of the thermal coefficient of expansion (CTE) on punchout development for the four sections in different climatic locations. The higher the CTE the higher the number of predicted punchouts. This result is due to two mechanisms. First, higher CTE results in wider crack openings and subsequently increased loss of LTE. Second, higher temperature curling of the CRCP slab results in higher bending stresses at the top of the slab and increased fatigue damage.

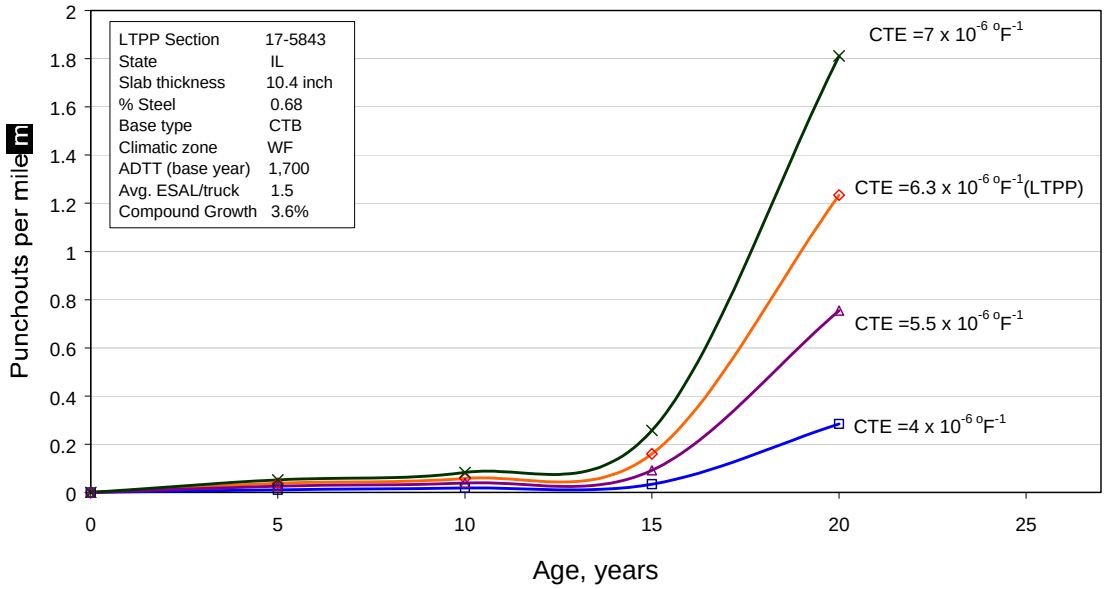

Figure 32. Predicted punchouts for sections with various PCC CTE for Illinois 17-5843.

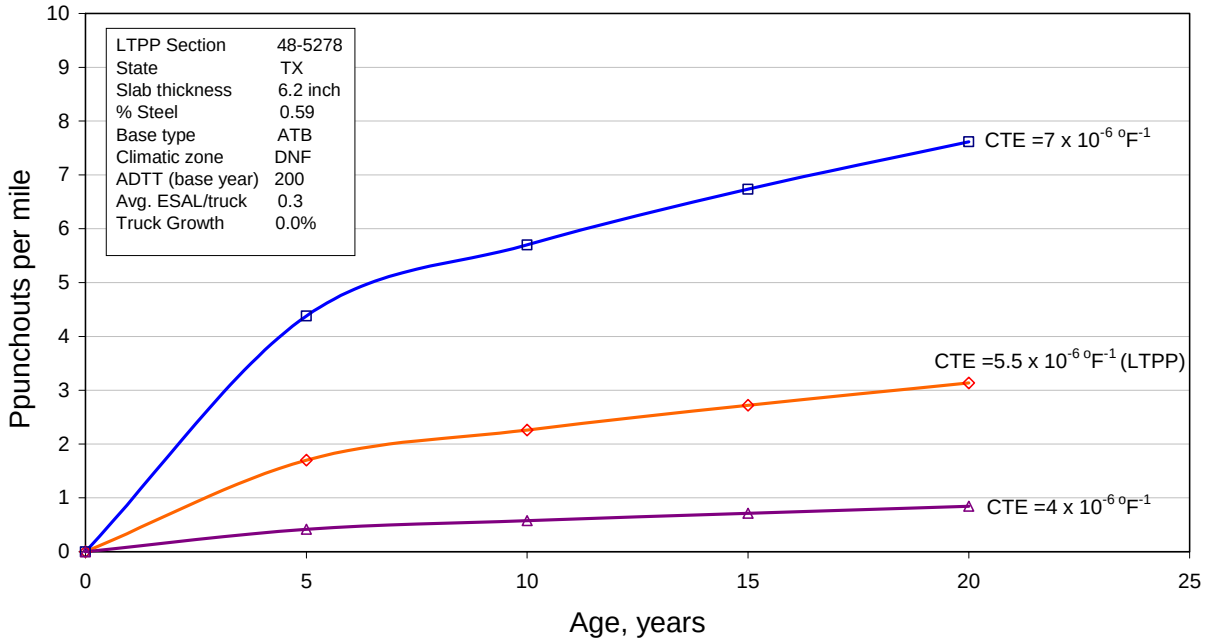

Figure 33. Predicted punchouts for sections with various PCC CTE for Texas 48-5278.

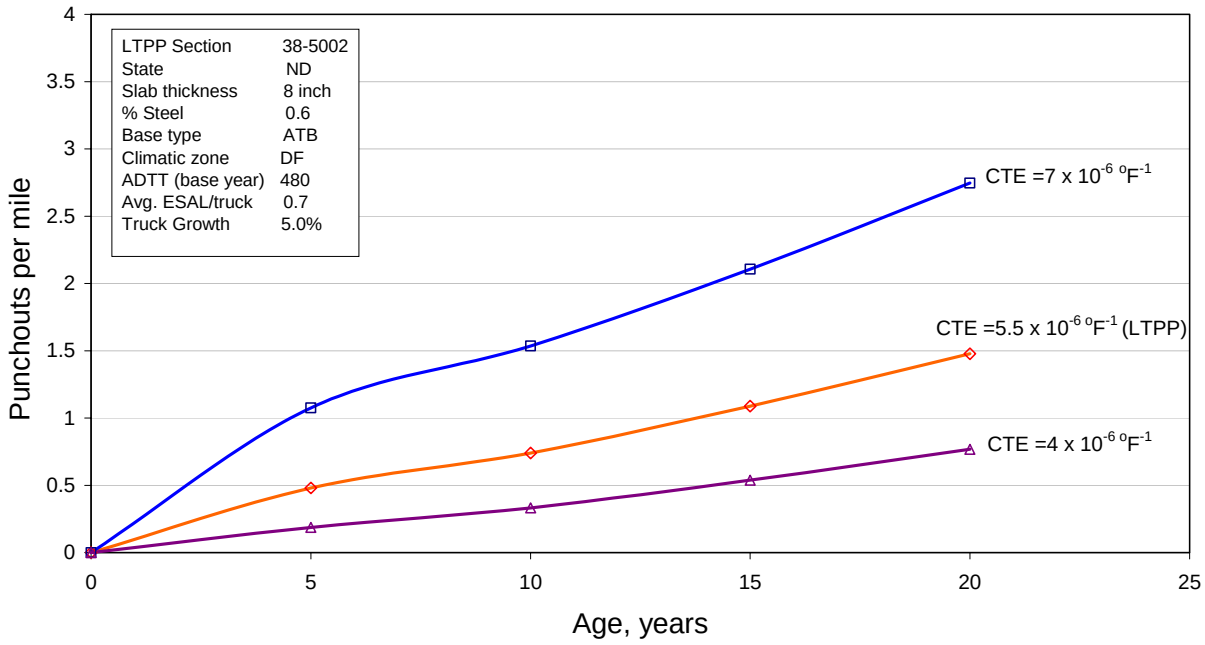

Figure 34. Predicted punchouts for sections with various PCC CTE for North Dakota 38-5002.

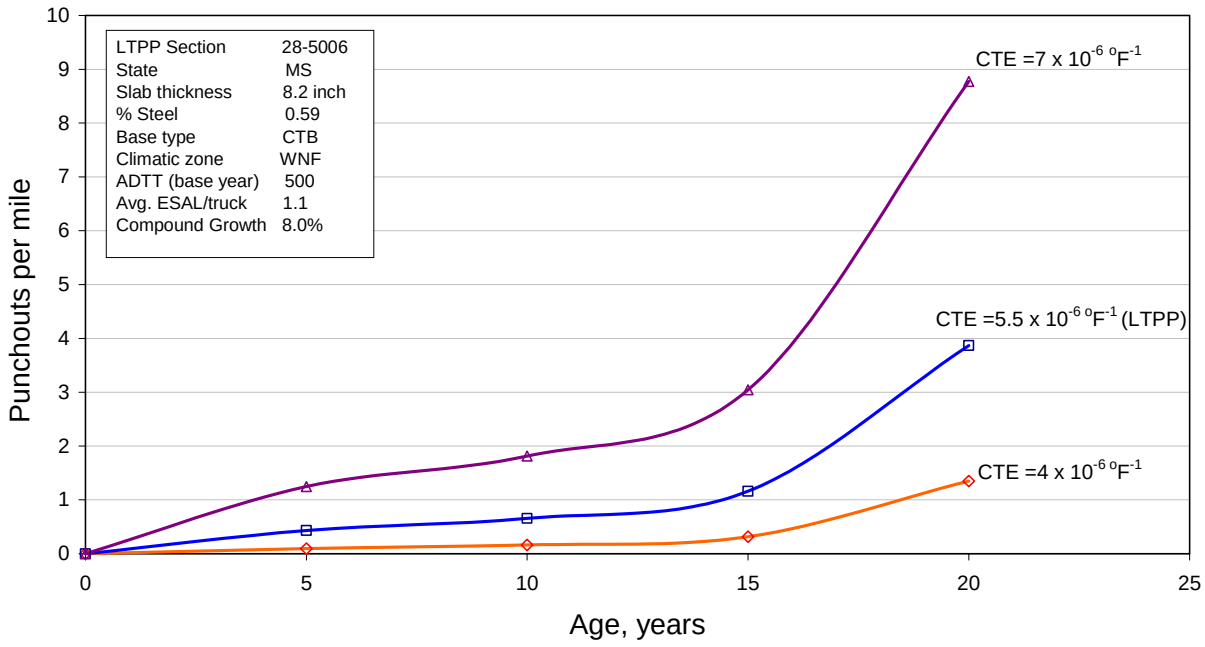

Figure 35. Predicted punchouts for sections with various PCC CTE for Mississippi 28-5006.

Permanent Slab Curl/Warp

Figures 36, 37, 38, and 39 show punchout prediction over a range of permanent curl/warp temperatures in the sections chosen for sensitivity analysis from different climatic areas of the nation. Permanent curl/warp is the combination of built-in temperature gradients and permanent moisture gradients expressed in terms of equivalent linear temperature differential between slab top and bottom. The nationally determined calibrated value was -10^0 F for JPCP and this value was used for all CRCP also. As it becomes larger, punchouts increase due to the increased negative curl which results in increased tensile stress at the critical top of slab location.

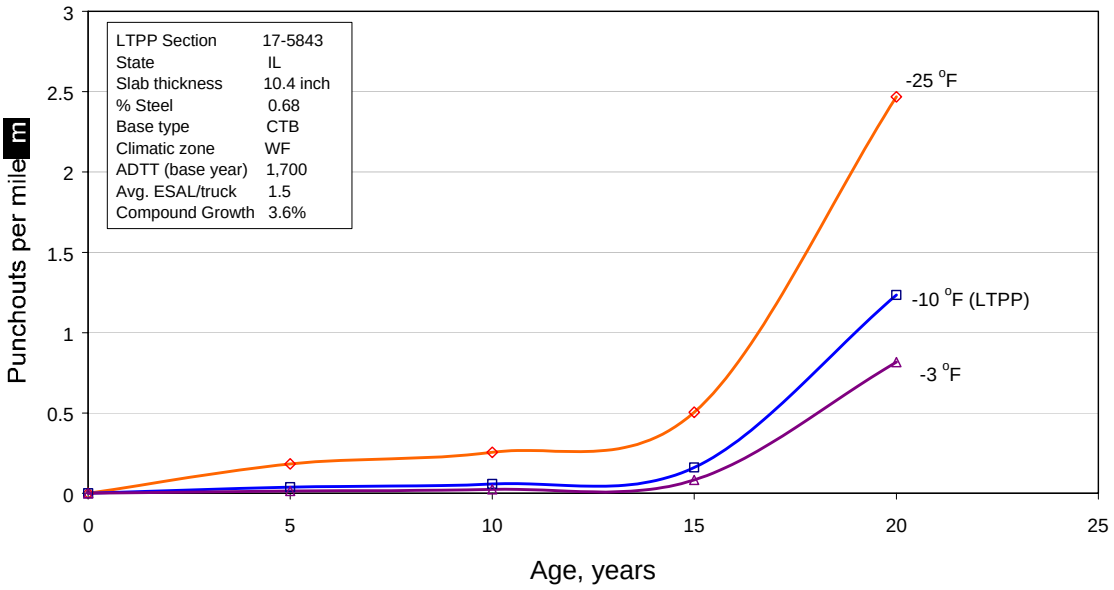

Figure 36. Predicted punchouts for various permanent curl/warp temperatures for Illinois 17-5843.

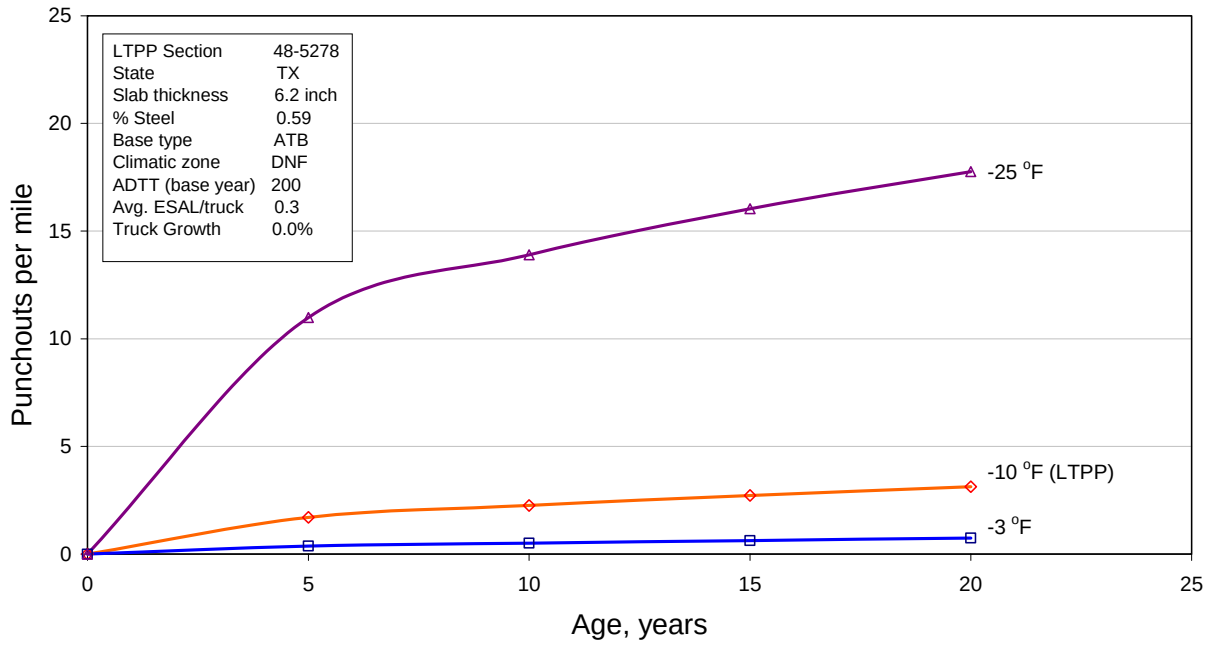

Figure 37. Predicted punchouts for various permanent curl/warp temperatures for Texas 48-5278.

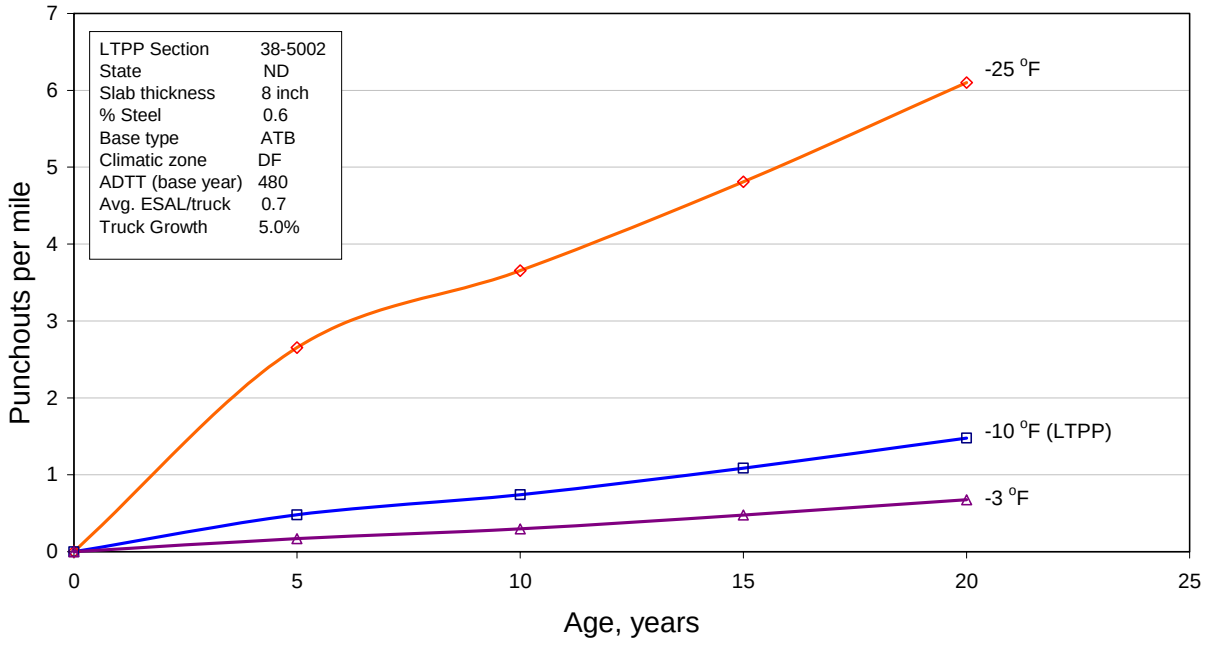

Figure 38. Predicted punchouts for various permanent curl/warp temperatures for North Dakota 38-5002.

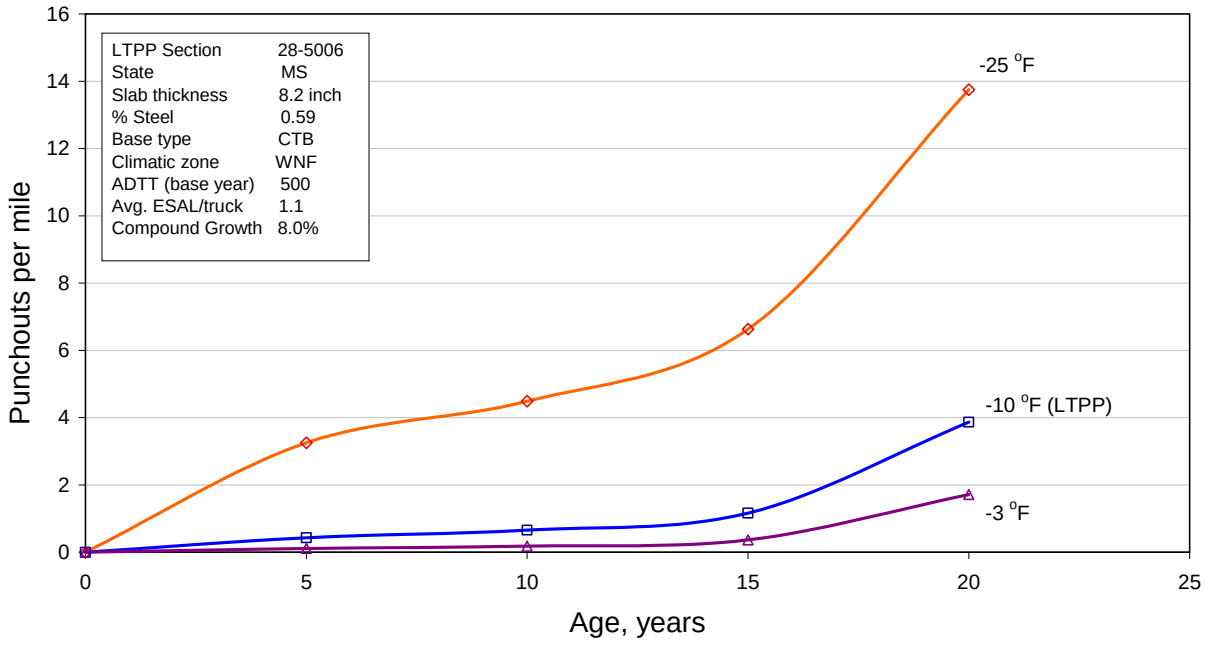

Figure 39. Predicted punchouts for various permanent curl/warp temperatures for Mississippi 28-5006.

Punchout Sensitivity to Traffic

Sensitivity of punchout prediction to the axle loads and axle load repetition was investigated. Only edge load applications were considered in sensitivity analysis based on the fact that edge loads result in the highest tensile stresses leading to punchout development. A hypothetical section with moderate deterioration of load transfer capacity across the transverse cracks was analyzed. Results of sensitivity analysis of punchout prediction to axle load spectrum characteristics are shown in Figure 40 for single and tandem axle load spectra.

Figure 40 indicates that punchout development mechanism is mostly insensitive to load applications less than 18 kip for single axle loads and 36 kip for tandem axle loads. However, heavy loads have a very profound contribution to punchout development. Accurate estimation of the number of heavy loads is very important for punchout prediction.

Single Axle

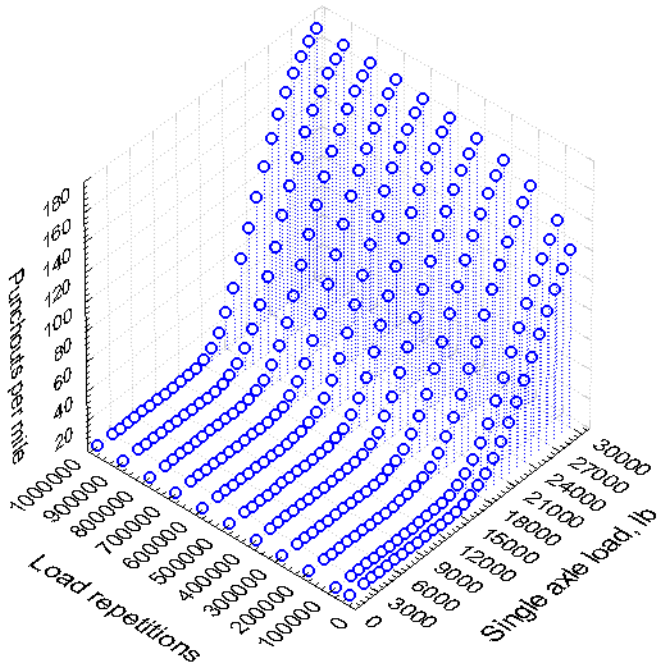

Tandem Axle

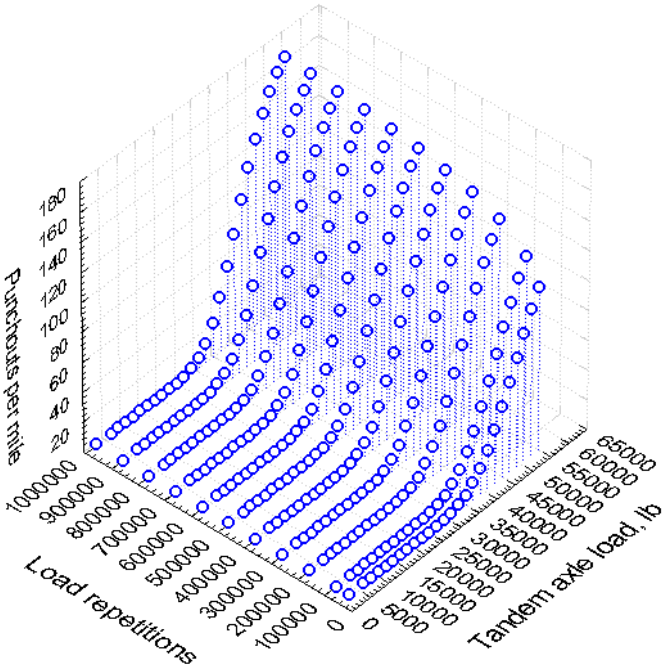

Figure 40. Sensitivity of punchout distress to load spectrum characteristics.

Lateral Load Position

The lateral movement of trucks across the lane has been shown in previous studies to be approximately normally distributed. The contribution of axle loading positioned at different lateral offsets to the overall damage was examined. The results of the fatigue damage analysis are presented in Figure 41. As can be seen, the relative contribution of a small number of edge loads to the overall damage is much more significant than contribution of large number of loads positioned away from the edge. The results in figure 41 also indicate that fatigue damage is very sensitive to LTE.

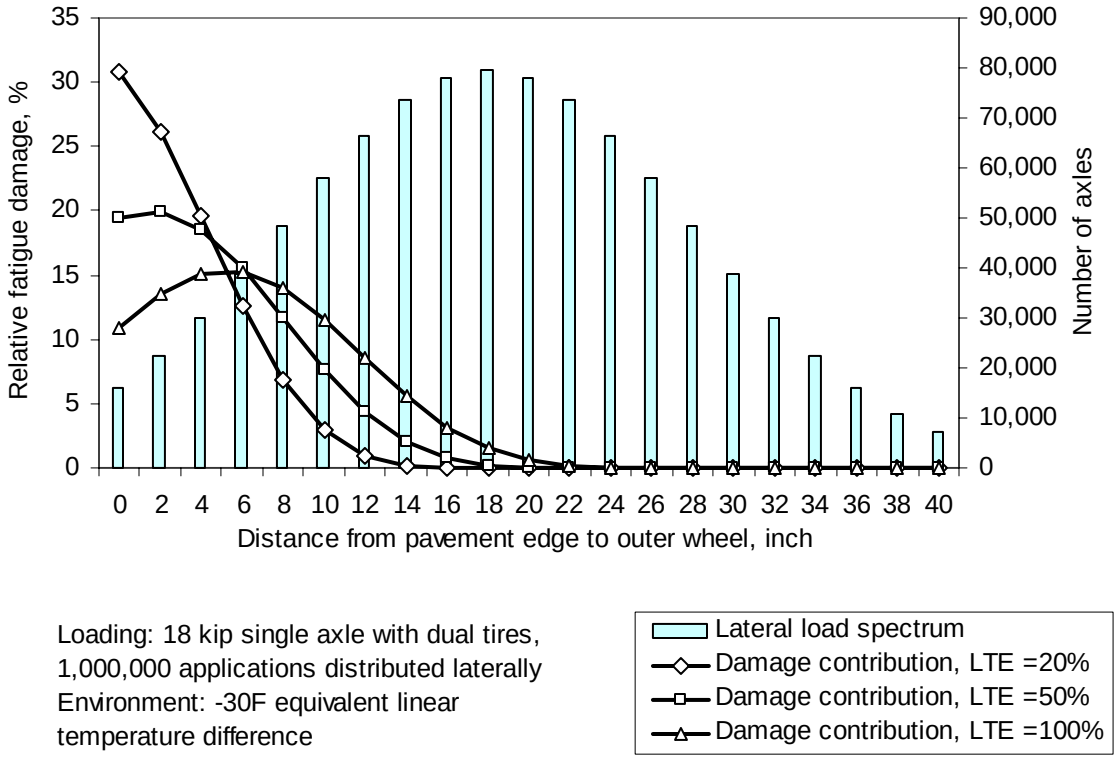

Figure 41. Sensitivity of fatigue damage to lateral traffic wander.

Sensitivity Analysis for Reliability

The CRCP punchout prediction model was run over a range of levels of design reliability. This was done for three different LTPP sections to gain knowledge of its magnitude and effect. Note that these three sections chosen are different from the four sections chosen for sensitivity analysis from different climatic areas. Figures 42, 43, and 44 show the results of reliability levels from 50 to 99.9 percent. Punchouts are plotted over time for each level of reliability. The results show that as the level of reliability increases, the number of predicted punchouts becomes greater. The rate of increase becomes higher as reliability becomes higher.

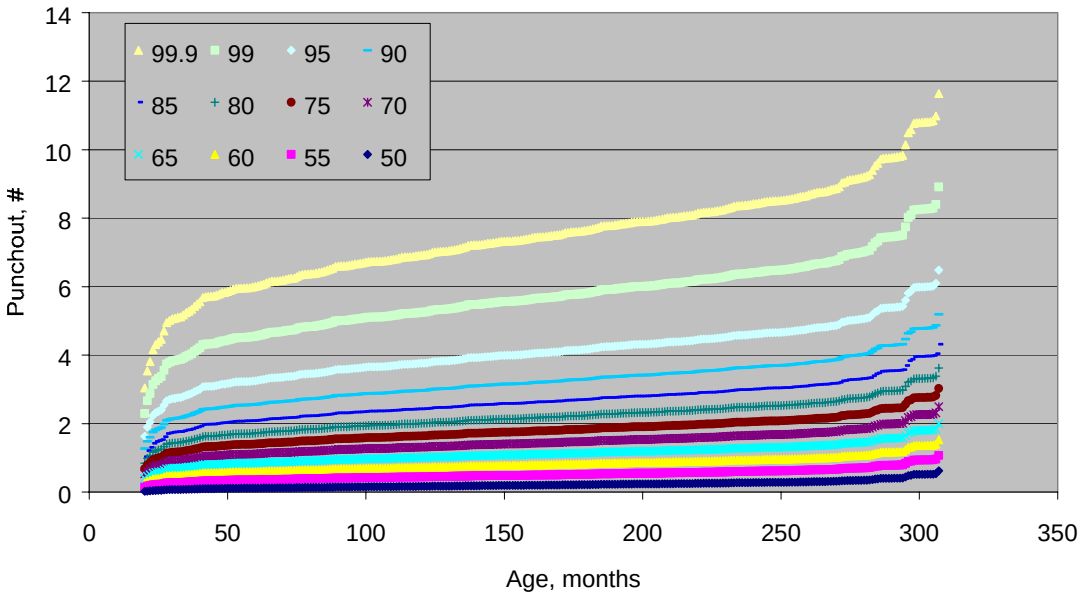

Figure 42. Predicted number of punchouts for section 01-5008.

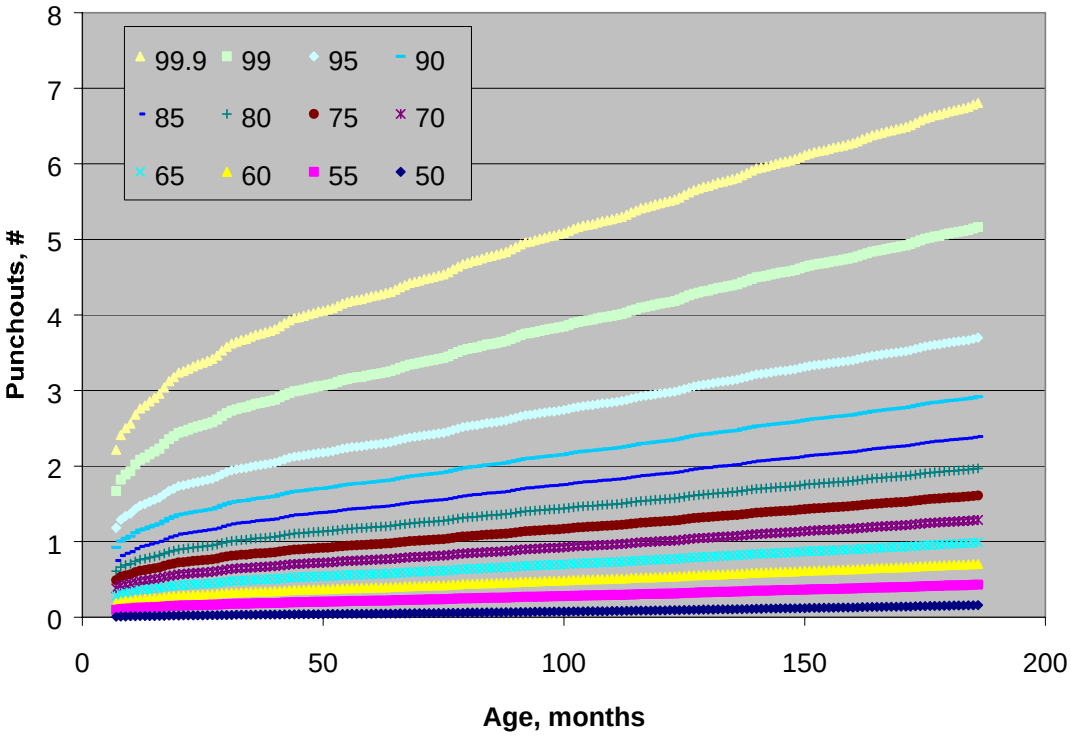

Figure 43. Predicted number of punchouts for section 17-5020.

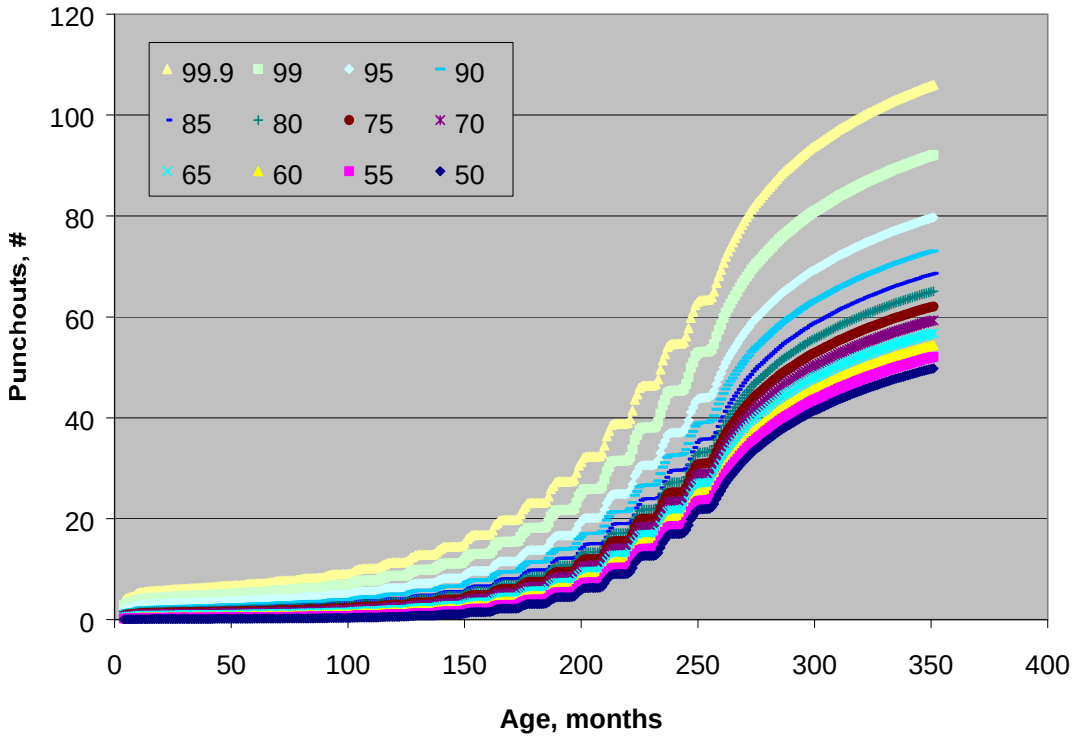

Figure 44. Predicted number of punchouts for section 37-5037.

IMPLEMENTATION CONSIDERATIONS

Any agency interested in adopting the CRCP design procedure described in this guide should prepare a practical implementation plan. The plan should include training of staff, acquiring of needed equipment, acquiring of needed computer hardware, procedures for obtaining all inputs, and calibration/validation to local conditions.

The use of mechanistic principles to both structurally and climatically (temperature and moisture) model the pavement/subgrade structure requires comprehensive input data to run such a model (including axle load distributions, improved material characterization, construction factors, and hourly climatic data such as ambient temperatures, precipitations, solar radiation, cloud cover, and relative humidity). Thus, a significant effort will be required to evaluate and tailor the procedure to the highway agency. This will make the new design procedure far more capable of producing more reliable and cost-effective designs, even for design conditions that deviate significantly from previously experienced (e.g., much heavier traffic).

Calibration to Local Conditions

Need For Calibration to Local Conditions

The national calibration-validation process has been successfully completed. The results appear to be reasonable as well as all of the sensitivity runs made using the final procedure. Although

this effort was very comprehensive, further validation study is highly recommended as a prudent step in implementing a new design procedure.

A highway agency (or several agencies geographically close) could develop a "local validation" CRCP database to confirm that the national calibration factors or functions are adequate and appropriate for the construction, materials, climate, traffic, and other conditions that are encountered within the agencies highway system. If no CRCP have been built in the area then the agency could utilize the national calibration models to develop the designs or check it against some data from nearby states.

The IRI models for CRCP are empirical in nature and were developed directly from the LTPP data. Further validation for a local agency may not be needed, but could be accomplished if desired as described in this section.

Approach to Local Calibration

Because this design procedure is based on mechanistic principles the procedures should work reasonably well within the inference space of the analytical procedure and the performance data from which the procedure was calibrated. However, this is a very complex design procedure and it must be carefully evaluated by highway agencies wishing to implement. The following is the recommended calibration/validation effort required to implement this 2002 mechanistic-empirical design procedure:

1. Review all input data and establish procedures for obtaining each input including the appropriate level. Laboratory and field testing to build a materials library will be required. Assessment of traffic data will also be required and it may be necessary to collect additional data to build an adequate traffic loadings library.
2. Conduct sensitivity analysis of all inputs.
3. Conduct comparative studies (with current design procedure).
4. Conduct validation/calibration studies using performance data from the agency.
5. Modify input defaults and calibration coefficients as needed.

Review All Input data

- Determine the desired method and level for obtaining each input on various types of design projects (low volume as compared to high volume where achieving an adequate design is more critical). The 2002 Guide allow three levels of inputs and each level has different procedures.

    - Level 1—site-specific testing data such as laboratory testing, FWD testing, ATC and WIM testing on site.
    - Level 2—regional factors and material properties from available testing procedures or correlation equations (e.g., use of compressive strength to estimate modulus of rupture).
    - Level 3— typical local values (if known) or default values

Note that the information available for the calibration under NCHRP Project 1-37A was generally Level 1 and Level 2 with some Level 3. Several inputs are very critical but are not well defined and these are the ones where the agency should conduct sensitivity analysis as described below.

- Determine if defaults provided with the 2002 software are appropriate for the agency and modify if needed.

- Select allowable ranges for inputs for various types of projects within the geographical area of the agency (low volume, high volume, different geographic areas within the state).

- Select procedures to obtain these inputs for regular design projects (e.g., traffic volume and weight inputs). Determine the effects of the accuracy of input values on the resulting design.

- Conduct necessary testing to establish specific inputs (e.g., PCC coefficient of expansion, PCC elastic modulus, PCC ultimate shrinkage, axle load distributions), acquire needed equipment for any testing required. Build materials and traffic libraries for those conditions to be used in design.

Sensitivity Analysis

Each agency should conduct sensitivity analysis of the new design procedure. This is accomplished by selecting a typical design situation with all design inputs. The software is run and the mean distresses and IRI predicted over the design period. Then individual inputs are varied, normally one at a time (unless two or more are correlated and then two or more are varied in unison as would occur in nature such as PCC modulus of elasticity and strength) and the change in all outputs observed. Appropriate tables and plots are prepared and the results evaluated. Inputs can be divided into three groups for example:

1. Those that have very significant effect on one or more outputs.
2. Those that have a moderate effect on one or more outputs.
3. Those that have only minor effect on one or more outputs.

Those inputs that belong to group No. 1 must be more carefully selected than No. 3 as they will have a very significant effect on design. The above sensitivity may be repeated for low, medium and high traffic project designs to see if that has an effect on inputs.

Comparative Studies

Conduct comparisons of designs from the new 2002 design procedure with those of the existing design procedure or other procedures such as those recommended by the industry associations. Select typical design situations (previous designs would be ideal) and obtain the design inputs for the 2002 Design Guide. Run the 2002 software and determine the distresses and IRI over the analysis period. Evaluate the adequacy of the design based on the results and agency

performance experience. If deficiencies exist in the 2002 design guide predictions, determine the reasons if possible.

Calibration to Local Conditions

Prepare a database of agency performance data and compare the new design procedure results with the performance of these "local" sections. This will require the selection of at least 20 CRCP sections around the state. If the state has very distinct climates this should be done in each climate. If no CRCP exists, utilize LTPP performance data from nearby states.

The goal of the calibration-validation process is to confirm that the performance models accurately predict pavement distress and ride quality on a national basis. For any specific geographic area, adjustments to the national models may be needed to obtain reliable pavement designs.

Modify the Calibrations/Inputs

If significant differences are found between the predicted and measured distresses and IRI for the agencies highways, appropriate adjustments must be made to the performance models. This study will also establish the level of accuracy desirable for key input parameters and default input values. Make modifications to the new procedure as needed based on all of the above results and findings.

Data Needs for Local Calibration

The 2002 Guide for CRCP design includes the following two performance models:

- Punchouts (crack spacing, crack width, punchouts)
- Smoothness

Punchouts (CRCP). Prediction of transverse crack spacing, transverse crack deterioration, and formation of longitudinal fatigue crack leading to punchout development are the main focus of CRCP slab thickness design in the 2002 Design Guide. Crack width and crack load transfer efficiency should be carefully evaluated within the climate and materials of the local agency. For calibration and validation of the punchout model, evaluation of the following factors is important:

- PCC zero-stress temperature—zero-stress temperature of the PCC is very critical as it has a direct affect on transverse crack spacing and transverse crack opening. No measured zero-stress temperature values were available during model development so predicted values were used instead. To test accuracy of the crack spacing and crack width prediction models, as applied to local conditions, one approach is to obtain data from previous CRCP projects and run the 2002 software to predict crack spacing and crack width to see how close to observed they predict. If model adjustment to local conditions is needed, the base friction values should be reviewed and the crack width

calibration constant (which has a default of 1.0 but can be varied lower or higher depending on which way the adjustment should be made) should be modified.

- PCC properties—various PCC properties are very important to accurate modeling of CRCP punchout, including the following:

  Coefficient of thermal expansion—curling stress has a significant affect on formation of longitudinal cracks. Accurate value of thermal coefficient is very important to ensure reliable results. Testing should be conducted to determine typical values for the type of aggregates and PCC mixes. Based on testing results, recommendations can be made on whether the use of typical value (based on mix design and aggregate type) is sufficient or project-specific testing is needed.

  PCC modulus of rupture and elastic modulus—The mean 28-day modulus of rupture is the proper input, not the minimum value required in the construction specifications. This value is often far lower than the mean commonly achieved. The agency should run tests on typical project mixes to establish the mean 28-day modulus of rupture. In the 2002 Guide, fatigue damage is calculated incrementally. Since PCC strength is a major factor affecting fatigue life, the consideration of strength gain over time is important. The validation study should include a testing program to verify the PCC strength-gain model incorporated in the 2002 Guide. An increase in PCC strength is typically accompanied by an increase in elastic modulus, which must be taken into consideration to obtain accurate analysis results. The testing program should include the modulus testing to ensure that the correlation between PCC strength and modulus is reasonable.

  PCC shrinkage—the surface of PCC pavements can dry significantly even while the relative humidity deeper in the PCC slab remains at 80 percent or higher. This difference in moisture condition can cause significant warping of PCC slabs, which affects curling stresses. Testing should be conducted to determine the shrinkage characteristics of PCC mixtures commonly used.

- Temperature profiles—the temperature conditions in PCC pavements vary continuously throughout a 24-hour day. For accurate fatigue damage assessment, consideration of hourly temperature profiles is highly desirable. In the 2002 Guide, this is accomplished through the use of an analytical model (Enhanced Integrated Climatic Model [EICM]) that predicts temperature profile in PCC slabs based on hourly climatic data, which are readily available from the National Oceanic and Atmospheric Administration. This model is capable of producing accurate results, but local calibration is highly recommended to ensure that the model predictions closely match actual temperature profiles. The calibration of EICM involves making adjustments to model parameters (e.g., thermal conductivity, heat capacity, emissivity) to match measured temperatures.

- Permanent Curl/Warp effective temperature difference—as a result of temperature gradients built into the PCC slabs during construction and differential shrinkage, PCC slabs are not flat even when no temperature gradient is present. The magnitude of built-in curling can be highly variable. In the 2002 Guide, a value of -10 F is used as a default. This value can be increased if poor curing is expected or construction under very hot conditions is expected. It could be lowered if water curing or night construction is expected.

- Base type—base type and quality (resistance to erosion) is a significant factor affecting CRCP performance. The performance of pavements constructed on different types of bases should be evaluated to verify model predictions and erosion index.
- Base friction —base friction has a significant effect on development of transverse crack spacing pattern and some effect on transverse crack opening. Transverse crack spacing patterns of CRCP pavements constructed on different types of bases should be evaluated to verify friction values used to predict mean crack spacing and mean crack opening for the agency.
- Crack opening—seasonal crack openings is an important parameter in the 2002 Guide punchout model; however, only limited data on crack openings were available. As a result, the punchout model was calibrated using mostly calculated joint opening values. The testing program for the validation study should include monitoring of the crack movements to ensure that the values used in calibration are realistic. It should be noted that the calculated crack widths in the output are at steel level. Those measured in the field are at the surface and are normally considerably higher.

Smoothness Ride quality/smoothness is one of the more common performance indicators used by State highway agencies (SHA's) for both design and pavement management purposes. One key concept included in the 2002 Guide is that there is a defined relationship between distress and smoothness (as measured by IRI). In other words, certain distresses have a significant effect on the IRI measured over time. Thus, smoothness is considered a key element or parameter in the experiment. Initial smoothness is a direct design input to the 2002 Guide and has a major effect on future smoothness. This input is highly dependent upon the smoothness specifications under which the project is constructed. Obtaining data from recently constructed projects is important to establishing this input.

REFERENCES

1. Darter, M.I., S.A. LaCourseiere, and S.A. Smiley, "Performance of Continuously Reinforced Concrete Pavement in Illinois." *Transportation Research Record No. 715*, Transportation Research Board, Washington, DC, 1979.
2. LaCourseiere, S.A., M.I. Darter, and S.A. Smiley, "Structural Distress Mechanisms in Continuously Reinforced Concrete Pavement," *Transportation Engineering Series No. 20*, University of Illinois at Urbana-Champaign, 1978.
3. Selezneva O.I., D. Zollinger, M.Darter, "Mechanistic Analysis of Factors Leading to Punchout Development for Improved CRCP design Procedures," Proccedings of the 7th International conference on Concrete Pavements, p. 731-745, September 2001.
4. Selezneva, O.I., "Development of Mechanistic-Empirical Damage Assessment Procedures for CRC Pavements with Emphasis on Traffic Loading Characteristics," Ph.D. Dissertation, West Virginia University, 2002.
5. Zollinger, D.G., N. Buch, D. Xin, and J. Soares, "Performance of CRCP Volume 6 - CRCP Design, Construction, and Performance," *FHWA-RD-97-151, Report*, U.S. Department of Transportation, Washington, DC, February 1998.

6. Zollinger, D.G., and E.J. Barenberg, "Continuously Reinforced Pavements: Punchouts and Other Distresses and Implications for Design", *Project IHR - 518, Illinois Cooperative Highway Research Program*, University of Illinois at Urbana-Champaign, March 1990.
7. Darter, M. I. "CRCP Distress Study on I-77 Fairfield and Chester Counties, South Carolina," ERES Consultants, Inc., 1988.
8. Tayabji S., Olga Selezneva, and Jiang, Y.J., "Preliminary Evaluation of LTPP Continuously Reinforced Concrete (CRC) Pavement Test Sections – Final Report," *FHWA-RD-99-086*, Office of Engineering and Highway Operations R&D, Federal Highway Administration, March 1999.
9. American Association of State Highway and Transportation Officials, "The AASHO Road Test, Report 5, Summary Report," *Highway Research Board*, Washington, D.C., Special Report 61G, 1962.
10. Spangler, M.G., "Stresses in the Comer Region of Concrete Pavements," *Bulletin 157, Iowa Engineering Experiment Station*, Iowa State College, Ames, 1942.
11. *The AASHTO Guide for Design of Pavement Structures*, American Association of the State Highway and Transportation Officials, Volume 1, 1986.
12. McCullough, B.F., A.A. Ayyash, W.R. Hudson, and J.P. Randall, "Design of Continuously Reinforced Concrete Pavements for Highways," *NCHRP 1-15*, Center for Highway Research, The University of Texas at Austin, August 1975.
13. Won, M., K. Hankins, and B.F. McCullough, "Mechanistic Analysis of Continuously Reinforced Concrete Pavements Considering Material Characteristics, Variability, and Fatigue," *Report No. 1169-2*, Center for Transportation Research, University of Texas at Austin, April 1990.
14. Zuk, W., "Analysis of Special Problems in Continuously Reinforced Concrete Pavements," *Highway Research Board, Bulletin 214*, 1959.
15. Vetter, C.P. "Stresses in Reinforced Concrete Due to Volume Changes," *ASCE, Proceedings, Paper No. 1848*, February 1932.
16. Palmer, R.P., Olsen, M., and Lytton, R.L., "TTICRCP-A Mechanistic Model for the Prediction of Stress, Strains, and Displacements in Continuously Reinforced Concrete Pavements," *Research Report 371-2F, Texas Transportation Institute*, Texas A&M University, August 1987, 275 pp.
17. Reis, Elmer E. Jr, John D. Mozer, Albert C. Bianchini, and Clyde E. Kesler, "Causes and Control of Cracking in Concrete Reinforced with High-Strength Steel Bars – A Review of Research," *Engineering Experiment Station Bulletin 479*, College of Engineering, University of Illinois.
18. Tang, T., D.G. Zollinger, and B. F. McCullough, "Field Tests and Analyses of Concrete Pavement in Texarkana and La Porte, Texas," *Research Report 1244-7*, Texas Transportation Institute, Texas A&M University, College Station, Texas, October 1996
19. Grzbowski, M. and S.P. Shah, "Model to Predict Cracking in Fiber Reinforced Concrete Due to Restrained Shrinkage," *Magazine of Concrete Research, 41*, No. 148, September 1989, pp. 125-135
20. Parrott, L.J., "Moisture Profiles in Drying Concrete," *Advances in Cement Research,* Vol. 1, No. 3, July 1988.
21. Westergaard, H.M., "Analysis of Stresses in Concrete Pavements Due to Variations of Temperature," *Highway Research Board Proceedings, 6*, (1927) p. 201-215.

22. Bradbury, R.D., “Reinforced Concrete Pavements,” Wire Reinforcement Institute, Washington, D.C., 1938.
23. Mohamed, A.R., and W. Hansen. (1997). "Effect of Nonlinear Temperature Gradient on Curling Stresses in Concrete Pavements," In *Transportation Research Record 1568*, National Academy Press, Washington, D.C., pp. 65-71.
24. Gharaibeh, N.G., M.I. Darter, and L.B. Heckel, “Field Performance of CRCP in Illinois,” *Paper presented at the 78th Annual Meeting of the Transportation Research Board*, Washington, DC, January 1999.
25. Van Wijk, A. J. and C. W. Lovell, “Prediction of Subbase Erosion Caused by Pavement Pumping,” *Transportation Research Record No. 1099*, Washington, D.C. pp. 45 – 57.
26. Van Wijk, A. J., “Rigid Pavement Pumping: (1) Subbase erosion and (2) Economic Modeling,” Joint Highway Research Project File No. 5-10, School of Civil Engineering, Purdue University, West Lafayette, Indiana, 1985.
27. L. Khazanovich, O.I. Selezneva, H.T. Yu, M. I. Darter, “Development of Rapid Solutions for Prediction of Critical CRCP Stresses,” *Transportation Research Record 1778*, Washington, D.C., 2001